# ISOMERIC SEPARATIONS OF PHARMACEUTICAL INTEREST USING HIGH PERFORMANCE CAPILLARY ELECTROPHORESIS

by

LI LI ZHOU

A Dissertation submitted to the Graduate Faculty in Chemistry in partial fulfillment of the requirements for the degree of Doctor of Philosophy. The City University of New York.

1996

**This manuscript has been read and accepted by the Graduate Faculty in Chemistry in satisfaction of the dissertation requirement for the degree of Doctor of Philosophy.**

10 Sept. 96 — David C. Locke

**Date:** **David C. Locke** **Chair of Examining Committee**

Sept. 10, 1996 — Richard Pizer

**Date:** **Richard Pizer** **Executive Officer**

Thomas C. Strekas

**Thomas C. Strekas** **Supervisory Committee**

Gary Mennitt

**Gary Mennitt** **Supervisory Committee**

Angelos Dovletoglou

**Angelos Dovletoglou** **Supervisory Committee**

**The City University of New York**

## ABSTRACT

ISOMERIC SEPARATIONS OF PHARMACEUTICAL INTEREST USING HIGH PERFORMANCE CAPILLARY ELECTROPHORESIS

Adviser: Professor David C. Locke

The mechanisms of isomeric separation by capillary zone electrophoresis (CZE) of several pharmaceutical compounds are investigated.

In the first chapter, the mechanisms of various diastereomeric separations, such as those for *cis*- and *trans*-aminoindanols and diastereomers of dorzolamide, are discussed. The separations are achieved based upon differences in the pKa values of the *cis*- and *trans*-diastereomers. The separation of *cis* and *trans*-aminoindanols using non-aqueous CZE is also studied and shows better resolution in comparison to the aqueous system. The isomeric separation based on pKa differences can also be applied to various positional isomers. The cationic positional isomers of aminoquinoline and the anionic positional isomers of difluorophenyl-acetic acid are successfully separated.

In the second chapter, the separations of aminoindanol enantiomers through the utilization of α- and β-cyclodextrins (CDs) as chiral selectors are discussed. Thermodynamic studies establish a dynamic separation model of the inclusion complex between the enantiomers and CDs. Binding of the *cis*-aminoindanol enantiomers to the CDs is stronger than the *trans*-enantiomers. van't Hoff plots indicate that inclusion complex formation is enthalpically-driven

in the temperature range from $15^0$C to $35^0$C. The CZE separation mechanism is also supported by HPLC and molecular modeling calculation. The effects of the buffer pH, urea additive, size of the chiral selectors and the presence of a hydroxyl group on the analyte are analyzed by examining the thermodynamic parameters.

In the third chapter, the enantiomeric separation of a novel orally active growth hormone secretagogue, using β-cyclodextrin as a chiral selector is discussed. The resolution, the effective electrophoretic mobility of analytes, and the electroosmotic flow are studied as function of the concentrations of β-CD, organic modifier and ion pairing reagents in the electrolyte. The effects of CZE operating conditions, such as the temperature, the applied voltage, and the apparent pH of the electrolyte are also examined. The results of these experiments demonstrate that the concentrations of β-CD and L-tartaric acid, pH, and temperature are the key parameters for the enantiomeric separation. This separation technique is fully validated according to cGMP standards for limits of detection (LOD) and quantitation (LOQ), detection linearity, precision, accuracy, and ruggedness.

## Acknowledgments

I would especially like to express my appreciation to my thesis advisor, Dr. David Locke, for his guidance and assistance in the preparation of this dissertation, and for his constant concern and encouragement during the entire period of my graduate study at the City University of New York.

I would also like to thank my committee members, Dr. Angelos Dovletoglou, Dr. Thomas Strekas, and Dr. Gary Mennitt for their solid support and advice.

Many thanks to Dr. Pascal H. Toma for providing help for the molecular modeling calculation.

I extend my thanks to all my colleagues, especially Dr. Richard Thompson, Dr. Peter Maligres and Dr. Nelu Grinberg for many valuable discussions. And also thanks to Dr. Ioannis Houpis and Dr. Sunil Prabhu for providing some very useful chemicals.

Special appreciation to Dr. Richard Egan for encouraging me to finish this study.

Very special thanks to my husband, Dr. Yun Fang, and my son, John Z. Fang for their patience, understanding, and encouragement during these years.

Finally, I would like to acknowledge the Doctoral Study Program II of Merck Research Laboratory which gave me the financial support and the chance to prepare this dissertation.

*Dedicated to those who made this thesis possible:*

*My research mentor, my husband, my son, my parents, and my parents in-law.*

## TABLE OF CONTENTS

## Chapter Two: Study of Separation Mechanism of Aminoindanol Enantiomers Using CDs

## LIST OF FIGURES

**Chapter** **Page**

**Chapter One**

Chapter Two

**Chapter Three**

## LIST OF TABLES

**Chapter** **Page**

**Chapter Three**

# ISOMERIC SEPARATIONS OF PHARMACEUTICAL INTEREST USING HIGH PERFORMANCE CAPILLARY ELECTROPHORESIS

## General Introduction

Isomers are chemical compounds which have identical molecular compositions but differ structurally from each other. Positional isomers differ from one another because their atoms are linked in a different order. Stereoisomers differ from one another because their atoms are arranged differently in space. Two stereoisomers that are non-superimposable mirror images are called enantiomers. Diastereomers are non-enantiomeric stereoisomers having two or more asymmetric centers. The positional isomers or diastereomers usually have different physical and chemical properties. The enantiomers usually have same physical and chemical properties, but different optical and biological properties [1].

Isomeric separation is a important task in the pharmaceutical industry. Many pharmaceutical drugs contain one or more chiral centers and may have several isomeric forms. In many cases, only one of the isomeric forms is biologically active while the other isomer is either much less active, or sometimes even toxic. For example, a new HIV protease inhibitor, Crixivan®, (Merck & Co., Inc., Whitehouse Station, NJ, USA) which was approved by the U.S. Food and Drug Administration (U.S. FDA) in March, 1996, has five chiral centers. This means the compound could have 32 ($2^5$) possible chemical configurations. Only one of the thirty two configurations provides optimal efficiency and tolerability[2-3]. The structure of Crixivan® is shown in Figure 1-1. The isomeric separation of the

major isomer from all others as mentioned above is quite challenging. When a new drug is applied for US FDA approval, it is now required to provide detailed information regarding the enantiomeric purity and therapeutic or toxic effects of the individual enantiomer.

Isomeric separations can be achieved using several separation techniques, such as gas chromatography (GC), high performance liquid chromatography (HPLC), supercritical fluid chromatography (SFC), and high performance capillary electrophoresis (HPCE) [4-12]. HPCE was introduced in the early 1980s and has become one of the most powerful and popular separation techniques. Compared with HPLC, HPCE has advantages in terms of high efficiency, easy exchange of the separation media, extremely small amount of sample and media needed, hence low cost, etc.[13-16].

HPCE combines some of the most powerful aspects of traditional electrophoresis. chromatography, and capillary technology. Numerous authors have given overviews of the basics, some equipment criteria, and the various modes of HPCE [17-22]. An HPCE system can be as simple as a high voltage power supply connected to two buffer reservoirs that are bridged by a fused silica capillary. Samples are loaded onto the capillary by replacing one of the reservoirs (at the anode or cathode) with a sample reservoir and applying either an electric field (electrokinetic injection mode) or an external pressure or vacuum (hydrodynamic injection model). After injection of the sample solution, an electric field is

applied to the capillary and the separation is based upon the mobility and the size of analytes. The analytes are monitored by a detector(s), such as UV/Vis, fluorescence, MS, etc. With UV/Vis and fluorescence detectors, the fused silica capillary can serve as the sample cell by removing a short section of the polyimide coating and placing the resultant "window" in a modified HPLC detector. The detector trace, which looks like a chromatogram, is called an electropherogram.

Several different HPCE separation modes, including capillary zone electrophoresis (CZE), capillary gel electrophoresis (CGE), and micellar electrokinetic chromatography (MEKC), have been developed during the past years [8,27-30]. A variety of compounds, such as ionic compounds, neutral compounds, and biopolymers, can be all separated by one or other of the different modes of HPCE. Among the HPCE techniques, CZE is the simplest and the most used mode.

In CZE, the capillary is filled only with a buffer. Separation occurs because analytes migrate in discrete zones at different velocities. The separation of both anionic and cationic analytes is possible by CZE. Neutral analytes do not migrate and elute with the electroosmotic flow (EOF). EOF is a fundamental constituent of HPCE. It is the bulk flow of liquid in the capillary and is a consequence of the surface charge on the interior capillary wall. The EOF results from the effect of the applied electric field on the solution double-layer at the wall. The EOF controls the amount of time analyte remain in the capillary by superposition of

flow on to analyte mobility. It can be measured using a neutral marker (NM) that moves at a velocity equal to the EOF [32].

Since 1990, more and more applications using CZE for the separation of isomers, especially optical isomers, have been reported. However, for the separation of positional isomers or diastereomers (which usually result by derivatizing enantiomers with a chiral reagent), the common mode used is MEKC [23-25]. For most enantiomeric separations, the enantiomers contain only one chiral center [26, 31]. Many theoretical aspects and application problems of CZE are still unknown and require further investigation. My thesis focuses on the area of isomeric separation of compounds of pharmaceutical interest using CZE. In this study, both theoretical discussions and experiments were conducted. The body of the study is divided into three chapters according to aspects that different chapters covered and emphasized.

In the first chapter, the separations of the *cis-* and *trans-* diastereomers and positional isomers using simple aqueous or non-aqueous buffer systems were demonstrated. *Cis-* and *trans-* aminoindanol diastereomers and *cis-* and *trans-* dorzolamide diastereomers were used as model compounds of the diastereomers. Four aminoquinoline isomers were used as model compounds of cationic positional isomers and five difluorophenyl acetic acid isomers were used as model compounds of anionic positional isomers. The separations were based on differences in pKa or size which exists in the diastereomers and positional

isomers. For the separation of the anionic positional isomers, a polyvinyl alcohol (PVA) capillary was used to suppress the EOF. The separation mechanism was interpreted in detail. The results were compared with those from HPLC and molecular modeling.

In the second chapter, the CZE enantiomeric separation of new compounds, *cis*(+/-) and *trans*-(+/-) aminoindanol enantiomers, with cyclodextrins as chiral selectors was described. A theoretical separation model was established through thermodynamic studies. The effects of *cis* and *trans* structural features on the enantiomeric separation were investigated in detail. HPLC and molecular modeling were conducted to confirm the interpretation of the separation mechanism. The effects of temperature, buffer pH, concentration of the chiral selector or urea additive, size of the chiral selector, and the presence of a hydroxyl functional group on the target compounds were also studied.

In the third chapter, the separation of *R/S* enantiomers of a novel growth hormone secretagogue, MK-0677 was discussed. By using a theoretical model, a practical CZE method was developed and validated according to the standards of current good manufactory practice (cGMP) in terms of precision, accuracy, ruggedness, linearity, and sensitivity. Furthermore, the effects of composition of the electrolyte were investigated in detail via experiments and the theoretical modeling.

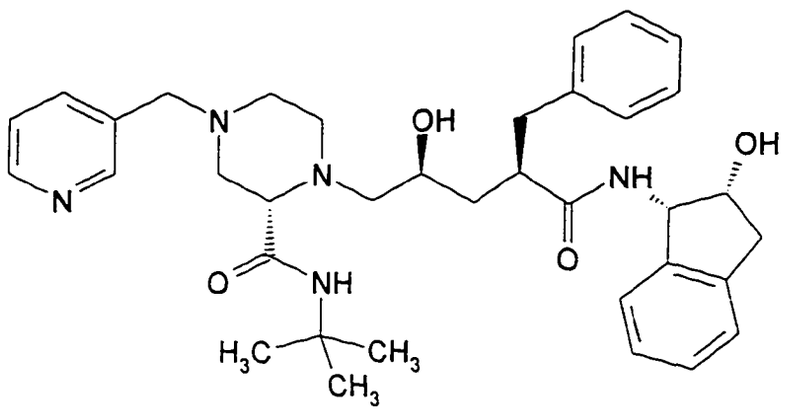


**Figure 1-1. The Structure of Indinavir (Crixivan®)**

The chemical name of Indinavir (Crixivan)® is *N*-(2(*R*)-Hydroxyl-1(*S*)-indanyl-2(*R*)-(phenylmethyl)-4(*S*)-hydroxyl-5-{1-[4-(3-pyridylmethyl)-2(*S*)-(*N*-*tert*-butylcarbamoyl)piperazinyl]}pentanamide. Indinavir contains five chiral centers in its structure.

# CHAPTER ONE

## Study of the Separation Mechanism of *Cis/Trans* Diastereomers and Positional Isomers

## 1-1 Introduction

Aminoindanol is an important key raw material used to introduce a benzocycloalkyl amine functional group into the HIV protease inhibitor Indinavir® [1]. It contains two chiral centers and exists as four stereoisomers. They are (1S,2R)-*cis*-1-aminoindan-2-ol [*cis*(-)]; (1R,2S)-*cis*-1-aminoindan-2-ol [*cis*(+)]; (1S,2S)-*trans*-1-aminoindan-2-ol [*trans*(-)]; and (1R,2R)-*trans*-aminoindan-2-ol [*trans*(+)], based on the Cahn-Ingold-Prelog conversion system. The stereoisomeric relationship between these isomers is shown in Figure 1-2. Pharmacological studies show that the *cis*(-) gives the best biological activity[1]. During the synthetic process of making *cis*(-), it is very important to develop an analytical methodology to separate the stereoisomeric impurities from the major compound. In many cases, if a compound contains more than one chiral center, the most important thing is to separate the diastereomers from the major isomeric form. Until now, only a few examples of diastereomeric separations using CZE have been reported. These diastereomeric separations were reported either using MEKC [2] or involving derivatizing reagents and buffer additives such as β-cyclodextrin [3]. There are no literature reports on the separation of *cis* and *trans* diastereomers using CZE.

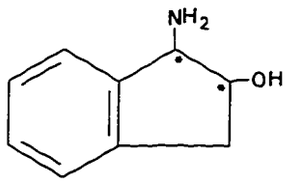


1-Aminoindan-2-ol

**(a)**

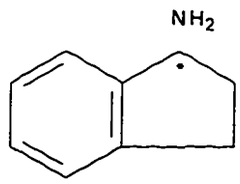


Aminoindan

**(b)**

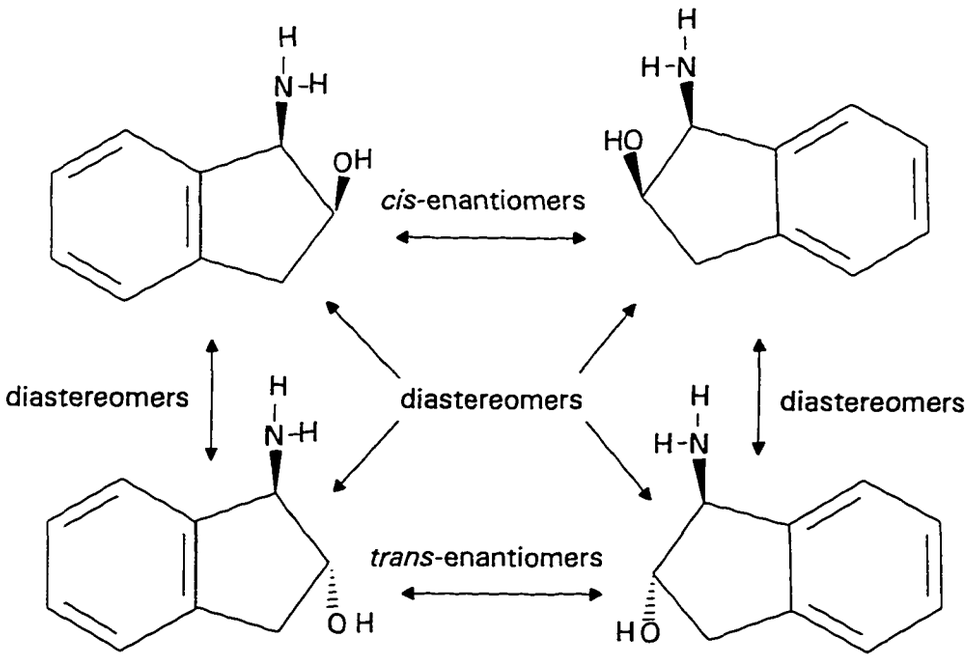


Stereoisomeric Relationship of the Aminoindanol Stereoisomers

**Figure 1-2. Structures of Aminoindanol and Aminoindan**

It is known that for aromatic compounds containing several functional groups, several isomers are possible because substituted groups can be located at different positions on the aromatic ring. These isomers may have differences in their pKa values, depending on the characteristics of the substitutents and the position on the aromatic ring. MEKC is usually used to separate this kind of isomer with some buffer additive(s) such as cyclodextrins, but the separations are usually limited to two isomers [4-5].

In this chapter, CZE methods with simple aqueous buffer solutions or non-aqueous solutions are described. Several diastereisomers and positional isomers were separated based on their pKa differences. The study employed several test compounds, aminoindanol and dorzolamide isomers as diastereomers, aminoquinoline isomers as cationic positional isomers and difluorophenylacetic acid used as anionic positional isomers. All these compounds are very important raw materials or intermediates in the pharmaceutical industry. The separation mechanisms were also investigated and some questions about the CZE separation of *cis/trans* diastereomers, which are listed as follows, were answered by the study.

1) Is it possible to separate *cis/trans* diastereomers, such as *cis/trans* aminoindanol isomers, by CZE without buffer additive?

2) If so, what are the key factors that differentiate *cis* and *trans* aminoindanol (or other diastereomers) during the separation? How can we take advantage of these key differences in order to develop a simple CZE diastereomeric separation procedure?

3) Is it possible to use results obtained from other methodologies to support the explanations of the CZE separation mechanism for the *cis/trans* diastereomers ?

4) Is it possible to separate *cis/trans* diastereomers using non-aqueous solutions by CZE? If so, how does the non-aqueous CZE separation compare with the aqueous CZE separation ?

## 1-2 Study Design

Before the study is designed to answer the questions above, we should consider the physical and chemical properties of the target compounds, especially differences between *cis*- and *trans*-aminoindanol. Their qualitative physiochemical properties are given in Table 1-1 based on their compound structure. If these physiochemical properties make some difference in the charge/size ratio between *cis* and *trans* diastereomers, a simple CZE separation should be possible. Based on this concept, the experiments were designed as follows:

1) Study the effect of buffer pH over the range from 2 to 10 on the separation of the *cis/trans* aminoindanol and *cis/trans*-dorzolamide diastereomers.

2) Determine the pKa values of *cis/trans* aminoindanol diastereomers using both acid/base titration and CZE methods to correlate the pKa with structures.

3) Determine the minimization energy of the *cis/trans* aminoindanol diastereomers by molecular modeling to support the interpretation of the separation mechanism.

4) Use non-aqueous buffers to separate the *cis/trans* aminoindanol diastereomers and compare with aqueous CZE.

5) Apply the same separation strategy to the positional isomers to test the generality of the model.

**Table 1-1. Comparison of Physical-Chemical Properties of the *Cis/Trans* Aminoindanol Diastereomers** [18]

| **Characters** | ***Cis* Isomer** | ***Trans* Isomer** |
|---|---|---|
| Dipole moment | higher | lower |
| Symmetry | less | more |
| Steric crowding | more | less |
| Total strain | more | less |
| Size | smaller | larger |
| Form intermolecular H bond | possible | possible |
| Form intramolecular H bond | possible | impossible |
| pKa | higher? | lower? |

## 1-3 Experimental

### 1-3A Instrumental

Unless otherwise specified, all CZE experiments, for both aqueous and the non-aqueous systems, were performed using a Hewlett-Packard CE instrument ($HP^{3D}$, Hewlett Packard, Piscataway, NJ). Information on capillaries and applied voltages used in the different experiments are given in Table 1-2. All experiments were performed using hydrodynamic pressure (50 mbar) sampling injection with injection time 3 seconds. A diode-array UV detector was set at 200 nm for all aqueous electrolytes and 254 nm for the non-aqueous analysis. Capillary temperature was controlled by the instrument's internal thermostat at 25°C. Data analysis and collection were accomplished using a NELSON ACCESS CHROM data system (Perkin Elmer Corp., Cupertino, CA).

The potentiometric acid/base titrations were performed using a Brinkmann 716 DMS titrino (Metrohm Titrator, Switzerland). For titration of weak bases, 0.01 N HCl was used as the titrant. For titration of weak acids, 0.01 N NaOH was used as the titrant.

### 1-3B Chemicals

The (*1S,2R*)-*cis*-1-aminoindan-2-ol [*cis*(-)], (*1R,2S*)-*cis*-1-aminoindan-2-ol [*cis*(+)], and a racemic mixture of *trans* pair enantiomers, (*1S,2S*)-*trans*-1-aminoindan-2-ol [*trans*(-)], and (*1R,2R*)-*trans*-aminoindan-2-ol [*trans*(+)], *cis*-dorzolamide, and *trans*-dorzolamide were synthesized by Merck Research Laboratories, Merck & Co. Inc. (Rahway, NJ). 1-Aminoindan, aminoquinoline, difluorophenylacetic acid, and mesityl oxide were purchased from Aldrich Chemical (Milwaukee, WI) and used without further purification. Ammonium acetate, sodium phosphate, phosphoric acid, lithium hydroxide, glacial acetic acid, sodium hydroxide solution, 0.01N HCl and 0.01N NaOH solutions, and methanol were purchased from Fisher Scientific (Springfield, NJ) and used without further purification. Hydroxymethyl-aminomethane (tris) was purchased from Bio-Rad (Richmond, CA, USA). Water was purified with a Milli-Q system (Millipore Corp, Milford, MA).

### 1-3C Solution Preparation

Several electrolyte solutions were prepared as follows:

Buffer solution 1-1 (BF 1-1): BF 1-1 was prepared by dissolving 4.8 grams (g) of tris in one liter (L) of the deionized water (D.I. water). The concentration of the solution was 40 mM. The solution was subdivided into different 100-mL beakers and each solution was adjusted to the designated pH with phosphoric acid.

Buffer solution 1-2 (BF 1-2): BF 1-2 was prepared by dissolving 3.1 g of ammonium acetate in one L of D.I. water. The concentration of the solution was 40 mM. The resulting solution was subdivided into different 100-mL beakers and each solution was adjusted to the designated pH with LiOH or perchloric acid.

Buffer solution 1-3 (BF 1-3): BF 1-3 was prepared by dissolving 3.1 g ammonium acetate in one L of 99.99% pure methanol. The concentration of the solution was 40 mM. The resulting solution was subdivided into different 100-ml beakers and each solution was adjusted to the designated pH with LiOH or perchloric acid. The pH of all solutions is apparent pH.

Several sample solutions were prepared as follows:

Sample solution 1-1 (SP 1-1): SP 1-1 was prepared by dissolving 5 mg of *cis*(-)-aminoindanol and 7 mg of *trans*(+/-)-aminoindanol racemic mixture in 50 mL D.I. water.

Sample solution 1-2 (SP 1-2): SP 1-2 was prepared by dissolving 5 mg each of *cis*-dorzolamide and *trans*-dorzolamide in 50 mL D.I. water.

**Table 1-2. Summary of Capillaries and Applied Voltages Used In the Study**

| **Experiment** | **Fused Silica Capillary Information** | **Applied Voltage (kV)** |
|---|---|---|
| pKa determination | 40-cm effective length (47-cm total length, 50μm I.D. with a preburned window) | 16 |
| Aqueous/ non-aqueous separation | 56-cm effective length (63-cm total length, 50μm I.D. with a preburned window) | 20 |
| Separation of *cis/trans* dorzolamide | 56-cm effective length (63-cm total length, 75μm I.D. with a preburned window) | 20 |
| Anionic structural isomers separation | a PVA coated 56-cm effective length, (63-cm total length, 50μm I.D. with a preburned window) | 20 reverse polarity |
| Cationic structural isomers separation | 56-cm effective length (63-cm total length. 50μm I.D. with a preburned window) | 20 |

Neutral marker solution (NM 1-1): NM 1-1 was prepared by dissolving 30 mg of mesityl oxide in 100 mL 99.99% pure methanol.

Titration solutions: About 35 mg of each *cis*-(-)-aminoindanol, or *cis*-(+)-aminoindanol, or *trans*(+/-)-aminoindanol racemic mixture, or 1-aminoindan racemic mixture was accurately weighed into 100 mL beaker. 50 mL D.I. water was added to each beaker.

### 1-3D Procedure

All new capillaries were washed sequentially with 1N NaOH solution for 30 min, D.I. water for 10 min, and 0.2 N NaOH solution for 60 min. Before each injection, the capillary was also rinsed sequentially with 0.2 N NaOH solution for 3 min, then the test buffer solution for 3 min. This operating procedure is necessary to successfully obtain reproducible results from experiments. All test and sample solutions were filtered through 0.45μm Nylon syringeless filters before use. The neutral marker solution (NM) was added into all sample solutions quantitatively.

## 1-4 Results and Discussion

### 1-4A Separation of *Cis/Trans* Diastereomers

Electrophoretic separation is achieved through velocity differences of the analytes in a electric field. The velocity of an ion is

$$v = \mu_e E \qquad [1\text{-}1]$$

where v is ion velocity; $\mu_e$ is the effective electrophoretic mobility, and E is the applied electric field [6].

The electrophoretic mobility in Equation 1-1 is determined by the electric force, the molecule experiences, balanced by its frictional drag through the medium. Combination of both forces yields an equation that describes the mobility in terms of physical parameters

$$\mu_e = q / 6\pi \eta r \qquad [1\text{-}2]$$

where q is the ionic charge, $\eta$ is the solution viscosity, and r is the ion radius.

Since the target compounds, *cis*- and *trans*- aminoindanol, are weakly basic compounds, the thermodynamic dissociation equilibrium for the weak base can be expressed as:

$$B H^+ \rightleftharpoons B + H^+ \qquad [1\text{-}3]$$

The dissociation constant, Ka, is calculated by the following equation:

$$Ka = \frac{\gamma_B [B] \gamma_{H^+} [H^+]}{\gamma_{(BH^+)} [BH^+]} \quad [1\text{-}4]$$

where $\gamma_B$ is the activity coefficient of the nondissociated base, which is assumed reasonably to be 1 at the low concentration used. Equation 1-4 can be rewritten:

$$pKa = pH + \log\gamma_{(BH^+)} - \log\frac{[B]}{[BH^+]} \quad [1\text{-}5]$$

Activities can be calculated using the Debye-Huckel theory according to the equation:

$$-\log \gamma_i = \frac{0.5Zi^2 [B] \sqrt{\mu}}{1 + a\sqrt{\mu}} \quad [1\text{-}6]$$

$$\mu = 0.5 \sum (Ci\, Zi^2) \quad [1\text{-}7]$$

where a is the hydrated diameter for ion *i* in Å, $C_i$ is the molar concentration for ion *i*, $Z_i$ is the charge on ion *i*, and the $\mu$ is the ionic strength of the solution. In general, the exact value of the parameter of a is range from 1-11Å, which is usually unknown. In this study, the value 5 Å is assumed.

Let us look at the relationship between $pK_a$ and the effective mobility. In CZE, a voltage (V) is applied across a capillary of length (L) resulting in an electric field strength (E) given by

$$E = \frac{V}{L} \quad [1\text{-}8]$$

The electrophoretic mobility of an ion is generally expressed as:

$$\mu = \frac{lL}{tV} \qquad [1\text{-}9]$$

where $l$ is the effective capillary length which is the length from the injector end to the detector.

In the presence of electroosmotic flow (EOF), the measured mobility is called the apparent mobility($\mu_a$). The effective mobility ($\mu_e$)is determined from $\mu_a$ and the mobility of a neutral marker ($\mu_{EOF}$) which is caused by EOF.

$$\mu_e = \mu_a - \mu_{EOF} \qquad [1\text{-}10]$$

$$\mu_{EOF} = \frac{l \times L}{V \times (t_{EOF})} \qquad [1\text{-}11]$$

$$\mu_e = \frac{l \times L}{V \times \left(\frac{1}{t} - \frac{1}{t_{EOF}}\right)} \qquad [1\text{-}12]$$

where t is the migration time of the analyte and the $t_{EOF}$ is the migration time of the neutral marker.

The electrophoretic mobility of weak acids and bases can be conveniently adjusted by varying the pH of the running electrolyte. When a base is protonated, the net electrophoretic mobility $\mu_e$ in the buffer solution at a certain concentration also equal [7]:

$$\mu_e = \alpha \mu_b \qquad [1\text{-}13]$$

where $\mu_b$ is the electrophoretic mobility of the fully protonated species, $BH^+$, and $\alpha$ is the fraction of the analyte ionized, which is defined as:

$$\alpha = \frac{[BH^+]}{[BH^+]+[B]} \qquad [1\text{-}14]$$

Combination of equations 1-13 and 1-14 gives [17,21-22]:

$$\frac{[BH^+]}{[B]} = \frac{\alpha}{1-\alpha} = \frac{\mu_e}{\mu_b - \mu_e} \qquad [1\text{-}15]$$

Substituting equation 1-14 into Equation 1-5,

$$pKa = pH + \log\left(\frac{\mu_e}{\mu_b - \mu_e}\right) + \log \gamma_{[BH^+]} \qquad [1\text{-}16]$$

Based on the above discussion, if the target compounds, *cis*- and *trans*-aminoindanol, differ in either molecular size or dissociation constant, the CZE separation should be achievable.

Several experiments were conducted to separate *cis*-and *trans*-aminoindanol by CZE using tris-phosphate buffer solutions with pH values from 2 to 10. Figure 1-3 shows the separation of the *cis*- and *trans*-aminoindanol. The front peak is *cis*-aminoindanol and the later eluting peak is *trans*-aminoindanol. It can be seen from Figure 1-3, as the buffer pH increases, the migration time of both *cis*- and *trans*-aminoindanol diastereomers decreases except between pH 2.4 and 3.3 where it increases. The resolution of two peaks increases along the pH axis up to a maximum point and then decreases. When the pH is ≥ 10.0, the resolution is completely lost (Figure 1-5). This phenomenon indicates the resolution of *cis*- and *trans*-aminoindanol diastereomers is a function of pH.

In order to explain the separation behavior shown in Figures 1-3 and 1-5, the effective mobilities for both *cis*- and *trans*-aminoindanol diastereomers and neutral marker were calculated based on Equations 1-11 and 1-12, and plotted vs. pH values in Figure 1-4. The pKa values for both *cis*- and *trans*-aminoindanol diastereomers were determined based on the $\mu_e$-pH plots and Equation 1-16 [16,17]. The results show the pKa value for the *cis*-aminoindanol is 0.8 units higher than that of *trans*-aminoindanol (See Table 1-3).

Since *cis*- and *trans*-aminoindanol diastereomers have different pKa values, the separation behavior can be attributed to differences of charge/size ratio between *cis*- and *trans*-aminoindanol diastereomers. Based on Equation 1-13, the $\mu_e \propto \alpha$. At a low pH (pH=2), $\alpha \rightarrow 1$, both aminoindanol diastereomers are fully charged and the effective mobilities of both *cis*- and *trans*-aminoindanol diastereomers approach their highest values because both analytes are completely ionized. There is no charge difference between the *cis*- and *trans*-aminoindanol diastereomers, and there is no separation between them if the sizes are same. However, experimental results show resolution about 1.0 between the two diastereomers even at pH =2. That indicates there is a size difference between the two diastereomers which will be discussed below. In the region of pH between 2.4 to 3.3, the EOF is almost eliminated. As the buffer pH increases, the $\alpha$ decreases, results in a reduction in the overall charges on the diastereomers, hence increase the migration time (Figure1-3) which corresponding a reducing of

effective mobilities. At pH=pKa, $\alpha$=0.5, only half of the diastereomers are ionized, $\log(\frac{\alpha}{1 - \alpha}) = 0$ and the effective mobilities start to dramatically decrease. In the region of pH ≥ pKa+2, the $\alpha \rightarrow 0$, the charge $\rightarrow 0$, the $\mu_e \rightarrow 0$. In the region of pH>4.0, the EOF increases significantly, the migration times of both *cis*- and *trans*- aminoindanol diastereomers are reduced although the effective mobilities are decreased. Since the pKa of the *trans*-aminoindanol is 0.8 units lower than the *cis*-aminoindanol, by increasing the pH, the charge difference between *cis*- and *trans*- aminoindanol diastereomers becomes larger because of $\alpha_{trans} < \alpha_{cis}$, which results in a better resolution. There is an optimum pH at which maximum resolution should be achieved, as is presented in Figure 1-5. In the region of the pH ≥ pKa+2 units (eg. at pH=10.0), both *cis*- and *trans*-aminoindanol diastereomers are almost completely deprotonated, analytes turn into neutral species and coelute with the neutral marker peak because of the EOF.

The change of the EOF with the buffer pH can be seen from Figure 1-4 as well. For the pH < 4.0, the EOF is small because the capillary surface is protonated. As the pH is increased from 4.0 to 8.0, the EOF increases rapidly due to the significant increase in the number of ionized silanol groups. When the buffer pH changes from 8.0 to 10.0, the EOF increases slowly and up to a maximum value since the silanol groups are almost completely ionized.

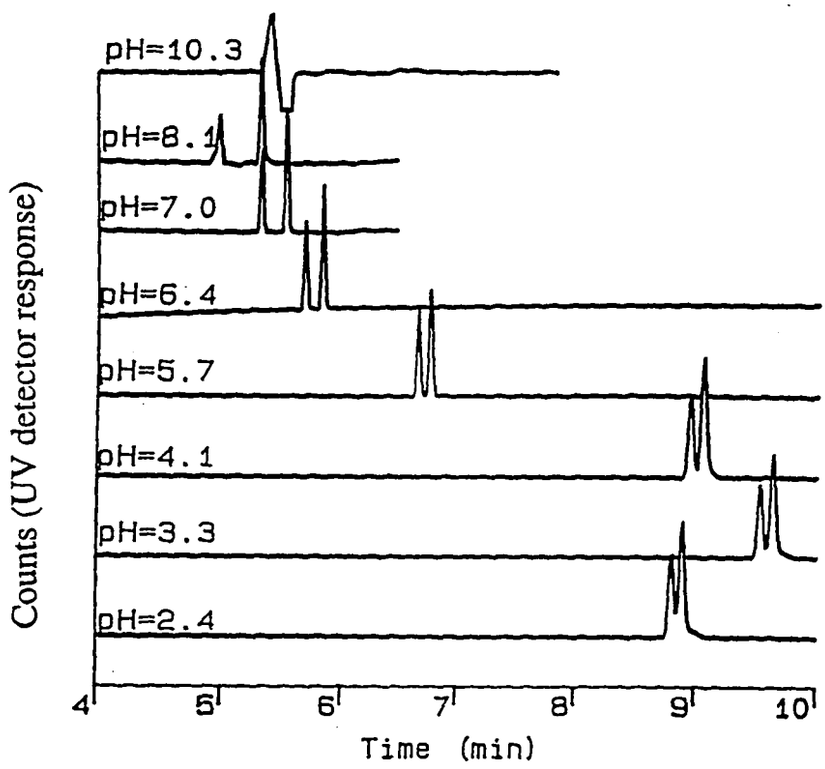


**Figure 1-3. Electropherograms of *Cis/Trans* Aminoindanol Diastereomers Obtained by CZE at Various pH.**

Experimental conditions: buffer solution: BF 1-1; capillary: 50 μm I.D., 40 cm effective length (47 cm total length); detection: 200 nm; temperature: 25°C; applied voltage: 16 kV.

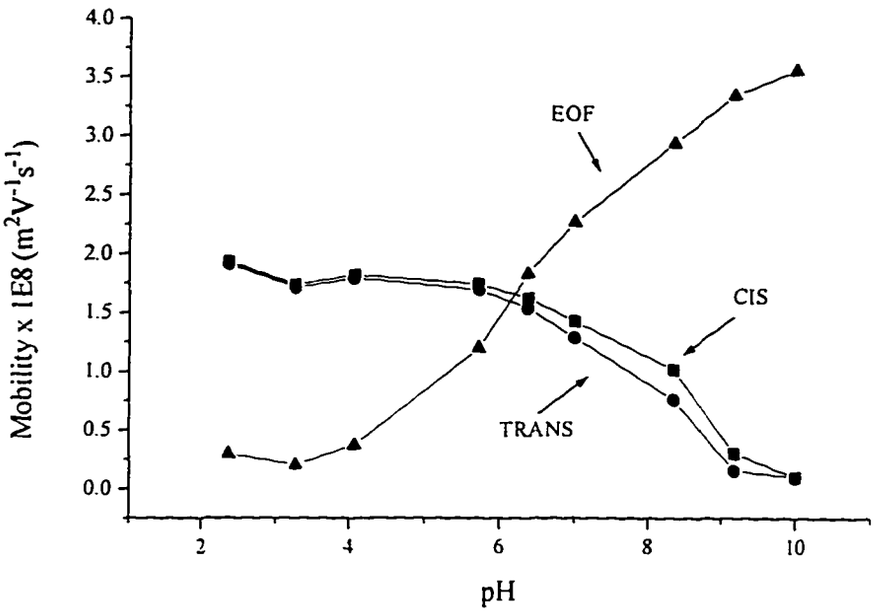


**Figure 1-4. Relationship Between Buffer pH, Effective Mobility, and Mobility of Neutral Marker.**

The experimental conditions are the same as those in Figure 1-3.

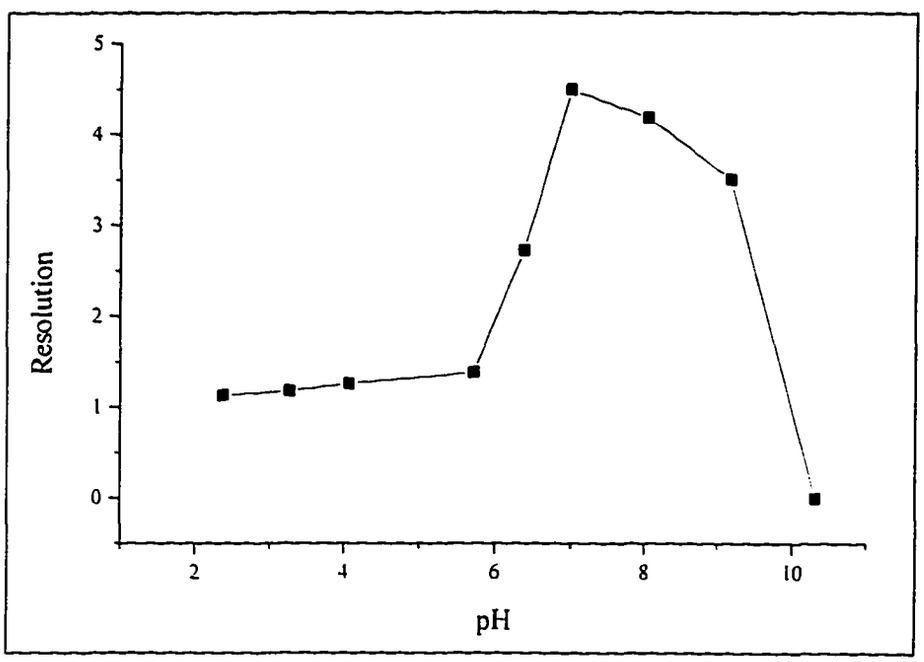


**Figure 1-5. Resolution of *Cis/Trans* Isomers at Different Buffer pH.**

The experimental conditions are the same as those in Figure 1-3.

### 1-4B Acid/Base Titration

In order to confirm the pKa difference between *cis*- and *trans*-aminoindanol diastereomers, an acid/base titration was conducted to measure the pKa values of the *cis*- and *trans*- aminoindanol diastereomers. The relationship between the analyte pKa and the buffer pH can be expressed as [23-24]:

$$pKa = pH + \log\gamma_{[BH^+]} + \log \frac{[BH^+]}{[B]} \qquad [1\text{-}17]$$

When the titration is 50% completed, the concentration of the untitrated base equals the concentration of the conjugate acid formed, $[BH^+]=[B]$, then Equation 1-17 can be changed to:

$$pKa = pH + \log\gamma_{[BH^+]} \qquad [1\text{-}18]$$

The pKa values of *cis/trans* aminoindanol were determined by a potentiometric titration using 0.01N HCl as titrant. About 0.3 mol. of each diastereomer was dissolved in 50 ml D.I. water. The pH at the half equivalence point was obtained from the titration curve, $\log\gamma_{[BH+]}$ was calculated using Equation 1-6.

In order to determine the end point more clearly, the first derivative of the titration curve, d(pH)/d(vol) was plotted vs. the titrant volume. A typical titration curve for *cis*-aminoindanol is shown in Figure 1-6.

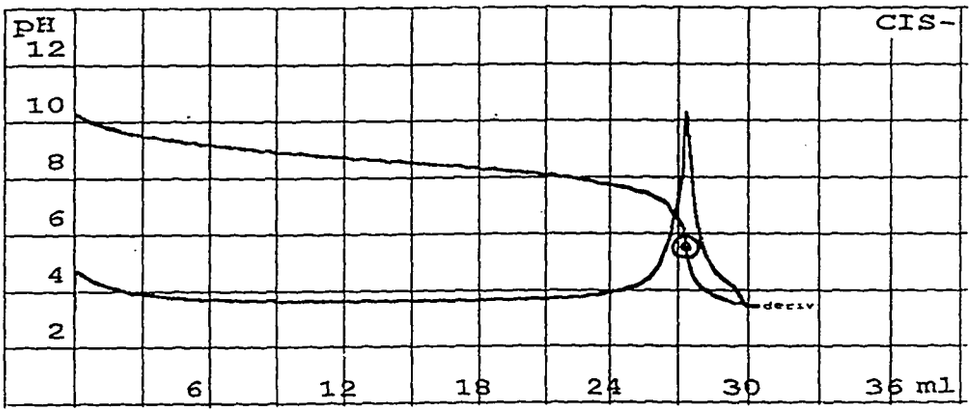


**Figure 1-6. Typical Acid/Base Potentiometric Titration Curve**

**Table 1-3. Measured pKa Values of *Cis* and *Trans* Isomers**

| Compound name | pKa Acid/Base Titration | pKa CZE Experiment |
|---|---|---|
| *cis*-Aminoindanol | 8.5 | 8.4 |
| *trans*-Aminoindanol | 7.7 | 7.7 |

The measured pKa values are summarized in Table 1-3. These results confirm the CZE separation of the *cis/trans* aminoindanol diastereomers is based on the pKa difference.

### 1-4C Spatial Arrangement and pKa

Why do the *cis*- and *trans*-aminoindanol diastereomers have different pKa values? Let us analyze the spatial orientation of the *cis*- and *trans*-aminoindanol diastereomers. The amine functional group, which is basic, and the alcohol functional group, which is weakly acidic, are attached to the same side of the ring in *cis*-aminoindanol, but attached to the opposite side of the ring in the *trans* isomer, as indicated in Figure 1-2. Because the -OH group is in the opposite direction to the $-NH_2$ group, the basicity of the amino group could be reduced through dipole-dipole cancellation, making the *trans* isomer less active. On the other hand, for the *cis*-aminoindanol, both -OH and $-NH_2$ groups are on the same side of the ring, both -OH and $-NH_2$ have nonbonding electron pairs, and it is possible for an intramolecular hydrogen bond to form between the two functional groups. The oxygen can be considered as an electron-donor, and the nitrogen is not as strong electronegative as the oxygen. Therefore, the hydrogen bond should increase the electron density on the nitrogen, making the positive $RNH_3^+$ ion more stable, and increasing the basicity of the whole structure [18-20 ].

Although steric hindrance of the -OH group might affect the solvation process to reduce the basicity of the amine, the net effect still results in a relatively higher basicity in the *cis*-aminoindanol than the *trans* isomer. Aminoindan was used to confirm that there is a steric hindrance effect between the -OH and $-NH_2$ groups in *cis*-aminoindanol. Aminoindan has a structure similar to that of aminoindanol, except absence of an -OH group, so there is no steric hindrance for the $-NH_2$ group. The pKa value of aminoindan is determined by titration to be 9.8, which is higher than that of both *cis*- and *trans*-aminoindanol diastereomers. This indicates a steric hindrance effect exists in the *cis*-aminoindanol.

The effect of the hydrodynamic radius of the *cis*- and *trans*-aminoindanol diastereomers on the separation should also be considered. Since the *cis*- and *trans*-aminoindanol diastereomers have different spatial orientations, it should be expected that they have different hydrodynamic radii. The *trans*-isomer should have a larger hydrodynamic radius than the *cis* [8]. As indicated in Figure 1-7. In the low pH buffer solution, both *cis*- and *trans*- aminoindanol diastereomers should be almost fully protonated, so that two isomers carry the same amount of charge. However, the *trans*-aminoindanol has relatively larger hydrodynamic radius because of its spatial orientation, and it should migrate more slowly than the *cis*-aminoindanol due to its smaller charge/radius ratio. The experimental results show that the *cis* isomer does migrate earlier than the *trans* isomer in the low pH range, which is consistent with the above explanation. The ratio of the

hydrodynamic size between the *cis*- and *trans*- aminoindanol diastereomers ($\mu_{e,cis}$/ $\mu_{e,trans} = r_{trans}/r_{Cis}$) is 1.011 based on their electropheroretic mobilities.

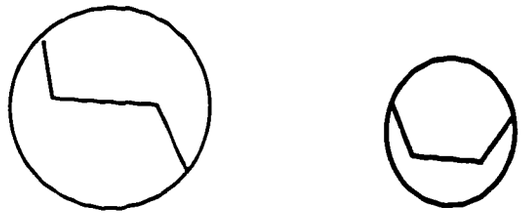

*Trans* isomer *Cis* isomer

**Figure 1-7. Size Difference of *Cis* and *Trans* Aminoindanol**

## 1-4D Molecular Modeling

In order to find out which configuration of aminoindanol is more stable, an energy minimization was applied using a Cerius$^2$ molecular simulations program in collaboration with Dr. Pascal Toma [9]. The program is built based upon the Open Force Field Modules (OFFM), which utilizes energy routines that form the basis of many property prediction methodologies. A simple analytical expression is used to describe each interaction, allowing rapid evaluation of the forces on all particles. From the force field, the optimum geometry or the dynamic motion can be evaluated. The Cerius$^2$ OFFM includes two important simulation modules, Minimizer and Dynamics. The minimizer module provides molecular mechanical methods for energy minimization of structures. Minimization results in structural configurations which correspond to the minimum energy of the system. During an energy minimization, the atomic coordinates and unit cell (if present) are adjusted in order to reduce the molecular energy. The dynamics module performs molecular dynamics on structures and analyzes the results. Unlike molecular mechanics, molecular dynamics enables us to investigate the behavior and properties of the system at non-zero temperatures. The effects of thermal motion or the applied external pressure on a system can be determined.

The energy expression is the heart of the OFFM method. The potential energy is described in the energy expression as the sum of various two-, three-, and four-body force terms. Valence terms describe the force between bonded atoms, and the nonbonded terms describe the through-space interaction of atoms that are not

necessarily connected. The potential energy is expressed as a sum of valence interactions and nonbonded interactions:

$$E_{total} = E_{valence} + E_{nonbonded} \quad [1\text{-}16]$$

The valence interactions consist of diagonal terms, namely bond stretching ($E_{bond}$), bond angle bending ($E_{angle}$), dihedral angle torsion ($E_{torsion}$), inversion ($E_{inversion}$), and Urey-Bradley interactions ($E_{UB}$) between atom pairs having 1-3 interactions (atoms bound to a common atom):

$$E_{vlance} = E_{bond} + E_{angle} + E_{torsion} + E_{inversion} + E_{UB} \quad [1\text{-}17]$$

The nonbonded interactions consist of van der Waals ($E_{vdw}$), electrostatic ($E_{coulomb}$), and hydrogen bond ($E_{hbond}$) terms:

$$E_{nonbond} = E_{vdw} + E_{coulomb} + E_{hbond} \quad [1\text{-}18]$$

For the investigation of energy differences between the *cis*- and *trans*-aminoindanol configurations, the lowest energy is sought using the dynamic and minimizer simulation modules. These heat each molecule and let it change conformations freely, and then cool it back down in a force field. The calculation process is iteratively calculated until a converge value is reached in which the lowest energy conformation has been determined.

Table 1-4 shows the calculated energy values for the *cis*- and *trans*-aminoindanol isomers. As expected, the molecular modeling calculation shows that the total configuration energy of the *trans* isomer is 0.8 Kcal/mol lower than that of the *cis* isomer, which indicates the *trans* configuration is more stable than the *cis* configuration. The calculated energy results indicate that the low configurational

energy of the *trans* isomer might be caused by dipole-dipole cancellation through the -OH and -$NH_2$ groups in the *trans* isomer structure, which supports the explanation made previously in Section 1-4C.

## 1-4E CZE Separation of Dorzolamide-HCl and Its Cis-distereomer

Dorzolamide-HCl is one of *cis/trans* pair of six-membered heterocyclic compounds that contain two chiral centers and exist in *cis* and *trans* diastereomeric forms. The structure is shown in Figure 1-8. For this compound, the methyl and amino groups are located on the two chiral centers of the heterocyclic ring, which results in four stereoisomers. It should be mentioned that the dorzolamide-HCl is the first topically active carbonic anhydrous inhibitor to be developed for the treatment of glaucoma and ocular hypertension. It is an effective and well-tolerated agent as monotherapy for patients who cannot tolerate ophthalmic beta-blockers, and for those who need add-on therapy to a beta blocker [10-11]. For the same reasons that apply to the *cis/trans* aminoindanol, it is expected that dorzolamide-HCl and its *cis*-distereomer might have different pKa values and they might be separated by CZE. Figure 1-9 shows electropherograms of the dorzolamide and its *cis*-distereomer separation at the different buffer pH values.

**Table 1-4. Configurational Energy for *Trans* and *Cis* Aminoindanol**

| | ***Trans* Isomer** | ***Cis* Isomer** |
|---|---|---|
| Valence Terms | Energy (kcal/mol) | Energy (kcal/mol) |
| Bonds | 1.53404 | 1.67029 |
| Angles | 5.27866 | 5.08526 |
| Torsions | 3.86495 | 4.49186 |
| Inversions | 0.01195 | 0.001838 |
| Urey-Bradley | 0.00000 | 0.00000 |
| Cross-Terms | 0.00000 | 0.00000 |
| Nonbonded Terms | | |
| van der Waals | 13.7691 | 14.4239 |
| Electrostatic | 1.56659 | 1.15146 |
| Hydrogen Bonds | 0.00000 | 0.00000 |
| Restraints | 0.00000 | 0.00000 |
| Total Energy | 26.1042 | 26.8758 |

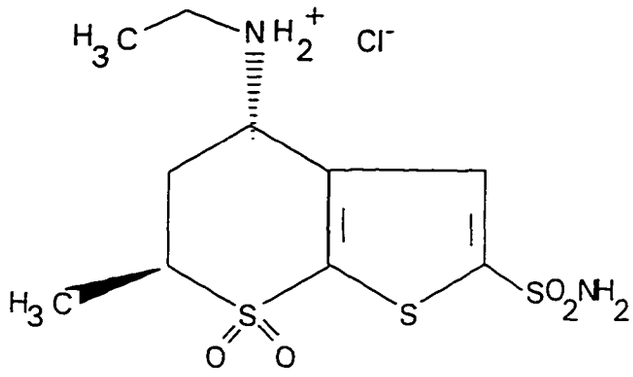


**Figure 1-8. The Structure of Dorzolamide-HCl**

**(4S,6S)-4-Ethylamino-5,6-dihydro-6-methyl-4H-thieno-[2,3-β] thiopyran-2-sulfonamide-7,7-dioxide.**

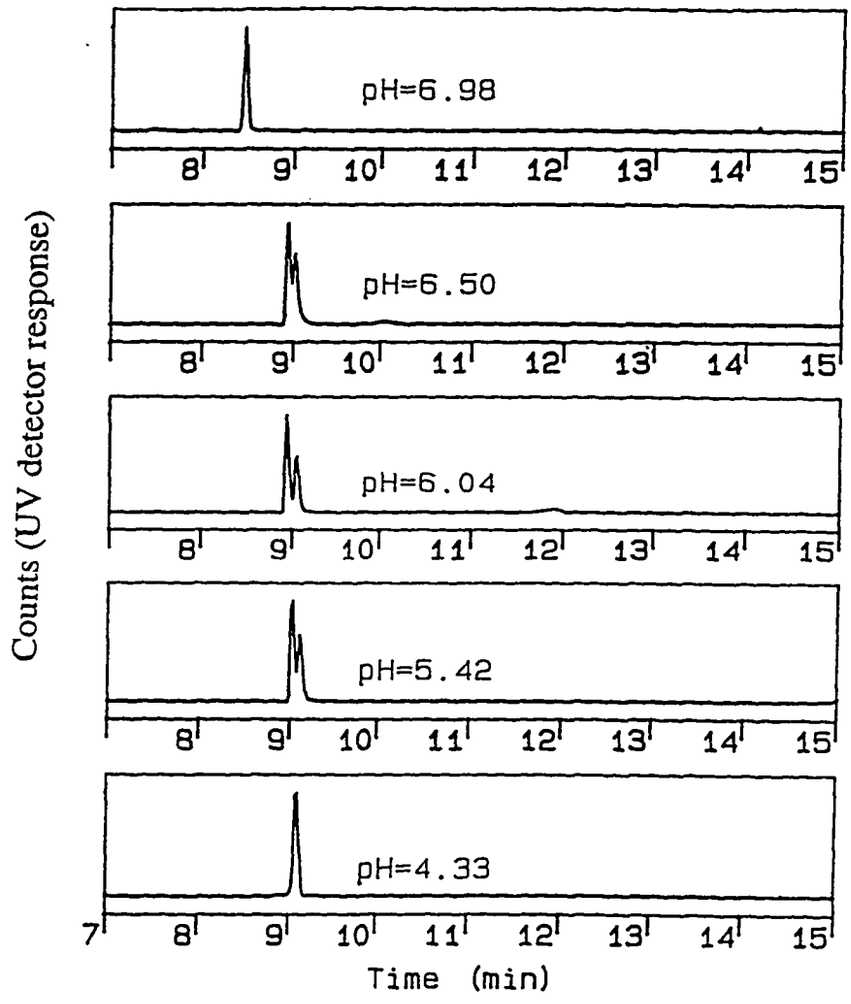


**Figure 1-9. Electropherograms of *Cis/Trans* Dorzolamide Isomers At Different Buffer pH**

Experimental conditions: buffer solution: BF 1-2; capillary: 75 μm I.D., 56 cm effective length (63 cm total length); temperature: 25°C; detection: 200 nm; applied voltage: 20 kV.

## 1-4F Separation of Diastereomers in Non-aqueous CZE

Non-aqueous CZE analysis is a relatively new and unexplored field. There are many applications using organic modifiers in CZE analysis, but only a few papers describe applications using 100% non-aqueous electrolytes [13-15].

Many organic weak acids or weak bases must be titrated in non-aqueous media because of the enhancement of their solubility and ionization. Since the separation by CZE depends on ionization constant differences, the investigation of the CZE separation mechanism in a non-aqueous medium should be very interesting.

Figure 1-10 shows the separation of *cis/trans* aminoindanol diastereomers in methanol containing 40 mM ammonium acetate. The apparent pH was adjusted with lithium hydroxide and perchloric acid to the value in the range from 2.2 to 10.1 (BF 1-3). Figure 1-11 shows that separation of *cis/trans* aminoindanol diastereomers in aqueous solution which also contains 40 mM ammonium acetate over a similar pH range (BF 1-2). The selectivity of *cis/trans* aminoindanol separation using non-aqueous CZE is much better than that in the aqueous buffer, especially in the pH range between 5 to 9, although the separation is faster in the latter case.

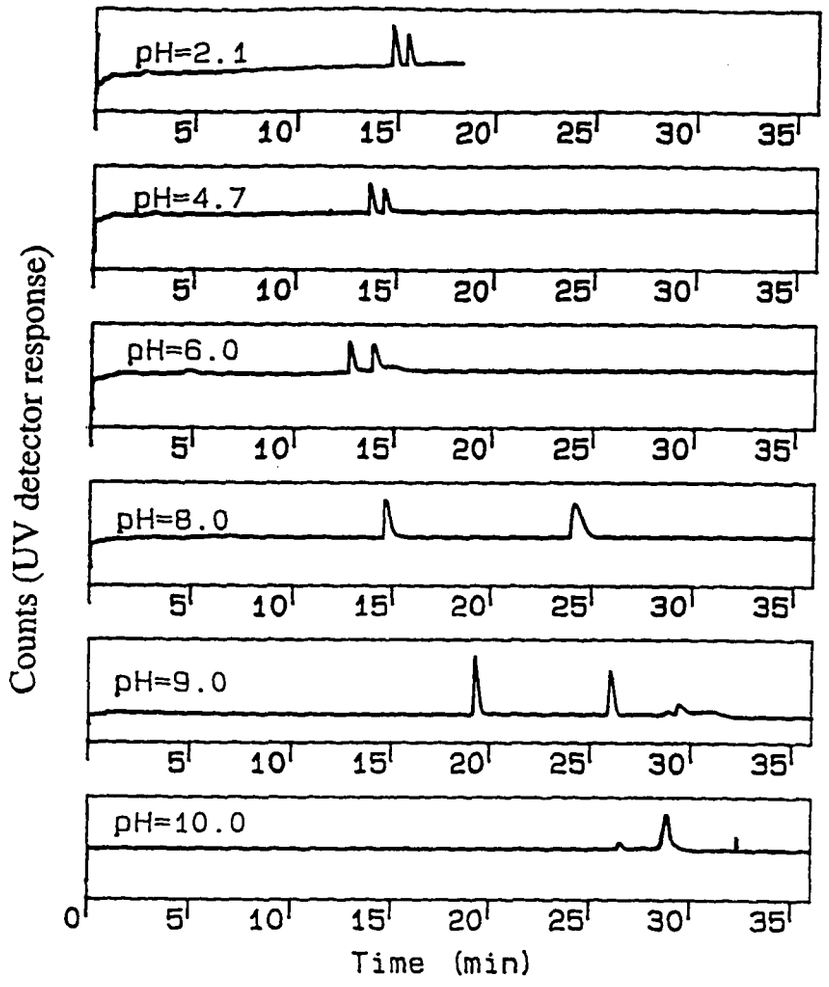


**Figure 1-10. Electropherograms of *Cis/Trans* Aminoindanol Using Non-aqueous CZE at Various pH**

Experimental conditions: buffer solution: BF 1-3; capillary: 50 μm I.D., 56 cm effective length (63 cm total length); temperature: 25°C; detection: 254 nm; applied voltage: 20 kV.

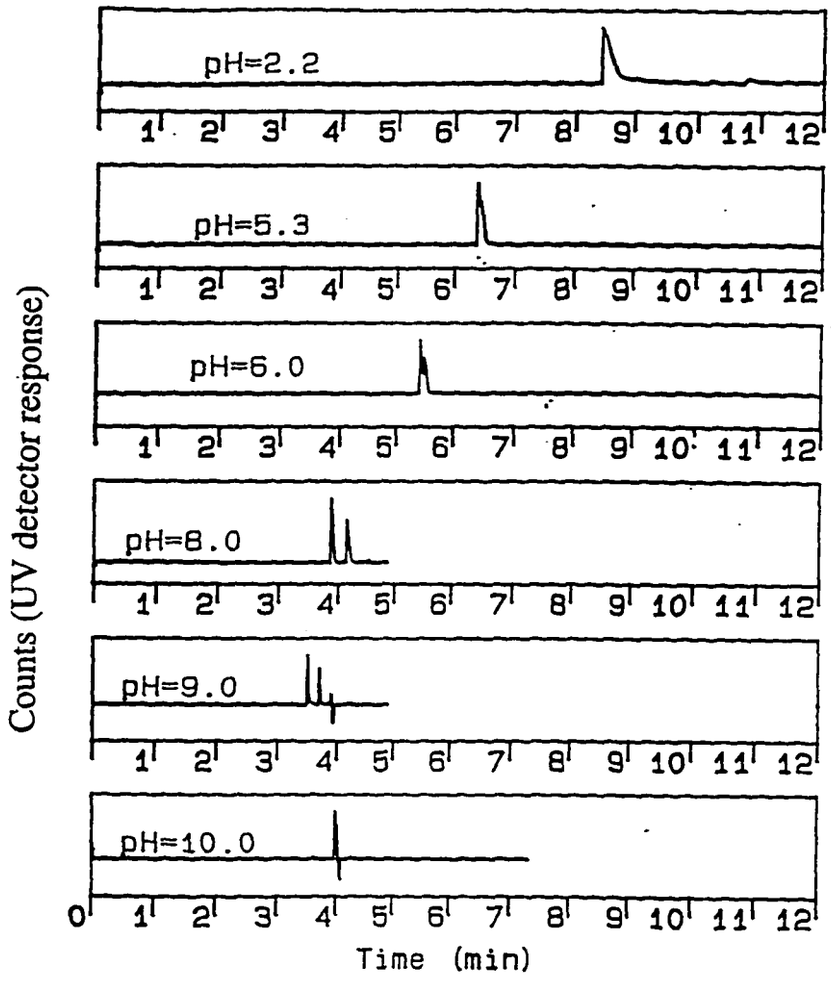


**Figure 1-11. Electropherograms of *Cis/Trans* Aminoindanol Using Aqueous CZE at Various pH**

Experimental conditions: buffer solution: BF 1-2; capillary: 50 μm I.D., 56 cm effective length (63 cm total length); temperature: 25°C; detection: 200 nm; applied voltage: 20 kV.

**Reduction of Joule Heat In Non-aqueous CZE System**

Why is the separation of *cis/trans* aminoindanol diastereomers in the non-aqueous electrolyte better than in the aqueous electrolyte? The effects of Joule heating and EOF are apparently most important.

Joule heating is one of the major limitations of the traditional electrophoretic techniques. Because Joule heating can cause nonuniform temperature gradients, density gradients in the electrophoresis medium can be induced, which in turn cause natural convection, resulting in zone broadening. Modern CZE in narrow-bore capillaries reduces the effects of Joule heating, but does not eliminate it completely. Ohm's law can be used to calculate the Joule heating generated by passage of electric current. The relationship between the electric field strength E and the electrophoresis current produced in the capillary is:

$$E = i / \kappa A \qquad [1\text{-}19]$$

where $\kappa$ is the specific conductance of the liquid electrolyte and A is the cross sectional area of the capillary. The heat produced, W, is given by:

$$W = E\, i / A \qquad [1\text{-}20]$$

substituting Equation 1-19 into Equation 1-20, we get the following equation:

$$W = i^2 / \kappa A^2 \qquad [1\text{-}21]$$

Although the heat is produced uniformly throughout the capillary, it can be dissipated only at the periphery. The maximum temperature is found at the center of the capillary.

To reduce the Joule heating, one can reduce the current in the capillary. In this study, experiments were conducted to determine the relationship between current and applied voltage in the aqueous and non-aqueous electrolytes. The experimental conditions were kept similar for the aqueous and non-aqueous electrolytes, except methanol was used in the non-aqueous electrolyte instead of the water used in the aqueous electrolyte. Figure 1-12 shows relationships between the current and applied voltage in both electrolytes. At the apparent pH 9.0 and the same concentration of ammonium acetate, the current produced in the non-aqueous electrolyte is only half of the current generated in the aqueous electrolyte. In fact, the current generated in methanol with 60 mM ammonium acetate is still lower than that in the aqueous electrolyte with 40 mM ammonium acetate.

The main reason for the reduction of the current in the non-aqueous solvent is the lower dielectric constant of the methanol (32.7 $C^2$/J-m) compared to water (80 $C^2$/J-m). As a result, the methanol electrolyte has lower conductivity than the water electrolyte, hence lower Joule heating and better resolution.

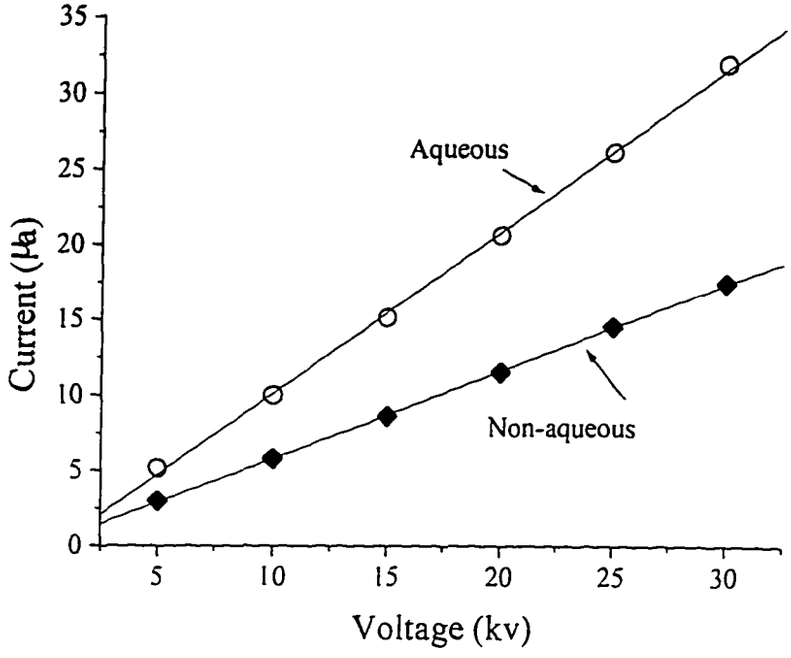


**Figure 1-12. Relationship Between Current and Applied Voltage In Aqueous and Non-aqueous CZE Systems**

The experimental conditions for the aqueous system and the non-aqueous system are the same as those in Figure 1-10 and in Figure 1-11, respectively.

**Reduction of EOF**

The measurement of the EOF is accomplished by determining the mobility of a neutral marker as shown in Figure 1-13 from aqueous and non-aqueous electrolytes with the same concentration of ammonium acetate over the apparent pH range from 2-11.5. It is clear that the EOF in the non-aqueous medium is consistently lower than that in the aqueous, especially at the higher pH values. The reason for the EOF change in the aqueous electrolyte was discussed in Section 1-4A. In the non-aqueous electrolyte, the EOF is also small at the low pH value, but it increases only slightly over the entire studied pH range. The electroosmotic mobility is related the zeta potential, $\xi$, dielectric constant, $\varepsilon$, and buffer viscosity, $\eta$, by equation [22]:

$$\mu_{eof} = \varepsilon \xi / \eta \qquad [1\text{-}22]$$

The viscosity ($\eta$) of the water (0.84 cp at 25°C) is higher than that of methanol (0.54 pc at 25°C), however, the dielectric constant ($\varepsilon$) of methanol (32.7 $C^2$/J-m) is much lower than that of water (80 $C^2$/J-m) [13]. Overall, the $\varepsilon/\eta$ of the methanol is 0.64 times less than water, which leads a lower EOF. The zeta potential essentially depends on the surface charge on the capillary wall. For the fused-silica capillary, the surface charges are mainly anionic silanol groups ($SiO^-$) and the $OH^-$ groups from water. It was reported the pKa value of the surface silanol groups is about 5.3 in the pure aqueous, but it is shifted toward higher values when the organic solvent is added [24-25]. Therefore, in the pure

methanol, the silanol charges on the capillary wall should be much less than those in the water. Furthermore, in the non-aqueous, methanol molecules can substitute water molecules which adsorb on the surface silanol groups, hence decreasing the adsorbed $OH^-$ groups. All these factors lead the zeta potential in methanol lower than in the aqueous, hence reduce the EOF in a non-aqueous. Since the mobilities of *cis/trans* aminoindanol diastereomers are the sum of the electrophoretic mobilities of the analytes and the EOF, which is in the same direction as electrophoresis, the lower the EOF is, the longer time the analytes migrate electrophorically and hence, the better the separation.

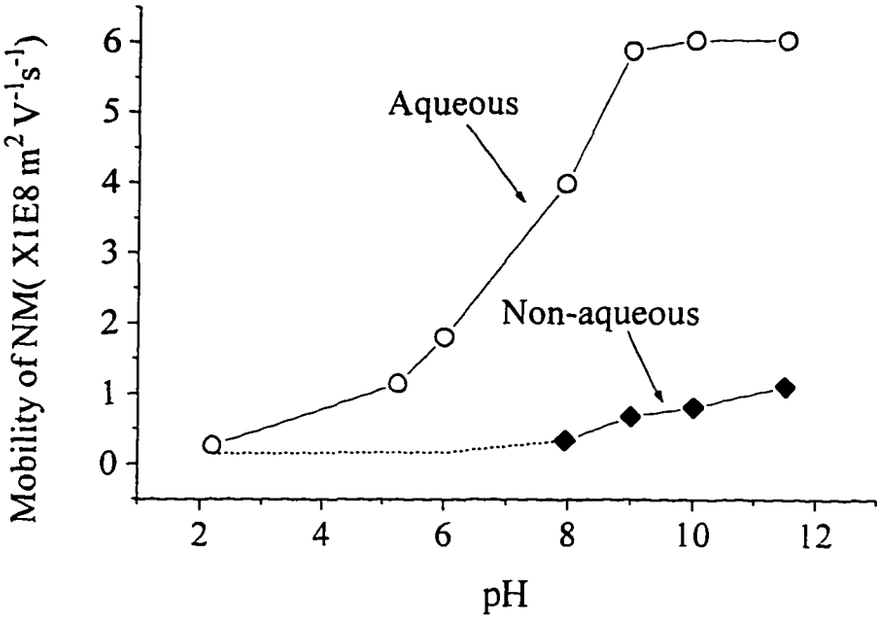


**Figure 1-13. Mobility Of Neutral Marker In Aqueous and Non-aqueous Electrolytes**

The experimental conditions for the aqueous system and the non-aqueous system are the same as those in Figure 1-10 and in Figure 1-11, respectively.

## 1-4G Separation of Positional Isomers by CZE

### Separation of Aminoquinoline Isomers

Aminoquinolines are used as examples of cationic positional isomers. A representative structure is shown in Figure 1-14. The amino group can be located on different positions in the quinoline ring to produce a series of positional isomers. The amino group can be protonated at low pH values and the aminoquinolinium carries a positive charge. Table 1-5 lists the pKa values of four aminoquinolines [12].

As discussed earlier, for two isomers with different pKa values, the maximum difference of the effective mobility in CZE will be achieved at the electrolyte pH between their two pKa values. Figure 1-15 shows a successful separation of four aminoquinoline isomers at pH 3.3. In the electropherogram, the elution order of isomers corresponds to the order of pKa values. The larger the pKa, the later it elutes. These experimental results demonstrate that positional isomers can be separated by CZE as long as their pKa values differ.

**Table 1-5. pKa Values of Aminoquinolines**

| Aminoquinoline | pKa |
|---|---|
| 3-Aminoquinoline | 4.95 |
| 5-Aminoquinoline | 5.46 |
| 6-Aminoquinoline | 5.63 |
| 8-Aminoquinoline | 3.99 |

**Table 1-6. pKa Values of Difluorophenylacetic Acids**

| Difluorophenylacetic acid | pKa |
|---|---|
| 2,4-Difluorophenylacetic acid | 4.94 |
| 2,5-Difluorophenylacetic acid | 4.78 |
| 2,6-Difluorophenylacetic acid | 4.69 |
| 3,4-Difluorophenylacetic acid | 5.17 |
| 3,5-Difluorophenylacetic acid | 4.56 |

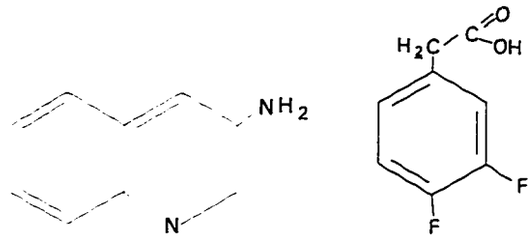


a) b)

3-Aminoquinoline 3,4-Difluorophenylacetic acid

**Figure 1-14 Typical Structures of Some Positional Isomers**

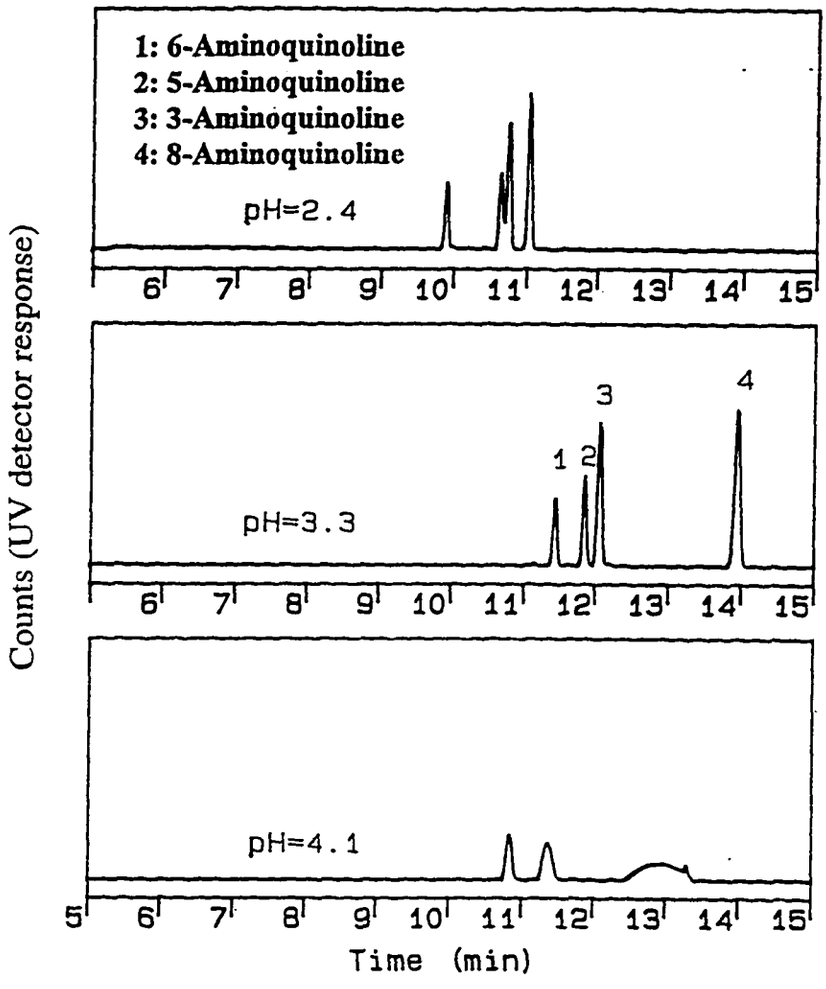


**Figure 1-15. CZE Separation of Aminoquinoline Isomers**

Experimental conditions: buffer solution: BF 1-1; capillary: 50 μm I.D., 56 cm effective length (63 cm total length); temperature: 25°C; detection: 200 nm; applied voltage: 19 kV.

**Separation of Difluorophenylacetic Acid Isomers**

Difluorophenylacetic acids are used as examples of anionic positional isomers. A representative structure is shown in Figure 1-14(b). The two F atoms can attach to different positions on the benzyl ring to generate a series positional isomers. The pKa values of five isomers were determined using the acid/base potentiometric titration with 0.01 NaOH as the titrant, as described in Sections 1-3A and 1-4B. The results, listed in Table 1-6, show that the different positional difluorophenylacetic acid isomers do have different pKa values, but differences are so small that there will be difficulty to achieve the CZE separation.

It is often difficult to separate anionic analytes using silica capillaries because of the effect of EOF on the separation. There are two common approaches taken to separate anionic compounds. One is to reverse the polarity of the applied voltage and add cationic surfactants in the electrolyte to reverse the EOF by forming a surfactant double layer on the capillary wall, and in this way, the direction of the EOF is the same as that of the anionic analytes. The second is to use a high pH electrolyte to generate strong EOF which can push anionic analytes out of the capillary, even though the electrophoretic direction of anionic analytes is opposite that of the EOF.

In this study, a new approach was conducted. In order to eliminate the EOF effect, a polyvinyl alcohol-coated (PVA) capillary was used. The PVA shields the

silanol groups on the surface of the fused silica, effectively eliminating the EOF[6]. Using reversed polarity of the applied voltage, anionic analytes migrate electrophoretically to the anode without the interference of the EOF. The larger the analyte ratio of charge/size, the faster it migrates. Electrolyte pH can be optimized to achieve the best separation of the isomers. As seen from Figure 1-16, the five difluoro-phenylacetic acid isomers were successfully separated even though the maximum difference of their pKa is only 0.61 and the minimum difference is only 0.09. 3,5-difluorophenylacetic acid, which has the lowest pKa value, elutes fastest and 3,4-difluorophenylacetic acid, which has the highest pKa value, elutes slowest. The results indicate that the pKa dominates the elution order and the size is not the important effect..

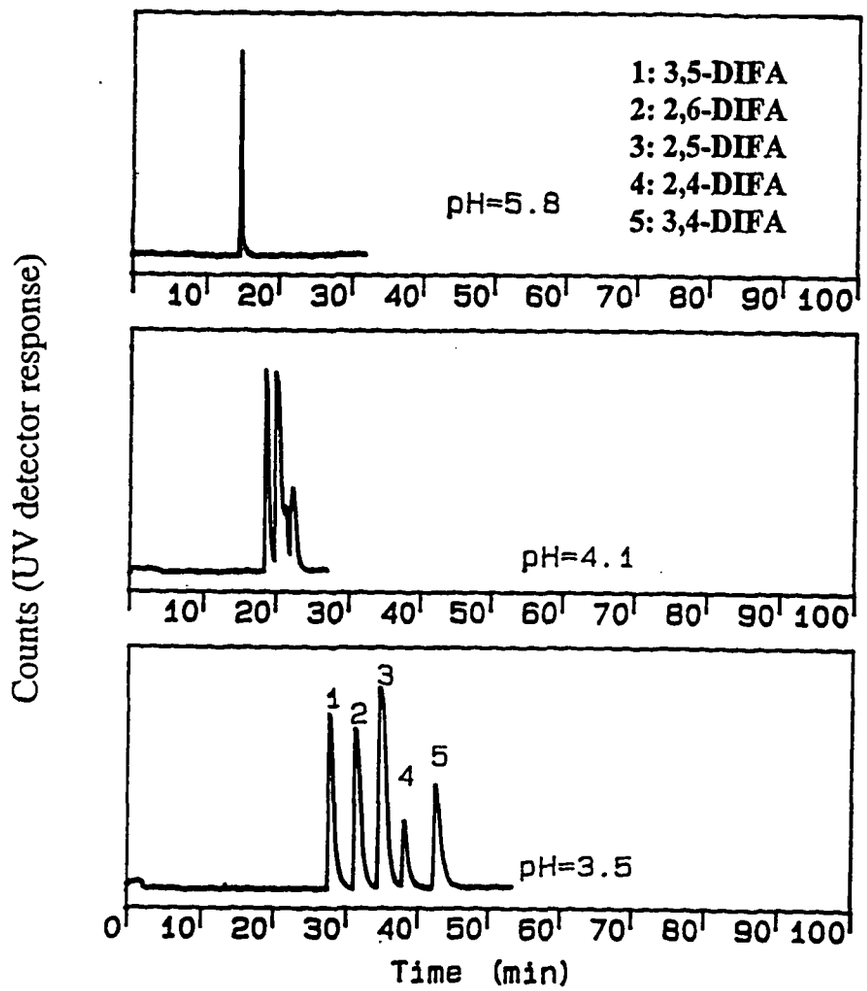


**Figure 1-16 CZE Separation of Difluorophenylacetic Acid Isomers**

Experimental conditions: buffer solution: BF 1-1; capillary: PVA coating capillary with 50 μm I.D., 56 cm effective length (63 cm total length); temperature: 25°C; detection: 200 nm; applied voltage: reversed polarity at 20 kV.

## 1-5 Conclusions

1) The CZE diastereomeric separations were successfully achieved for several tested compounds based on the difference of their pKa.

2) The pKa difference of *cis*- and *trans*-aminoindanol diastereomers has been discovered and confirmed using both CZE and acid/base titration. The *cis*-aminoindanol has a higher pKa than the *trans*-aminoindanol.

3) The reasons for the different pKa values of *cis*- and *trans*- aminoindanol diastereomers is interpreted in terms of their spatial structural orientations. For the *trans* isomer, because the -OH group is in the opposite direction from the $-NH_2$ group, the basicity of amino group is reduced through dipole-dipole cancellation.

4) The molecular modeling results indicate the *trans* isomer has a lower configurational energy than the *trans* isomer, which might be caused by dipole-dipole cancellation through the -OH group and $-NH_2$ group in the *trans* isomer. The configurational energy data are consistent with the above interpretation.

5) The principle of CZE separation based upon different pKa values was extensively explored for the separation of positional isomers which are

either cationic positional isomers or anionic positional isomers. Four aminoquinoline positional isomers were separated by CZE at the optimization of the electrolyte pH. Five positional isomers of difluorophenylacetic acid were successfully separated using a capillary coated with PVA.

6) The separation of *cis*- and *trans*-aminoindanol diastereomer using non-aqueous CZE was also studied. The selectivity of the *cis*- and *trans*-aminoindanol diastereomers in a non-aqueous buffer was much better than that in aqueous buffer. This phenomenon was interpreted in terms of a) the higher conductivity of the aqueous electrolyte, which results a higher current and higher Joule heating, and b) the lower EOF in the non-aqueous electrolyte due to the lower $\varepsilon/\eta$ and the lower $\xi$ of the non-aqueous medium.

# CHAPTER TWO

## Study of Separation Mechanism of Aminoindanol Enantiomers Using CDs

## 2-1 Introduction

Generally, enantiomers have identical internal energies, and therefore they have the same physicochemical properties. In order to separate enantiomers, chiral environments must be created. In CZE chiral analysis, adding a chiral selector to the electrolyte buffer is the most common approach. The separation of enantiomers results from the formation of transient diastereomeric complexes, which are resolvable due to their different formation constants and hence different electrophoretic mobilities. CDs (or CD derivatives) [1-5], proteins [6-7], crown ethers [8-9], and polysaccharides [10] can be used in CZE as chiral selectors.

Cyclodextrins (CDs) are the most common chiral selectors because of their commercial availability at relatively low cost, and wide selectivity for many compounds. CDs are cyclic oligosaccharides composed of either six, seven, or eight glucose units, which are named $\alpha$-, $\beta$-, and $\gamma$-CDs, respectively. The schematic structure of a CD is shown in Figure 2-1, and some properties of CDs are listed in Table 2-1 [11-12]. Cyclic oligosaccharides in CDs are built of *D*-(+)-glucopyranose units, which are bonded together via $\alpha$-(1,4)-glycosidic linkages. Each glucose unit has five centers of a defined chirality, that allow CDs to be used to discriminate chiral compounds in GC, HPLC and CE. The top of the cone has a larger diameter with a rim that is lined with secondary hydroxyl groups bonded to carbon atoms at positions 2 and 3 in each glucose unit. The smaller opening of

the cone has a line of more polar primary hydroxyl groups joined to the glucose ring at the C-6 position. The central cone of the CD is relatively hydrophobic because of the presence of two rings of C-H bonds and the glycosidic oxygen atoms that form the inner wall of the molecule. The hydrophilic groups that line both openings allow CDs to be dissolved in water. Based on the specific characteristics of the CD configuration, a CD might look like a hollow cone with a cavity, the size of the which depends on the number of cyclicoligosaccharides [17-18,33]. However, recent studies show that a CD can be shaped like a twisted basket, which indicates the CD cone structure may be more flexible [33]. CDs are stable molecules that are unaffected by large pH changes or light. As chiral selectors, the most important property of CDs is their ability to form highly selective molecular inclusion complexes with a variety of chiral compounds [31].

Enantiomeric resolution by CZE with CDs as the chiral selectors was first introduced by Fanali's group [1]. Wren and Rowe [2,13-15] described a separation model and suggested that there is an optimum concentration of CD, which gives a maximum enantioselectivity. Goodall and co-workers [16] modified the model and successfully applied this model to the enantiomeric separation of tioconazole. Some thermodynamic parameters for the binding of tioconazole enantiomers to cyclodextrins were reported based on the experiments. Rawjee, Vigh and co-workers [3,27-30] described a more complex model of CD-CZE and demonstrated that the resolution of the enantiomer separation is not only

a function of the chiral selector concentration, but also of the pH of the CZE buffer [3,27-30].

During 1976 to 1978, Bergeron and co-workers [12,17-18] investigated the thermodynamics of cyclodextrin-analyte complexation. They suggested that the binding energy of cyclodextrin-analyte inclusion complexes is the result of van der Waals-London dispersion forces, releasing of cyclodextrin strain energy, and releasing of enthalpy-rich cavity water. The inclusion process should be associated with a favorable enthalpy change.

In this study, the separation model described by Wren and Rowe [2,13-15] was used to study the separation mechanism of aminoindanol enantiomers. Thermodynamic studies were established based upon the dynamic interaction for aminoindanol and CDs. The effects of temperature, buffer pH, concentration of urea additive, size of chiral selectors, and presence of a hydroxyl group on the analyte were discussed in terms of the thermodynamic parameters. HPLC and molecular modeling were also conducted to support the CZE results to explain the enantiomeric separation mechanism.

Aminoindanol has two chiral centers, resulting in two pairs of enantiomers named *cis*(-) and *cis*(+), and *trans*(-) and *trans*(+) as discussed in Chapter One (see Figure 1-2). It should be noted that aminoindanol contains a hydrophobic

aromatic ring, hydrophilic amino, and alcohol functional groups around the chiral centers. CZE experiments were designed to separate two pairs of enantiomers: *cis*(-) and *cis*(+), *trans*(-) and *trans*(+) using CDs as chiral separation selectors. Under the optimized conditions, the four enantiomers can be successfully separated. The separation mechanism is discussed in detail.

## 2-2 Study Design

The study of CZE enantiomeric separation using CDs was designed as follows:

1) Establish a "host:guest" dynamic separation model of interaction between enantiomers and chiral selectors.

2) Set up series of experiments based upon the model to determine thermodynamic parameters, the binding constant (K), gibbs free energy (G), enthalpy change (H), and entropy change (S) for "host-guest" complexation of aminoindanol with chiral selectors.

3) Study the enantiomeric separation mechanism through interpretation of the thermodynamic parameters.

4) Investigate the size effects of the chiral selectors on the enantiomeric separation by using $\alpha$, $\beta$, and $\gamma$ CDs.

5) Study the pH effect and the urea additive effect on the enantiomeric separation .

6) Use HPLC and molecular modeling to support the established "host-guest" model.

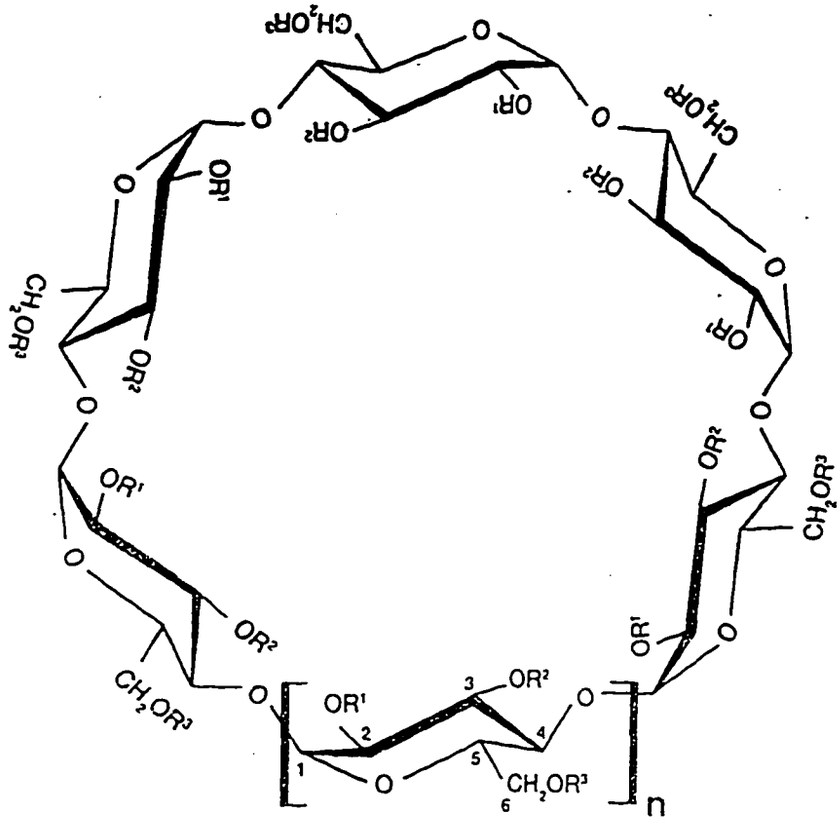

**Figure 2-1. Schematic Structure of Cyclodextrin** [32]

$R^1$, $R^2$, and $R^3$ are H in the study.

**Table 2-1. Physico-Chemical Properties and Structure of CDs** [11-12]

| **Parameter** | **Type of CD** | | |
|---|---|---|---|
| | α- | β- | γ- |
| Number of glucose units | 6 | 7 | 8 |
| Number of $H_2O$ in the cavity | 6 | 11 | 17 |
| Molecular mass | 972 | 1135 | 1297 |
| Inner diameter of cavity (Å) | 5.7 | 7.8 | 9.5 |
| Outer diameter of cavity (Å) | 13.7 | 15.3 | 16.9 |
| Cavity volume ($Å^3$) | 174 | 262 | 427 |
| Solubility in water ($25^0C$) (%,w/v) | 14.5 | 1.8 | 23.2 |

## 2-3 Experimental

### 2-3A Operating Conditions

Unless otherwise specified, the CZE experiments were performed on an $HP^{3D}$ CE instrument (Hewlett Packard) with a 33-cm effective length HP fused-silica capillary (40-cm total length), 50-μm I.D. with a preburned window. Hydrodynamic pressure sampling injection was applied. The injection time was 2 seconds. The injection pressure was 50 mbar. The applied voltage was 16 kV. A Diode-array UV detector was employed at 200 nm wavelength. The temperature was controlled by the instrument vs. an internal thermostat device. Data analysis and collection were accomplished using a PE NELSON ACCESS CHROM system.

Unless otherwise specified, the high performance liquid chromatography (HPLC) experiments were performed on a Shimadzu HPLC instrument (Model 10-A) with a C-4 column (YMC®, 15cm x 4.1mm I.D. x 5μm). The stationary phase of the C-4 column is bonded with butyl chain polymer. The isocratic mobile phases were the same as the buffer solutions used in the CZE experiments. Unless otherwise specified, the flow rate was set at 0.6 mL/min. Twenty minute re-equilibrium time was required for the system between each injection. A UV detector was employed at 200 nm. The column temperature was controlled at

ambient. The signals were also collected using the NELSON ACCESS CHROM data system (Perkin Elmer Corp, Cupertino, CA).

Two individual *cis*-enantiomers of aminoindanol, (1S,2R)-*cis*-1-aminoindan-2-ol [*cis*(-)] and (1R,2S)-*cis*-1-aminoindan-2-ol [*cis*(+)], and a racemic mixture of *trans*-enantiomers, (1S,2S)-*trans*-1-aminoindan-2-ol [*trans*(-)] and (1R,2R)-*trans*-aminoindan-2-ol [*trans*(+)], were made and purified by Merck Research Laboratories (Rahway, NJ). 1-Aminoindan and mesityl oxide were purchased from Aldrich Chemical Co (Milwauke, WI) and used without further purification. Phosphoric acid and 50% sodium hydroxide solution were obtained from Fisher Scientific (Springfield, NJ). α-CD, β-CD, and γ-CD were purchased from Sigma (St. Louis, MO). Tris (hydroxymethyl) aminomethane (tris) was obtained from Bio-Rad (Richmond, CA). Nylon syringeless filters were purchased from Whatman (Springfield, NJ). Water was purified with a Milli-Q system (Millipore Corp, Milford, MA).

### 2-3B Test Solutions

Several electrolyte solutions were prepared as follows:

Tris background electrolyte (tris-BGE): tris-BGE was prepared by dissolving 4.8 grams of tris in 1-L deionized (D.I.) water and adjusted pH to 2.2 using phosphoric acid. The tris concentration was 40 mM.

Tris-urea background electrolyte (tris-urea-BGE): tris-urea-BGE was prepared by dissolving 2.4 g of tris and 250 g urea in 500 mL D.I. water and adjusted to pH 4.4 using phosphoric acid. The tris concentration was 40 mM, and the urea concentration was 8 mM.

Buffer solutions 2-1 (BF 2-1): BF 2-1 were made by dissolving various amounts of α-CD in tris-BGE. The concentrations of α-CD were in the range from 0 to 64 mM.

Buffer solutions 2-2 (BF 2-2): BF 2-2 were prepared by dissolving various amounts of α-CD in the tris-urea BGE. The concentrations of α-CD were in the range from 0 to 92 mM.

Buffer solutions 2-3 (BF 2-3): BF 2-3 were prepared by dissolving various amounts of β-CD in tris-urea-BGE. The concentrations of β-CD were in the range from 0 to 84 mM.

Buffer solutions 2-4 (BF 2-4): BF 2-4 were prepared by dissolving 6.8 g α-CD in 200 mL tris-BGE. The concentration of α-CD was 35 mM. The solutions were subdivided into several 20 ml glass vials, and each solution was adjusted to the designated pH with 50% NaOH solution. The pH ranged from 2.2 to 9.2.

The pH of all solutions were apparent pH

Several sample solutions were prepared as follows:

Sample solution 2-1 (SP 2-1): SP 2-1 was prepared by dissolving 15 mg *cis*(-) or *cis*(+) aminoindanol in 100 mL D.I. water, then diluted 10 times with D.I. water. The concentration of each enantiomers was 0.1mM.

Sample solution 2-2 (SP 2-2): SP 2-2 was prepared by dissolving 15 mg *trans* (+/-)-aminoindanol racemic mixture in 50 mL D.I. water, then diluted 10 times with D.I. water. The concentration of each enantiomers was 0.1mM.

Sample solution 2-3 (SP 2-3): SP 2-3 was prepared by dissolving 30 mg aminoindan racemic mixture in 100 mL D.I. water, then diluted 10 times with D.I. water. The concentration of each enantiomers was 0.1mM.

Sample solution 2-4 (SP 2-4): SP 2-4 was prepared by mixing 5 mL SP 2-1 and 5 mL SP 2-2. The concentration of *cis* (-) or *cis* (+) or *trans*(+/-) was 0.05 mM.

Neutral marker solution (NM): NM was prepared by dissolving 30 mg mesityl oxide in 100 mL 99.99% pure methanol.

### 2-3C Procedure

The procedures of the capillary and the sample solution treatment are described in Section 1-3D, Chapter One.

## 2-4 Establishment of Separation Model and Discussion of Theory

### 2-4A "Host-Guest" Complex Model

As mentioned in the introduction, addition of cyclodextrin (host) to the electrolyte buffer can produce a chiral separation in CZE if enantiomers (guest) can complex with chiral selectors with different formation constants. The process is schematically illustrated in Figure 2-2. The neutral cyclodextrin added to the buffer migrates at the velocity of the electroosmotic flow. The migration of the analyte (R or S enantiomer) is controlled by the degree of its association with the cyclodextrin.

The binding constant calculation for chiral separations in the CZE was first introduced by Wren based upon the "host:guest" complex model [2,13-15]. The model assumes that the enantiomers and the chiral selector form 1:1 enantiomer-chiral selector (host-guest) complexes, and the complex formation is a much faster equilibrium process than the CZE separation process. If the complexes have different complexation binding constants, differences of the electrophoretic mobility of two complexes will result.

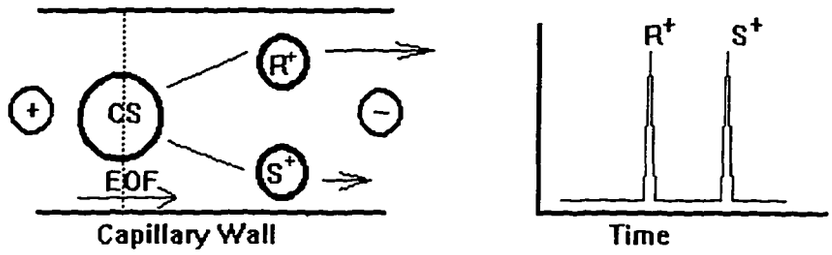


**Figure 2-2. Schematic Diagram of Chiral Separation by CZE**

CS is the chiral selector as a host; $R^+$ is *R*-enantiomer and $S^+$ is *S*-enantiomer as a guest.

Aminoindanol enantiomers are positively charged ($RNH_3^+$) compounds under the conditions used. The formation of the host-guest complex between the CD and the enantiomer can be expressed as:

$$CD + RNH_3^+ \rightleftharpoons CD{:}RNH_3^+ \qquad [2\text{-}1]$$

The equilibrium constant, K, is

$$K = \frac{[CD{:}RNH_3^+]}{[RNH_3^+][CD]} \qquad [2\text{-}2]$$

$$K[CD] = \frac{[CD{:}RNH_3^+]}{[RNH_3^+]} \qquad [2\text{-}3]$$

The $RNH_3^+$ moves in the capillary with an electrophoretic mobility, $\mu_0$. A $[CD{:}RNH_3^+]$ complex also carries a positive charge and has an electrophoretic mobility, $\mu_e$, which is smaller than $\mu_0$ because of the larger size of the complex.

Since the net mobilities of analytes reflect the fraction of time when $RNH_3^+$ is not bonded with the CD, and the fraction of time when $RNH_3^+$ is bound with CD (the "host:guest" complex), fractional times should be proportional to the equilibrium concentrations of the $CD{:}RNH_3^+$ complex and the free ion $RNH_3^+$ expressed as follows:

$$\frac{\mu_0 - \mu_e}{\mu_e - \mu_\infty} = \frac{[CD:RNH_3]}{[RNH_3^+]} \qquad [2\text{-}4]$$

Combining Equation 2-4 with Equation 2-3, the following equation is obtained [16]:

$$KC = \left(\frac{\mu_0 - \mu_e}{\mu_e - \mu_\infty}\right) \qquad [2\text{-}5]$$

where C is used instead of [CD], $\mu_0$ and $\mu_\infty$ are mobilities at C=0 and C$\rightarrow\infty$, respectively, and $\mu_e$ is the mobility at the concentration of free chiral selector.

Rearranging Equation 2-5, $\mu_e$ can be expressed as:

$$\mu_e = \left(\frac{\mu_0 - \mu_\infty}{1 + KC}\right) + \mu_\infty \qquad [2\text{-}6]$$

For a pair of enantiomers [eg, *cis*(-) and *cis*(+)], the binding equilibrium can be described as

$$CD + cis(-) = CD{:}cis(-) \qquad K_1 \qquad [2\text{-}7]$$

$$CD + cis(+) = CD{:}cis(+) \qquad K_2 \qquad [2\text{-}8]$$

$$\mu_{e1} = \left(\frac{\mu_0 - \mu_\infty}{1 + K_1 C}\right) + \mu_\infty \qquad [2\text{-}9]$$

$$\mu_{e2} = \left(\frac{\mu_0 - \mu_\infty}{1 + K_2 C}\right) + \mu_\infty \qquad [2\text{-}10]$$

The experimental set of data of mobility as a function of chiral selector concentrations can be fitted to Equations 2-9 and 2-10 to give an optimum value for binding constants of K.

*Cis*(-) and *cis*(+) have an identical values of $\mu_0$ because they have the same physical properties. The value of $\mu_\infty$ is considered effectively the same for *cis*(-)

and *cis*(+) [16]. Combination of Equations 2-9 and 2-10 with μ and K assigned subscripts 1 and 2 for *cis*(-) and *cis*(+) gives the difference in mobilities [2,13-16]:

$$\Delta\mu_e = \frac{C(\mu_0 - \mu_\infty)(K_2 - K_1)}{1 + C(K_2 + K_1) + K_2 K_1 C^2} \qquad [2\text{-}11]$$

The optimum concentration of CD ($C_{opt}$) at the maximum of $\Delta\mu_e$ is found by differentiating and setting $d\Delta\mu/d(CD) = 0$. $C_{opt}$ is:

$$C_{opt} = \frac{1}{\sqrt{K_1 K_2}} \qquad [2\text{-}12]$$

Based upon the above equations, the determination of mobilities of enantiomers with and without CD in the buffer solution allow us to calculate the binding constants directly.

It should be mentioned for the "host:guest" dynamic model to be used, several criteria must be satisfied:

a) The rate of the complex equilibration must be much faster than the rate of the separation process. The complexation can then be treated as a thermodynamically equilibrium process.

b) There must be significant proportions of both the selector (free CD) and [selector:analyte] complex in the system.

c) The mobilities of the free analyte and the complex must be different.

d) The equilibrium constants ($K_1$ and $K_2$) for selector-analyte binding or partition must differ for the two enantiomers.

It was found in this study that all these criteria are satisfied. The following sections gives the details.

## 2-4B Determination of Thermodynamic Parameters

Based on thermodynamic theory [16], the binding constants for the formation of complexes between the enantiomers and the chiral selectors are related to the Gibbs free energy change $\Delta G$ given by

$$\Delta G = -RT\ln K \qquad [2\text{-}13]$$

where T is the absolute temperature and R is the gas constant. The molar Gibbs free energy change $\Delta G$ is related to the enthalpy $\Delta H$ and entropy $\Delta S$ changes of complexation by:

$$\Delta G = \Delta H - T(\Delta S). \qquad [2\text{-}14]$$

Combinating those two equations gives:

$$\ln K = -\frac{\Delta H}{RT} + \frac{\Delta S}{R} \qquad [2\text{-}15]$$

From the plot of lnK versus 1/T, which is called a van't Hoff plot, $\Delta H$ and $\Delta S$ can be determined from the slope and the intercept, respectively. The thermodynamic parameters can be used to explain whether the complex model is reasonable or not.

## 2-5 Results and Discussions

### 2-5A Data Handling and Computer Calculation

In processing the data obtained from the CZE experiments for the determination of binding constants and other parameters, there are several important things that need to be considered. First of all, the migration time (t) is measured directly from the electropherograms, but the effective mobility ($\mu_e$) is calculated from Equation 2-16 [20,35], where $t_{EOF}$ is the migration time of mesityl oxide, *l* is the effective length of the capillary, L is the total length of the capillary and the V is the applied voltage.

$$\mu = \frac{l \times L}{V \times \left(\frac{1}{t} - \frac{1}{t_{EOF}}\right)} \qquad [2\text{-}16]$$

Second, since the viscosity ($\eta$) of buffer solutions containing CDs is a function of the concentration of the CDs and the mobility ($\mu$) is inversely proportional to the viscosity, it is necessary to correct the effect of the concentration of CD on the mobility. Since the current in the capillary is related to the viscosity, a correction for the effect of viscosity variation on the mobility can be accomplished by measuring the current:

$$\eta/\eta_0 = I_0/I \qquad [2\text{-}17]$$

where $\eta_0$ and $I_0$ are the viscosity of the buffer solution and the measured current with no CD in the buffer solution, respectively.

Third, the free CD concentration should be used for the calculation of binding constants, which equals to the total CD in the electrolyte minus the CD bound to the analyte. In this study, since the concentration of CD was much larger than that of analyte and the binding constants were not extremely large, the error is negligible.

Fourth, Joule heating, which is dependent on the power dissipation per unit length of the capillary, raises with the temperature of the capillary. A temperature increase will affect the thermodynamic equilibrium. This temperature increase should be corrected by calibrating the CE instrument. However, in this study, the currents generated were very small (~25-30 μA). the CE instrument had a good thermostatic control via a forced air cooling system, and the temperature of the capillary was accurately controlled within ±0.1°C. The results of the power dissipation calibration curve shows a linearity R square is greater than 0.9999. which indicates that any deviation in the mobility caused by a temperature increase is negligible.

Fifth, since the relationship between binding constants for the complex model and the effective mobility is not a simple linear relationship, a computer program, SAS non-linear least squares regression, written in $c^+$ computer language, was designed to calculate binding constants [19]. The program is shown in

Appendix I. The binding curves given in Figure 2-3 were fitted to $K_1$, $K_2$ and $\mu_\infty$ as variables at different temperatures according to the theory described above.

Sixth, thermodynamic parameters can be measured from the binding constants determination over the temperature range from 15 $^0$C to 35 $^0$C. van't Hoff plots can be generated by plotting 1/T vs. ln K. Figure 2-4 shows a typical van't Hoff plot for the binding of *cis*(+/-) aminoindanol enantiomers to the α-CD in BF 2-2. The thermodynamic parameters of the complex formation process, ΔH°, and ΔS°, can be calculated from the slopes and intercepts of the van't Hoff plots.

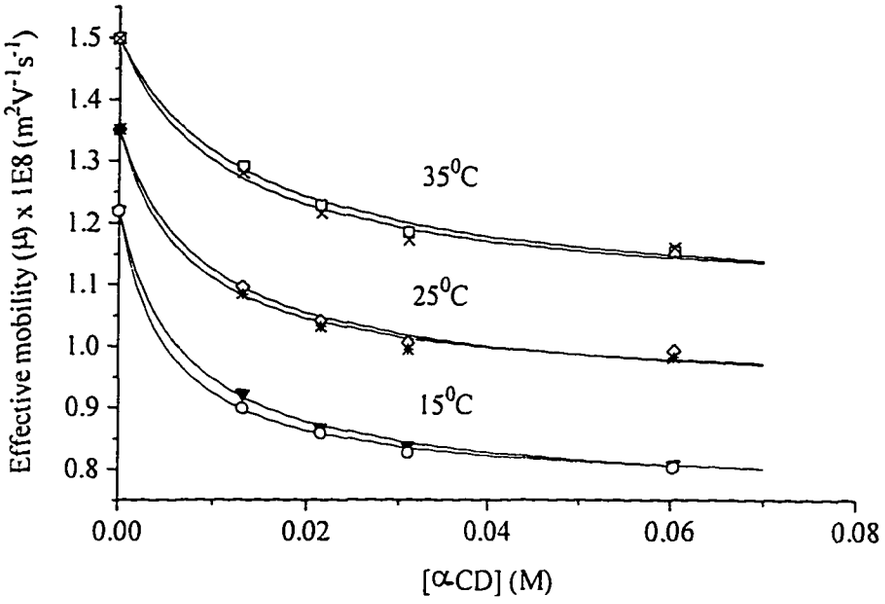


**Figure 2-3. Electrophoretic Mobilities of *Cis*(+/-) Enantiomers as Function of [α-CD] in BF 2-2 at Different Temperatures**

Experimental conditions: buffer: BF 2-2; capillary: 33 cm effective length (40 cm total length); applied voltage: 16 kV; temperature: 15-35$^0$C; UV detection: 200nm.

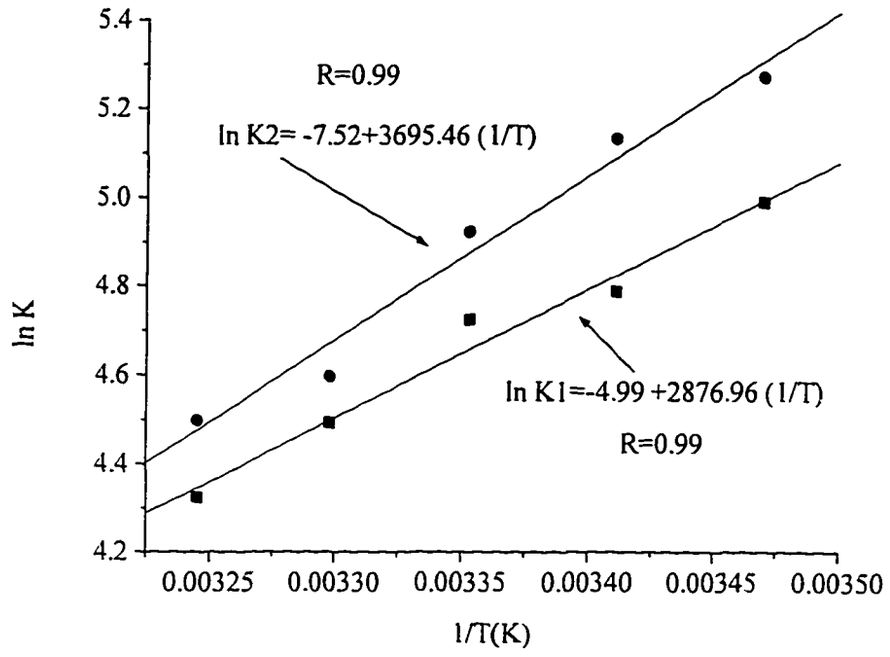


**Figure 2-4. van't Hoff Plot for the Binding of *Cis*(+/-) Aminoindanol Enantiomer to α-CD in the Presence of Urea**

Experimental conditions: temperature range: 15 $^{0}$C to 35 $^{0}$C, other conditions are the same as shown in Figure 2-3.

## 2-5B Effect of Structural Feature of Analyte

It was confirmed that different *cis/trans* configurations result different pKa values as described in Chapter One. It was also found that the different *cis/trans* configurations affect the enantiomeric separation.

Figure 2-5 shows the difference of the enantiomeric separation for *cis*(+/-) and *cis*(+/-) with α-CD as a chiral selector. As can be seen from the electropherograms, the separation of the *cis*(+/-) enantiomers is better than the *trans*(+/-) enantiomers at the same conditions. This observation indicates that the affinities of *cis*(+/-) enantiomers to the α-CD are stronger than *trans*(+/-) enantiomers.

In order to further investigate the effect of structure feature of analyte on the enantiomeric separation, the binding constant and thermodynamic parameters of the "host:guest" model will be determined.

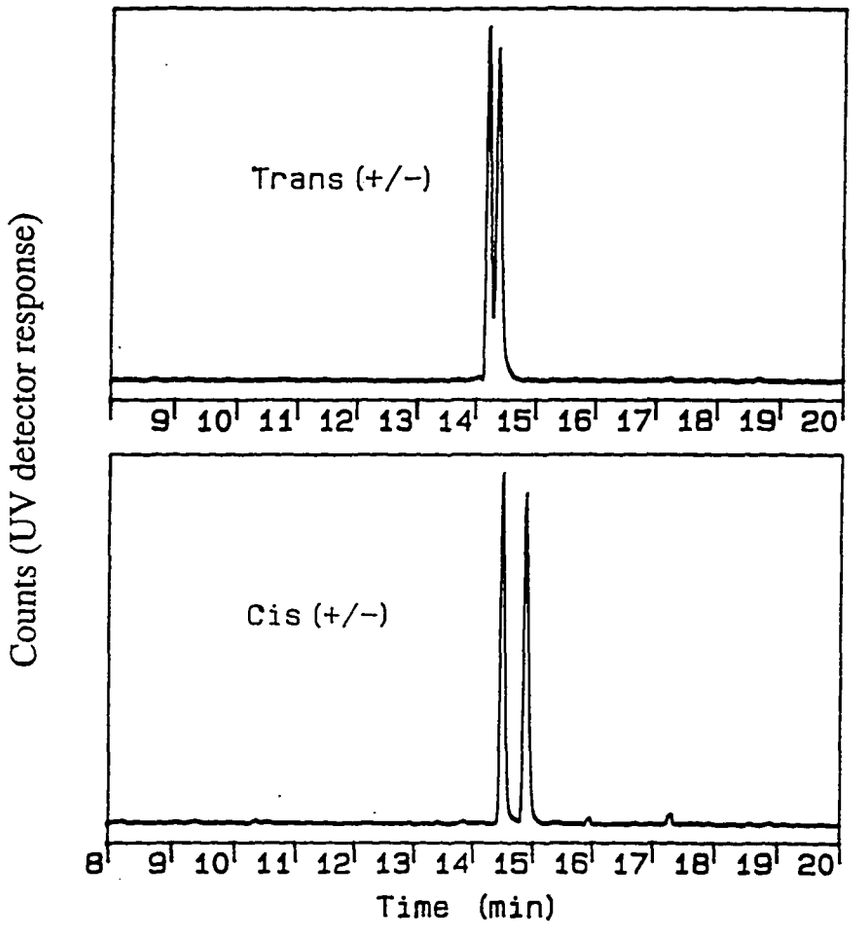


**Figure 2-5. Electropherograms of Aminoindanol Enantiomers Using α-CD**

Experimental conditions: buffer:30 mM α-CD in 40 mM tris-BGE; pH = 2.2; capillary: 50 μm ID, 56 cm effective length (63 cm total length); applied voltage: 16 kV; detector wavelength: 200 nm; operating temperature: 15 °C.

**Binding Constant**

As discussed in Section 2-4A, binding constants for enantiomers/chiral selector complexes can be determined from enantiomer mobilities at different concentrations of the chiral selector. BF 2-1 (with varied concentrations of α-CD from 0 to 92 mM) were used to determine the binding constants for the *cis*(+/-), *trans*(+/-), and the aminoindan enantiomers to the α-CD. Table 2-2 lists the binding constants at 25 °C calculated using the non-linear least squares regression computer program.

The binding constant represents the strength of the enantiomer:chiral selector binding. The larger the K value, the stronger the binding. According to Wren and Rowe's model, the stronger the binding in the [analyte:CD] complex, the lower the CD concentration needed to achieve an optimal resolution ($C_{opt}$) described in Equation 2-11. From Table 2-2, the binding constants for *cis*(+/-) are significantly larger than those for *trans*(+/-). This can be interpreted by the spatial configurations of *cis*(+/-) and *trans*(+/-) enantiomers. For the *cis*(+/-) enantiomers, the amino and the hydroxyl functional groups are on one side of the molecule. In contrast, the amino and the hydroxyl functional groups are on the opposite side of the molecule for *trans*(+/-) enantiomers. That makes the molecular size of *cis*(+/-) smaller than that of *trans*(+/-), and allows *cis*(+/-) to fit into the α-CD cavity more easily and tightly than for the *trans*(+/-).

**Table 2-2. Binding Constants for Testing Compounds**

**Using α-CD at 25°C**

| Analyte | $K_1(M^{-1})$ | $K_2(M^{-1})$ | $\Delta K\ (M^{-1})$ |
|---|---|---|---|
| *Cis*(+/-) | 93.5 | 103.5 | 10.0 |
| *Trans*(+/-) | 24.2 | 27.0 | 2.8 |
| Aminoindan(+/-) | 52.1 | 53.7 | 1.6 |

Since the binding constants for [α-CD:*trans*(+/-)] are much smaller than those for [α-CD:*cis*(+/-)], the optimized α-CD concentration for *trans*(+/-) complexes should be higher than that for *cis*(+/-) complexes according to Equation 2-12. The ratio of the optimized concentrations can be determined as follows:

$$C_{opt.\ trans}/C_{opt.\ cis} = (K_{cis}/K_{trans}) = 3.8$$

The results indicate that in order to gain the best separation of *trans*(+/-) enantiomers, the concentration of α-CD in the buffer must be about four times more than that for the *cis*(+/-) under the same conditions.

**Thermodynamic Parameters**

The binding constants for the *cis*(+/-), the *trans*(+/-), and the aminoindan enantiomers to the α-CD were determined over the temperature range from 15°C to 35°C using BF 2-1. The thermodynamic parameters for the binding process were calculated from the binding constants and van't Hoff plots as described in Section 2-5. The results are summarized in Table 2-3.

**Table 2-3. Thermodynamic Parameters for Testing Compounds Using α-CD**

| Analyte | $\Delta H^0$ (kJ/mol) | $\Delta S^0$ (J/mol T) | $\Delta G^0_{298}$ (kJ/mol) |
|---|---|---|---|
| *cis*(-) | -29.9 | -62.9 | -11.1 |
| *cis*(+) | -26.7 | -51.3 | -11.4 |
| *trans*(-) or (+) | -33.8 | -87.3 | -7.74 |
| *trans*(+) or (-) | -32.8 | -83.7 | -7.86 |
| Aminoindan(-) or (+) | -56.0 | -155.3 | -9.7 |
| Aminoindan(+) or (-) | -52.0 | -141.3 | -9.9 |

The formation of the inclusion complex between aminoindanol enantiomers and α-CD can be assumed to take several steps [12,17-18]:

1) Aminoindanol enantiomers approach the α-CD molecule;
2) The water molecules around aminoindanol (the positively charged ion) and inside the α-CD ring are displaced during the inclusion process;
3) A hydrophobic interaction forms between the aminoindanol aromatic ring and the rim on the inside of the α-CD;
4) Hydrogen bonds between the amino group, the hydroxyl group on the aminoindanol and the hydroxyl groups on the external side of the α-CD are formed;
5) The water-solvated charged side of the complexed enantiomer is reconstructed.

Based on the investigations of Bergeron and co-workers [12,17-18], the inclusion process between the solute and the CD is associated with both enthalpy and entropy contributions, but mainly controlled by enthalpy. The enthalpy change is associated with a) van der Waals-London dispersion forces and b) the release of enthalpy-rich cavity water. The van der Waals-London dispersion forces depend on the distance between the host and the guest. The water molecules associated in the cavity of CD are enthalpy rich because the water cannot be fully hydrogen

bonded. Hence, the inclusion process of the analyte into the cavity is favored by releasing the high energy water.

As can be seen from Table 2-3, the enthalpy change term provides a dominant contribution to $\Delta G^0$ for the binding of all enantiomers to the α-CD.

The entropy change is influenced by several factors [12,17-18]. A major contribution is that hydrating water molecules surrounding polar groups of the guest (-$NH_2$ and -OH groups) and in the host (hydrate water is contained in the α-CD cavity), which are highly ordered, become disordered and a large number of water molecules are released to the bulk solvent. These processes are associated with a positive entropy change. Simultaneously, the loss of the transitional and rotational degrees of freedom resulting the binding between the guest and the host is associated with a negative entropy change. Those two effects are usually balanced, and cancel each other to some extent, so that the net entropy change usually is small. As listed in Table 2-3, the entropy term, ΔS°, of the *trans*(+/-) is more negative than that for the *cis*(+/-). The loss of rotational freedom in the α-CD molecule (so-called glycosidic linkage) is higher for the *trans*(+/-) enantiomers because they have a larger hydrodynamic size than the *cis*(+/-) enantiomers. On the other hand, because *cis*(+/-) enantiomers have a greater chance to fit into the cavity of α-CD than the *trans*(+/-) enantiomers, more water

molecules surrounding the guest and in the cavity are stripped away, which makes the $\Delta S°$ of *cis*(+/-) enantiomers less negative than that of *trans*(+/-).

Because of the combination of enthalpy and entropy contributions, the Gibbs free energy change of the *cis*(+/-) is more negative than that of the *trans*(+/-). This can be interpreted in terms of their spatial arrangements. Figure 2-6 schematically illustrates possible spatial interaction of the *cis*(+/-) with α-CD and *trans*(+/-) with α-CD. The hydrophobic aromatic ring of the aminoindanol is included toward the cavity of the α-CD, and the amino group of the aminoindanol and the hydrogen atom on the chiral center might form a hydrogen bond on the edge of the α-CD. Similarly, the hydroxyl group of aminoindanol and the hydrogen atom on the another chiral center of the α-CD might also form a hydrogen bond.

For the [α-CD:*cis*(+/-)] complex, since *cis*(+/-) configurations have a high conformational energy in the chiral selector free solution, there is a strong driving force to form stable complexes to lower the conformational energy. Since the $-NH_2$ and -OH functional groups are in the same side for the *cis*(+/-), the hydrodynamic size of the *cis*(+/-) is smaller than that of the *trans*(+/-). It is easier for the *cis*(+/-) to include into the cavity. Also, because the $-NH_2$ and -OH are in the same side in the *cis*(+/-), the contact surface area between the benzene ring of enantiomers and the α-CD cavity is larger than that for the *trans*(+/-). See Figure 2-7. That gives more chance for the *cis*(+/-) to undergo the hydrophobic

interactions between the α-CD cavity and the aromatic ring of the *cis*-enantiomers. Furthermore, both -$NH_2$ and -OH can also form hydrogen bonds with α-CD toward in the same direction, which helps to obtain the chiral discrimination.

For the [α-CD:*trans*(+/-)] complex, the *trans*(+/-) configurations have lower conformational energies in the chiral selector-free solution, so there is a weaker driving force to form stable complexes. In the *trans*(+/-) structures, the -$NH_2$ and -OH functional groups are in the opposite direction, so the hydrodynamic size of the *trans*(+/-) is larger, which reduces the chance for the *trans*(+/-) to include into the α-CD cavity. Also, the contact surface area for the *trans*(+/-) between the benzene ring and the cavity of α-CD is less than that for the *cis*(+/-), which also reduces the hydrophobic interaction between the α-CD cavity and the enantiomers. Furthermore, both -$NH_2$ and -OH can form hydrogen bonds with the α-CD only in the opposite direction, which also reduces the chiral discrimination because of the dipole-dipole cancellation.

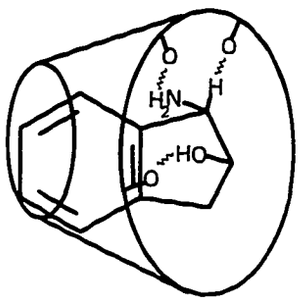


α-CD:*Cis*(+/-)

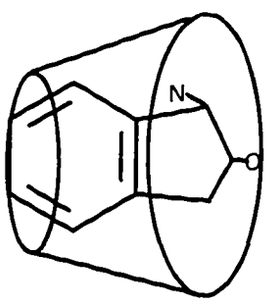


**Type I**

α-CD:*Trans*(+/-)

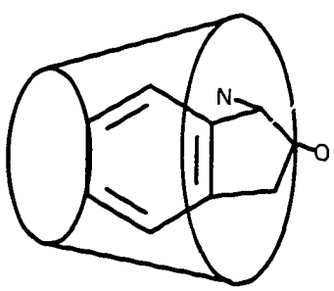


**Type II**

α-CD:*Trans*(+/-)

**Figure 2-6. Schematic Diagram for Possible Spatial Arrangements for *Cis*(+/-) and *Trans*(+/-) with α-CD**

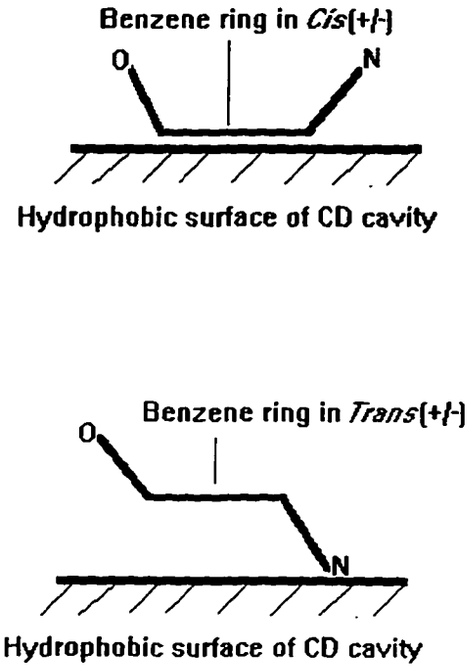


**Figure 2-7. Schematic Diagram for Possible Contact Between *Cis*(+/-) [*Trans*(+/-)] and α-CD Cavity**

## 2-5C Effect of Hydroxyl Group of Enantiomers

To study the effect of a hydroxyl group of the enantiomers on the complex between the aminoindanol enantiomers and the α-CD, aminoindan enantiomers (see Figure 1-2b) were used for comparison with the aminoindanol. Since the aminoindan molecule has the same structural configuration as aminoindanol but an absence of the hydroxyl functional group, the differences in the binding constants, separation resolution, and thermodynamic parameters between aminoindanol and aminoindan can be attributed to the hydroxyl functional group.

As can be seen from Table 2-2 and Table 2-3, the binding constants of the aminoindan are larger than those of the *trans*(+/-) aminoindanol, but lower than those of *cis*(+/-) aminoindanol. The optimum concentration of α-CD of the aminoindan is between those for the *cis*(+/-) and the *trans*(+/-) aminoindanol under the same conditions. The $\Delta G^0$ value for the aminoindan is also between those of the *cis*(+/-) and the *trans*(+/-) aminoindanol. The differences are associated with the hydroxyl group. For the *cis*(+/-), as discussed earlier, both -OH and $-NH_2$ are located on the same side of the structure, the actual hydrodynamic size is not much different from that of the aminoindan. The hydroxyl group on the cyclopentyl ring is available for the hydrogen bonding with both the primary and secondary hydroxyl groups on the α-CD, which enhances the binding between the α-CD and the aminoindanol. But for the aminoindan,

only the amino group can form a hydrogen bond with the α-CD. That allows *cis*(+/-) aminoindanol to have larger binding constants than the aminoindan. Compared with *trans*(+/-), the hydrodynamic size of aminoindan is smaller because it has no -OH group, which helps the aminoindan include into the α-CD cavity more easily, and have a larger binding constant than the *trans*(+/-). The entropy contribution for the aminoindan is the most negative in comparison with *cis*(+/-) and *trans*(+/-) aminoindanol, which is possibly caused by the large loss of the translational degree of freedom in the aminoindan molecule since it is less sterically hindered than the *cis*(+/-) and smaller than the *trans*(+/-) aminoindanol.

### 2-5D Effect of Chiral Selector Size

The cavity size of chiral selectors is also important in the determination of the binding constants, and the separation resolution. β-CD has seven glucose units; the inner diameter of the cavity is about 7.8 Å and there are 11 water molecules in the cavity of the β-CD [12]. The effect of chiral selector size was investigated by examining the binding constants and the thermodynamic parameters for the binding of *cis*(+/-) and *trans*(+/-) to the α-CD and to the β-CD. In this study, in order to enhance the solubility of the β-CD, urea was added into both electrolytes of α-CD system (BF 2-2) and β-CD system (BF 2-3) at the same concentration. Figure 2-8a shows the electropherograms of the aminoindanol enantiomers using β-CD. It can be seen that four enantiomers, *cis*(-), *cis*(+), *trans*(-), and *trans*(+),

can be completely separated. The *trans*(+/-) elute early, but the *cis*(+/-) can be separated more efficiently.

The binding constants are summarized in Table 2-4. The thermodynamic parameters, $\Delta G^0$, $\Delta H^0$, and $\Delta S^0$, for [β-CD:*cis*(+/-)] and [β-CD:*trans*(+/-)] complexes were determined in the same way as for [α-CD:*cis*(+/-)] and [α-CD:*trans*(+/-)] complexes described in Section 2-5A. The results are listed in Table 2-5.

The size effect of chiral selectors can be seen clearly from Table 2-4. The binding constants of the *cis*(+/-) to the β-CD are much less than that to the α-CD because of the large size cavity of the β-CD. According to the London dispersion force concept [12,17-18], the longer the distance between the host and the guest, the weaker the binding force. The binding constants of the [*trans*(+/-):β-CD] are larger than that for the [*trans*(+/-):α-CD ]. This is because the *trans*(+/-) has larger size than *cis*(+/-), which leads a better fitting to the β-CD. However, the binding constants of the [*cis*(+/-):β-CD] are still greater than thoes of the [*trans*(+/-):β-CD], which indicates that the structure feature of analyte is more important than the size of the selectors in this complexing process.

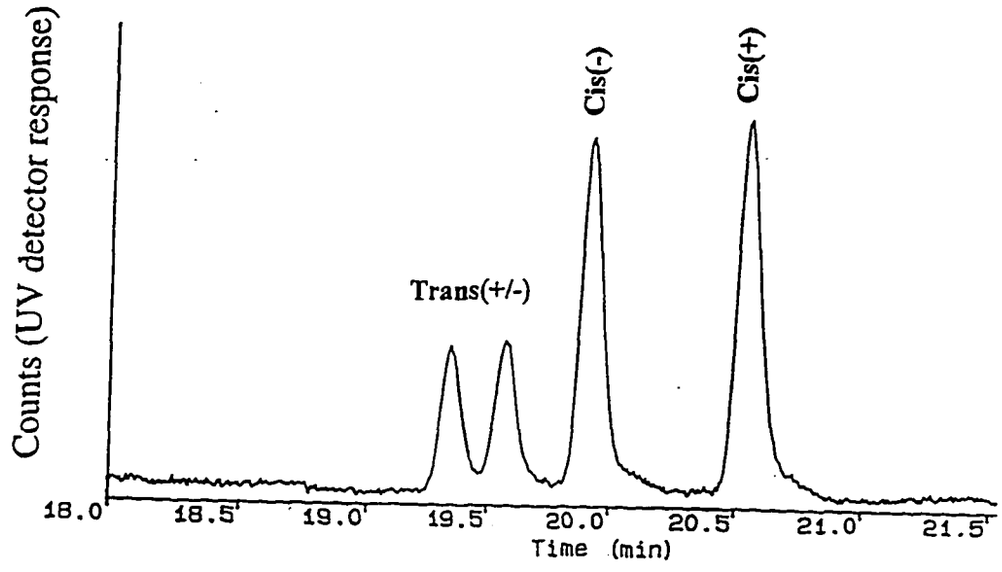


**Figure 2-8a. Electropherogram of Aminoindanol Enantiomers Using β-CD**

Experimental conditions: buffer solution: 50 mM of β-CD, 8 mM of urea (BF 2-3) at pH = 4.4; capillary: 50-μm ID, 56-cm effective length (63-cm total length); applied voltage: 16 kV; detector: 200 nm; temperature: 15°C.

**Table 2-4. Comparison Results of Binding Constants for *Cis*(+/-) and *Trans*(+/-)**

| Analyte | $K_1(M^{-1})$ | $K_2(M^{-1})$ | $\Delta K(M^{-1})$ |
|---|---|---|---|
| α-CD | | | |
| *cis*(+/-) | 112.5 | 147.4 | 24.9 |
| *trans*(+/-) | 25.6 | 27.7 | 2.1 |
| β-CD | | | |
| *cis*(+/-) | 38.3 | 42.1 | 3.8 |
| *trans*(+/-) | 33.1 | 35.1 | 2.8 |

**Table 2-5. Thermodynamic Parameters for *Cis*(+/-) and *Trans*(+/-)**

| Analyte | $\Delta G^0_{298}$ (kJ/mol) | $\Delta H^0$ (kJ/mol) | $\Delta S^0$ (J/mol T) |
|---|---|---|---|
| **α-CD** | | | |
| *cis*(-) | -11.5 | -23.9 | -41.5 |
| *cis*(+) | -12.1 | -30.7 | -62.5 |
| *trans*(-) or (+) | -7.78 | -59.7 | -174.2 |
| *trans*(+) or (-) | -8.05 | -65.0 | -191.0 |
| **β-CD** | | | |
| *cis*(-) | -8.89 | -40.4 | -105.7 |
| *cis*(+) | -9.18 | -46.5 | -125.3 |
| *trans*(-) or (+) | -8.66 | -18.2 | -32.1 |
| *trans*(+) or (-) | -8.77 | -18.3 | -32.0 |

As can be seen from Table 2-5, both the enthalpy and entropy changes for the [β-CD:*cis*(+/-)] complexes are more negative than those for the [α-CD:*cis*(+/-)]. It is possibly caused by the greater number of water molecules in the β-CD cavity than in the α-CD cavity [12], the displacement of which leads to a larger enthalpy change. In the case of the [β-CD:*cis*(+/-)] complexes, if the *cis*(+/-) approach the β-CD cavity from their narrow side, as into the α-CD cavity, the entropy of complexation should be expected to be less negative because of the larger diameter of the β-CD cavity and less restrictive rotation about the glycosidic linkages of β-CD. However, the approach of the *cis*(+/-) to the β-CD cavity from their wide side would lead to more restriction of the rotation about the glycosidic linkages of CDs and hence a higher entropy change, as observed. See Figure 2-8b.

For [β-CD:*trans*(+/-)] complexes, the entropy term is less negative, as expected. Because of the larger size of β-CD, the steric effect of the geometrical size for the *trans*(+/-) is not as important as in the case of [α-CD:*trans*(+/-)]. The *trans*(+/-) should fit into the β-CD cavity much easily than the α-CD cavity, and cause fewer restrictions on the rotation of the glycosidic linkages. On the other hand, the disorder of the water molecules during the inclusion process for the *trans*(+/-) is greater than that for the *cis*(+/-) because of the smaller steric hindrance of the *trans*(+/-) in the free β-CD buffer. The small enthalpy change of the formation of [β-CD:*trans*(+/-)] complexes can be attributed to the dominant contribution from

London dispersion forces. Because the β-CD cavity is large, there is a relatively large distance between the host and the guest molecules, and the binding strength of the [β-CD:*trans*(+/-)] should be weaker than that of the [α-CD:*trans*(+/-)] complex, as observed.

Enantiomeric separation could not be achieved for either *cis*(+/-) or *trans*(+/-) if γ-CD was used as a chiral selector because the cavity size of γ-CD is too large and the binding between the host and the guest is too weak to generate a chiral discrimination.

### 2-5E Effect of Urea Additive

Urea is used as an additive in many chiral separations to enhance the β-CD solubility [21,22,39,40]. It was confirmed that the solubility of β-CD was as high as 100 mM in the presence of 8 mM urea in the electrolyte in this study. Moreover, the effect of urea on the aminoindanol separation was investigated by comparison of the binding constants between the analytes and the α-CD with and without urea.

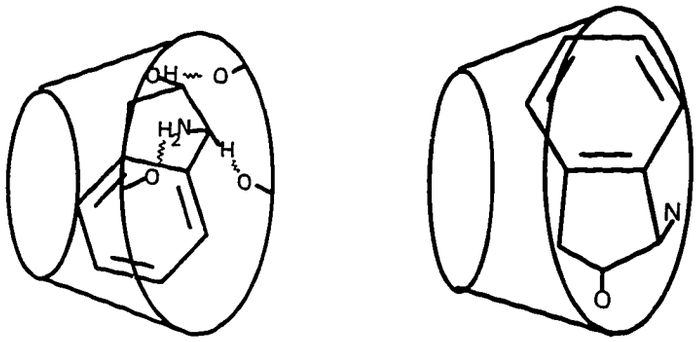


β-CD:*Cis*(+/-) β-CD:*Trans*(+/-)

**Figure 2-8b. Schematic Diagrams of *Cis*(+/-) and *Trans*(+/-) with β-CD**

According to the references [21,22,39-42], urea does not participate the binding with cyclodextrin. In this study, evidently urea did not bind to the α-CD. Table 2-6 shows that addition of urea did not decrease the binding constants, which confirms that no competitive binding exists between the urea and the α-CD. It was also noticed that the binding constants of the aminoindanol to the α-CD increased when urea was present, especially for the *cis*(+/-). Yoshinaga and co-worker [39] reported that enantioselectivity towards dansylamino acids were enchanced dramatically by addition of urea. That is in agreement with our results. It may be that urea can break up the water structure around the guest molecule by forming urea-water hydrogen bonds , which make the inclusion process easier [48]. However, the mechanism is not very clear at present. It warrants further investigation.

**Table 2-6. Binding Constants of *Cis*(+/-) and *Trans*(+/-)**

| Analyte | $K_1(M^{-1})$ | $K_2(M^{-1})$ | $\Delta K(M^{-1})$ |
|---|---|---|---|
| **Without Urea** | | | |
| *Cis*(+/-) | 93.5 | 103.5 | 10.0 |
| *Trans*(+/-) | 24.2 | 27.0 | 2.8 |
| **With Urea** | | | |
| *Cis*(+/-) | 112.5 | 137.4 | 24.9 |
| *Trans*(+/-) | 25.6 | 27.7 | 2.1 |

## 2-5F Effect of Buffer pH

The effects of the buffer pH on the chiral separation of *cis*(+/-), *trans*(+/-), and aminoindan enantiomers were studied using BF 2-4. In these solutions, 35 mM α-CD was used as a chiral selector and the buffer pH covered the range from 2.2 to 9.2. Typical electropherograms of the *cis*(+/-) obtained from various pH values are shown in Figure 2-9.

Vigh and his co-workers [3] reported that the resolution of enantiomers is a function of the binding constant of the complex formation, the concentration of the chiral selector, the EOF, and the effective charge of the enantiomers [27-30]. If the analyte is a weak base or a weak acid, the effective charge on the analyte strongly depends on the pH of the buffer solution. For a pair of basic enantiomers, two equations were derived [3,29] for the effective mobility of the S (or R) enantiomer:

$$\mu_{e(S)} = \frac{\mu^0_{HS^+} + \mu^0_{HSCD^+} \cdot K_{HSCD^+} \cdot [CD]}{1 + K_{HSCD^+} \cdot [CD] + \frac{[OH^-]}{K_b} \cdot (1 + K_{SCD}[CD])} \qquad [2\text{-}18]$$

$$\mu_{e(R)} = \frac{\mu^0_{HR^+} + \mu^0_{HRCD^+} \cdot K_{HRCD^+} \cdot [CD]}{1 + K_{HRCD^+} \cdot [CD] + \frac{[OH^-]}{K_b} \cdot (1 + K_{RCD}[CD])} \qquad [2\text{-}19]$$

where subscripts R and S describe the two enantiomers; $\mu^0_+$ is the ionic mobility of the free enantiomers; $\mu^0_{HRCD^+}$ and $\mu^0_{HSCD^+}$ and the ionic mobilities of the

complexed enantiomers; $K_b$ is the base dissociation constant of the enantiomers; $K_{RCD}$ and $K_{SCD}$ are the formation constants for the non-ionic form of the [enantiomer:CD] complexes; $K_{HRCD}^{+}$ and $K_{HSCD}^{+}$ are the formation constants for the ionic form of the [enantiomer:CD complexes], and [CD] and [$OH^-$] are the molar concentrations of CD and the hydroxyl ion in the background electrolyte.

Three different types of cyclodextrin-mediated capillary electrophoresis separations can be involved based upon the model parameters of the above two equations. The separation is called *Type I* when only the non-dissociated enantiomer complexes selectively with the cyclodextrin ($K_{RCD} \neq K_{SCD}$, but $K_{HRCD}^{+}=K_{HSCD}^{+}$). In this case, the separation will be only achieved at pH= pKa+0.5 units, at which most of the analytes are not ionized. The separation is called *Type II* when only the dissociated enantiomer complexes selectively with cyclodextrin ($K_{HRCD}^{+}\neq K_{HSCD}^{+}$, but $K_{RCD} = K_{SCD}$ ). In this case, the separation will be only achieved at pH $\leq$ pKa-1.5 units , at which all analyte are completely ionized. The separation is called *Type III* when both non-dissociated and dissociated complexes selectively with β-CD ($K_{RCD} \neq K_{SCD}$ and $K_{HRCD}^{+}\neq K_{HSCD}^{+}$). In this case, separation will be achieved at any pH. A simple way to determine the separation type is to make two buffers which contain same amount of chiral selector: One at pH $\leq$ pKa-1.5 units and the other at pH= pKa+0.5 units. If a separation is only achieved with the buffer pH= pKa+0.5 units, then it belongs to *Type I.* If the separation is only achieved with buffer pH$\leq$ pKa-1.5 , then it

belongs to *Type II*. If the separation is achieved with both buffers, then it belongs to *Type III* [3,36]. Since the test compounds, aminoindanol and aminoindan, are weakly basic compounds, their separation should depend on the pH of the buffer. Obviously, the enantiomeric separation for all three compounds does not belong to *Type I* because the separations were achieved at pH≤ pKa-1.5 and $K_{HRCD}^{+} \neq K_{HSCD}^{+}$ for all of them, as can be seen in Table 2-3. As shown in Figure 2-11, the enantiomeric separations of *trans*(+/-) and aminoindan(+/-) is lost at the pH= pKa+0.5 units, so that they belong to *Type II* separations. The enantiomeric separation of *cis*(+/-) is also achieved at the pH= pKa+0.5 units (pH=9.08). thus, it belongs *Type III* separation.

Why do the enantiomeric separations of *cis*(+/-), *trans*(+/-) and aminoindan (amd) belong to different separation types? It might be associated with the differences in the structure features of the analytes, especially the hydroxyl group on the analytes. As discussed in the section 2-5C, the binding constants of the three pairs of enantiomers are in the order of $K_{cis} > K_{amd} > K_{trans}$. This order results from the effect of the hydroxyl group. For the same reason, the -OH functional group on the same side of the *cis*(+/-) structure enhances binding and leads the nonionic form also complexing to the CD. But for the *trans*(+/-) or the aminoindan, the -OH functional group is either on the opposed side or is absent, which does not enhance the interaction between the nonionic form of the enantiomer and the CD.

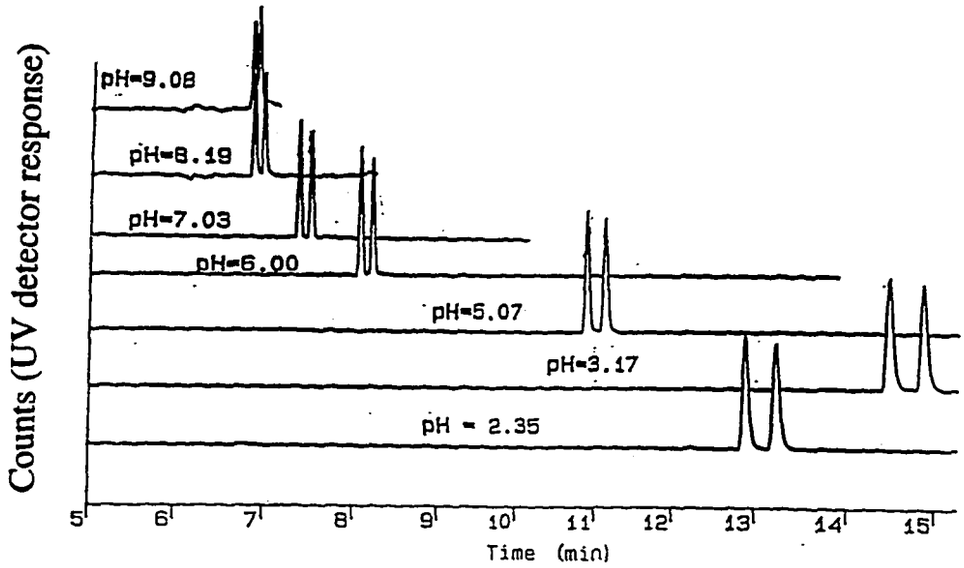


**Figure 2-9. Enantiomeric Separation of Cis(+/-) at Various pH**

Experimental conditions: buffer solution: BF 2-4; capillary: 50-μm ID, 56-cm effective length (63-cm total length); applied voltage: 16 kV; detector wavelength: 200 nm; operating temperature: 25 °C

Based on Equations 2-18 and 2-19, the effective mobilities of the enantiomers are strongly pH dependent. As can be seen from Figure 2-10, the buffer pH increases, the effective mobilities of all three enantiomers are slightly decreased, which is due to the increase in ionic strength because of the increasing $Na^+$ concentration. The dramatic decrease of the effective mobility occurs at the range of pKa-1 > pH > pKa+1, in agreement with Equations 2-18 and 2-19. As the pH increases close to the pKa of the enantiomers, the amino group starts to be deprotonated significantly, and the effective mobility becomes smaller because of loss of positive charge on the enantiomer ions. The terms $\mu^0_+$ and $\mu^0_{HRCD^+}$ (or $\mu^0_{HSCD^+}$) approach zero in Equations 2-18 and 2-19. The order of decreasing effective mobility along with pH axis is *trans* < *cis* < a*md*, which is the order of increasing pKa values, *trans* (7.7) < *cis* (8.5) < *amd* (9.8).

As shown in Figure 2-11, the decrease in resolution for *trans*(+/-) occurs at lower pH value than that for *cis*(+/-) and aminoindan(+/-), which is in agreement with the change in the effective mobility discussed above. However, the order of decreasing resolution with increasing pH is *trans* < *amd* < cis. This is because *trans*(+/-) aminoindanol and aminoindan(+/-) enantiomers belong to *type II* separation. The *cis*(+/-)-aminoindanol belongs to the *Type III* separation. Both the dissociated and the non-dissociated forms of the enantiomer complex selectively with the chiral selector, so the separation can be achieved at any pH

value. From a practical point of view, use of a low pH is the best approach to separation because in that region the EOF effect is minimized [3, 29].

Figure 2-12 presents the change in EOF with buffer pH in the presence of α-CD. . Comparing Figure 1-13 with Figure 2-12, it is clear that the EOF change in the presence of α-CD is similar to that in the absence of α-CD. The reason of the EOF change in the enantiomeric separation is the same as that in the diasteromeric separation, as discussed in Section 1-4F, Chapter One.

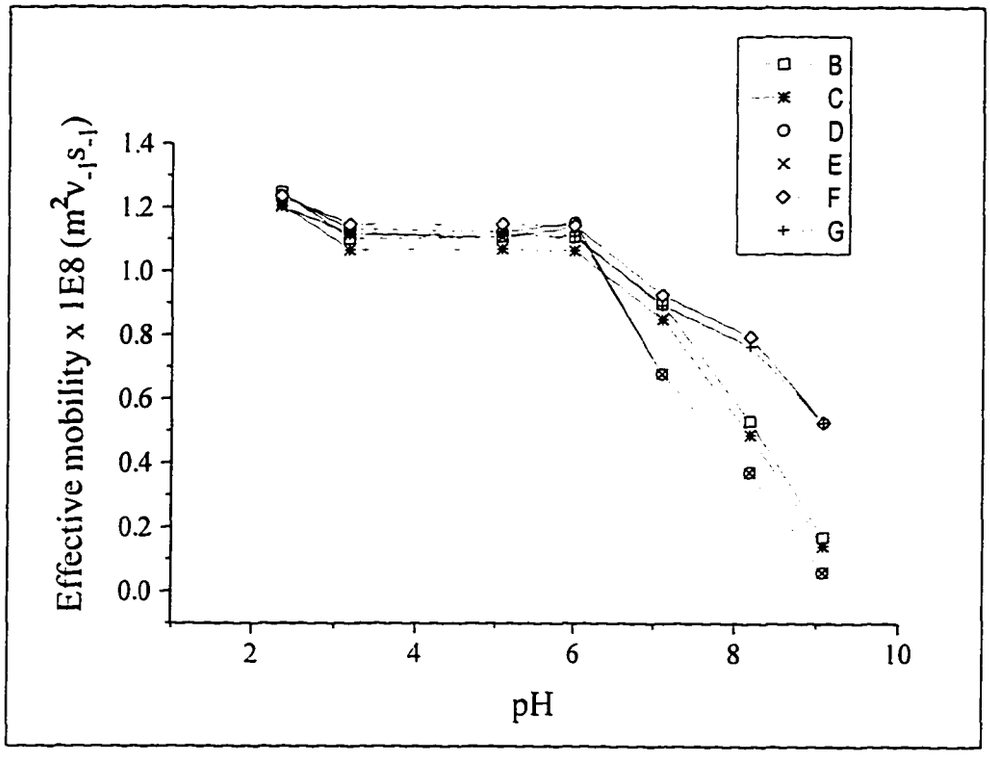


**Figure 2-10. Effective Mobility of Enantiomer Pairs vs. Buffer pH.**

B,C: *cis*(+/-); D,E: *trans*(+/-); F,G: aminoindan(+/-). Experimental conditions are the same as those in Figure 2-9.

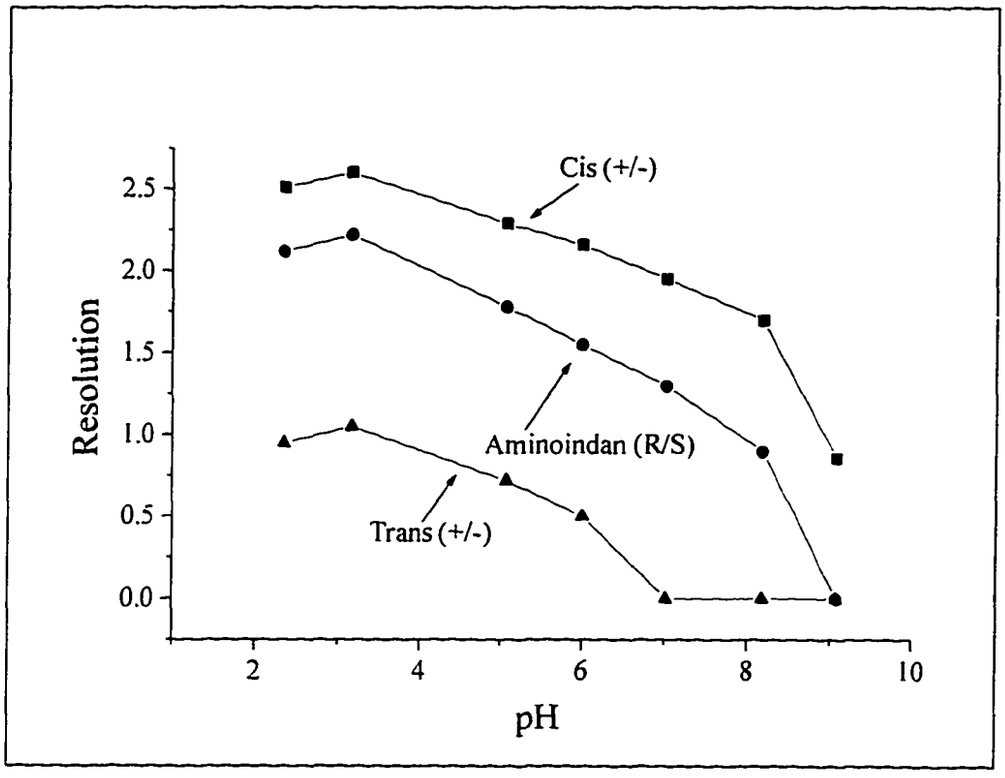


**Figure 2-11. Relationship Between Resolution and Buffer pH**

Experimental conditions are the same as thoes in Figure 2-9

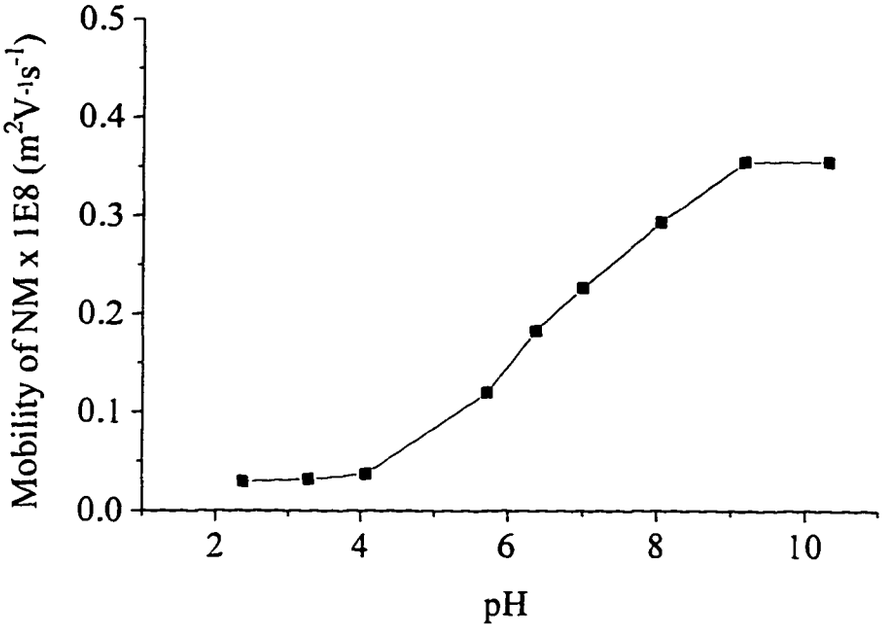


**Figure 2-12. Correlation of Buffer pH and EOF**

The experimental conditions are the same as thoes in Figure 2-9.

## 2-6 Supporting Results From HPLC and Molecular Modeling

The results obtained from HPLC and molecular modeling were also used to interpret the CZE results.

### 2-6A HPLC Enantiomer Analysis

HPLC can also be used to determine binding constants and thermodynamic parameters of complex formation. Based on the theory of reversed phase HPLC, if an inclusion complex equilibrium exists between a chiral selector (α-CD) and an enantiomeric analyte in the mobile phase, the retention time of the analyte should be reduced. This phenomena is due to the presence of -OH groups and a non-polar inner cavity of α-CD. With a polar surface, α-CD passes through a C-4 column unretained, hence, when the guest molecule complexes with α-CD, the [α-CD:analyte] complex should be retained less because of the reduced hydrophobicity of the complexed guest molecules in the mobile phase [37-38].

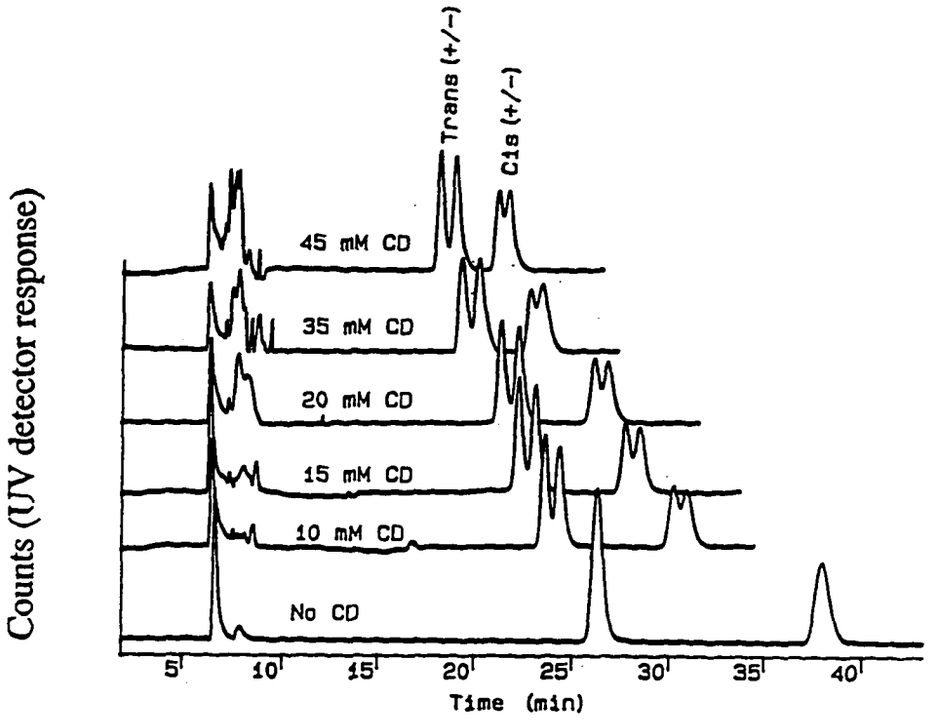


**Figure 2-13. Chromatograms of Aminoindanol Enantiomers with α-CD on C4 Column**

Experimental conditions: mobile phase: BF2-1. column: C-4 (YMC®, 15cm x 4.1mm I.D. x 5μm); isocratic, flow rate: 0.6 mL/min. A UV detection: 200 nm. The column temperature: ambient.

Serial HPLC experiments similar to the CZE experiments were conducted to measure binding constants between α-CD and *cis*(+/-) or *trans*(+/-) enantiomers using a YMC@ C4 column. Typical chromatograms are shown in Figure 2-14. The mobile phase was the same buffer solution (BF2-1) used in the CZE. Equation 2-5 used in CZE can be turned into Equation 2-20 for the HPLC system using the same strategy as in CZE, except substituting capacity factors for effective mobilities in Equation 2-20 [23,43-44]:

$$KC = \left(\frac{k'_0 - k'}{k' - k'_\infty}\right) \qquad [2\text{-}20]$$

where $k'_0$ is the capacity factor of the free analyte, $k'_\infty$ is the capacity factor of the [selector:analyte] complex, k' is the effective capacity factor at a particular concentration of the selector (C), and K is the binding constant. The same non-linear least squares computer program was used to solve Equation 2-20. Table 2-7 lists the Gibbs free energies of the complex formation of [α-CD:analyte] for *cis*(+/-) and *trans*(+/-) enantiomers using the YMC® C4 column at ambient temperature. The ΔG results from CZE in the same buffer solution are also listed in Table 2-7 for comparison.

As can be seen in Figure 2-13, the *trans*(+/-) elute faster than the *cis*(+/-). The major interaction between the stationary phase and the analyte is associated with the benzene ring of the analytes. The *trans*(+/-) have a smaller contact surface area because of the oppositely oriented -OH and $-NH_2$ groups, causing the plane

of benzene ring to be at an angle to the stationary phase; thus it is expected that the *trans*(+/-) are retained less.

The HPLC-determined ΔG of the *cis*(+/-) are larger than those for the *trans*(+/-), which indicates the effect of the structural feature of the analyte on the binding process to the α-CD in HPLC is similar to that in CZE. However, a discrepancy between the ΔGs was observed using these two techniques, especially for the *cis* (+/-) isomers. The discrepancy may be due to the HPLC experiments were performed at room temperature (25±2°C) but the CZE temperature was well controlled at 25±0.1°C by internal cooling device of the instrument. The second is that Equation 2-20 used in HPLC is used by analogy to Equation 2-5 for CZE. The interaction of the [CD:analyte] complex with the stationary phase is assumed to be negligible. However, it is possible that the [CD:analyte] complex loss interact with the stationary phase, causing the retention mechanism to be more complicated than thought [43, 45-46]. It is also probably related to the structural orientation. Further research work is warranted.

**Table 2-7. Comparison of ΔG Measured by CZE and HPLC**

| ΔG ( kJ/mol) | CZE ($25^0$C) | HPLC (ambient) |
|---|---|---|
| $\Delta G_{cis(-)}$ | -11.1 | -9.24 |
| $\Delta G_{cis(+)}$ | -11.4 | -9.55 |
| $\Delta G_{trans(-) \text{ or } (+)}$ | -7.74 | -7.47 |
| $\Delta G_{trans(+) \text{ or } (-)}$ | -7.86 | -6.31 |

## 2-6B Molecular Modeling Calculation

The molecular modeling calculation to predict the energy change for complexed [CD:analytes] was performed using a Cerius$^2$ molecular simulations system. [24] No solvent and solvation effects are considered in the calculation. The calculation assumes that α-CD and aminoindanol form a 1:1 ratio complex. The minimized crystal structure model of α-CD, which was introduced by the Cambridge Structure Database [25], is used in the Cerius$^2$ system. The minimized structures of the *cis*(+/-) enantiomers and the *trans*(+/-) enantiomers are built individually using the Cerius$^2$ system as discussed in Chapter One. The geometrical orientation and structural features of the inclusion complexes of α-CD with *cis*(+/-) and *trans*(+/-) were studied by calculating their energies at different stages, which included the individual analyte (or α-CD) is isolated in space, the analyte included to the α-CD at different angles, the analyte rotated in the α-CD to allow formation of specific interactions such as H-bonding and the interaction between α-CD and the analyte. The construction of the *cis*(+/-) or *trans*(+/-) enantiomers was accomplished using an individual isomer, separately optimized, as a building block. The host and the guest molecules were first put into separate spaces and were then arranged to the proper position to facilitate docking. The molecules were merged together. The merged structure was considered the initial geometric arrangement of the complex. The energy of complex formation was continuously calculated and then minimized using "Dynamic and minimizer

simulation modules". Initially, a rough energy change was estimated for the approach of the guest compound into the α-CD. The complex formation energy decreased as the guest compound entered the α-CD cavity. However, if it was pushed too far, the energy increased dramatically. Calculations were obtained repeatedly near the apparent energy minimum area while randomly rotating the compound relative to the α-CD fifteen times. In all cases, the most favorable interactions, ensuring the formation of the most stable complexes, were found as the benzene ring approached the α-CD from the more open side the cavity and hydrogen bonding occurred on the edge of the α-CD. Higher values of gas-phase binding energies, $\Delta E=E_{components}-E_{complex}$ correspond to more stable structures. Table 2-8 gives the average gas-phase binding energies. The binding energies between *cis*(+/-) enantiomers and *trans*(+/-) enantiomers are different and the energy difference between *cis*(+/-) enantiomers is greater than that between *trans*(+/-) enantiomers. These results match those obtained by CZE and HPLC. Furthermore, the molecular modeling calculation shows that when the benzene ring of *cis*(+/-) and *trans*(+/-) approaches the cavity of α-CD, the energy of the complex formation is the lowest comparison with any other routes of approach, which is also in agreement with the explanations given for the CZE and HPLC results.

It should be mentioned again that the molecular modeling calculation assumes no solvent or solvation, which is not a realistic assumption, because solvation will

affect the energy change for the complex formation of [α-CD:analytes] complex. Although the calculated energy values do not represent absolute values for the complex formation of [α-CD:analytes], but because of the structural similarity between *cis*(+/-) and *trans*(+/-), it is reasonable to assume that these compounds bind to α-CD through the similar mechanism, so the relative energy changes for the [α-CD:*cis*(+/-)] and [α-CD:*trans*(+/-)] complex formation should not be critically dependent on the presence of the solvent. The results obtained from the molecular model calculation should give a good qualitative picture.

**Table 2-8. Energy Change for Complex Formation of α-CD:Aminoindanol Using Molecular Modeling Calculation**

| | ***Trans*(-)** | ***Trans*(+)** | ***Cis*(-)** | ***Cis*(+)** |
|---|---|---|---|---|
| ΔE(kcal/mol) | 13.3 | 12.3 | 12.8 | 17.5 |

## 2-7 Conclusions

1) Enantiomeric separations were achieved for the multi-chiral center compound, aminoindanol, using CDs as chiral selectors.

2) The [host:guest] complex formation model was established for the aminoindanol enantiomeric separation. The experimental results demonstrate the inclusion complex formation is enthalpically-driven for aminoindanol in the temperature range from 15°C to 35°C.

3) For the *cis*(+/-) enantiomeric separation, the optimized α-CD concentration is less than 1/3 that required for the *trans*(+/-) separation. The binding constants for [α-CD:*cis*(+/-)] are much larger than those for [α-CD:*trans*(+/-)].

4) The binding constants and thermodynamic parameters calculated using the established model were confirmed by HPLC and the molecular model calculation. The host:guest complex formation model for aminoindanol and aminoindan was proved to be reasonable.

5) The presence of the hydroxy group of the aminoindanol enchances the binding of the [*cis*(+/-):α-CD] and reduces the binding of the *trans*(+/-) to the α-CD.

6) The binding of *cis*(+/-) to the β-CD is much weaker than that to the α-CD. The binding constants of the [*trans*(+/-): β-CD] are larger than those for the [*trans*(+/-):α-CD ], but the binding constants of the [*cis*(+/-):β-CD] are still greater than those of [*trans*(+/-): β-CD], which indicates that in this complexation process, the structural feature of the analyte is more important than the size of the selector cavity.

7) The enantiomeric separation cannot be achieved for either the *cis*(+/-) or the *trans*(+/-) using γ-CD as a chiral selector because the cavity size of γ-CD is too large and the binding between the host and the guest is too weak to generate chiral discrimination.

8) The enhancement of solubility of β-CD in aqueous solution by urea was confirmed. The results show no competition binding to the CDs between the analytes and urea.

9) The buffer pH affects the enantiomeric separation through the EOF and the characteristics of the enantiomers.

10) The trend of binding constants for the *cis*(+/-) and the *trans*(+/-) to the α-CD determined by HPLC are in agreement with those from the CZE study.

11) The results of the molecular modeling for the binding of *cis*(+/-) and the *trans*(+/-) to the α-CD are in agreement with those from CZE and HPLC.

# CHAPTER THREE

## Enantiomeric Separation of the Novel Growth Hormone Secretagogue by CZE

## 3-1 Introduction

The interest in growth hormone secretagogues has intensified during the past several years. MK-0677, made by Merck & Co. (Rahway, NJ) and shown in Figure 3-1, belongs to a new structural class of orally active growth hormone secretagogues [1]. Pre-clinical and clinical studies have shown the safety and efficacy of MK-0677, and indicated that important medical needs will be satisfied with MK-0677 [2]. Through biological studies, it is found that the *R*-isomer is the active form and the *S*-isomer, which is the enantiomeric impurity of *R*-isomer, is not biologically active. It is very important to develop an analytical method which can separate these two enantiomers and accurately detect the *S*-isomer at the level of 0.5%.

Initially, an HPLC method using an ovomucoid (OVM®) chiral recognition protein column (Ultrones Company, NJ) was employed to achieve the chiral separation. The major drawbacks of this method are that the OVM column is quite expensive and its lifetime is much shorter than that expected for this application. A CZE method is developed for separation of *S*-isomer from *R*-isomer. This method not only avoids the problems of the HPLC method, but also demonstrates much better separation characteristics, such as tailing factor and sensitivity.

The HPLC chromatogram and the CZE electropherogram of the separation of MK-0677 enantiomers are compared in Figure 3-2. It is obvious that the CZE peak efficiency for MK-0677 is much better than the HPLC. In this chapter, method parameters which affect the CZE separation will be discussed. These include effects of the concentrations of β-CD, *L*-tartaric acid, $NaH_2PO_4$, pH of the buffer, the organic modifiers, temperature, and applied voltage. The functions of ion-pair reagents and the separation mechanism are also studied. The method has been completely validated based on the standard of the cGMPs in terms of precision, accuracy, ruggedness, linearity, and sensitivity [3].

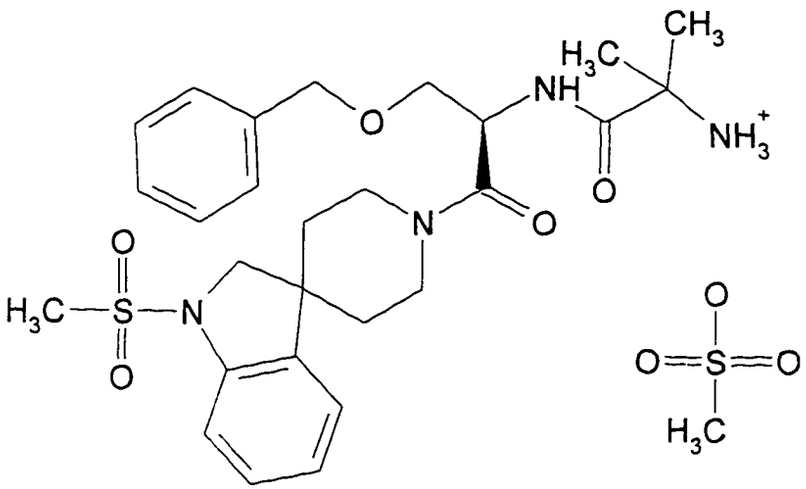

**Figure 3-1. Structure of MK-0677**

(*R*)-2-Amino-N-[2-[1,2-dihydro-1-(methylsulfonyl)spiro [3*H*-indole-3,4'-piperidin]-1'yl]-2-oxo-1-[(phenylmethoxy) methyl] ethyl-2-methylpropanamide-monomethanesulfonate (pKa = 7.8).

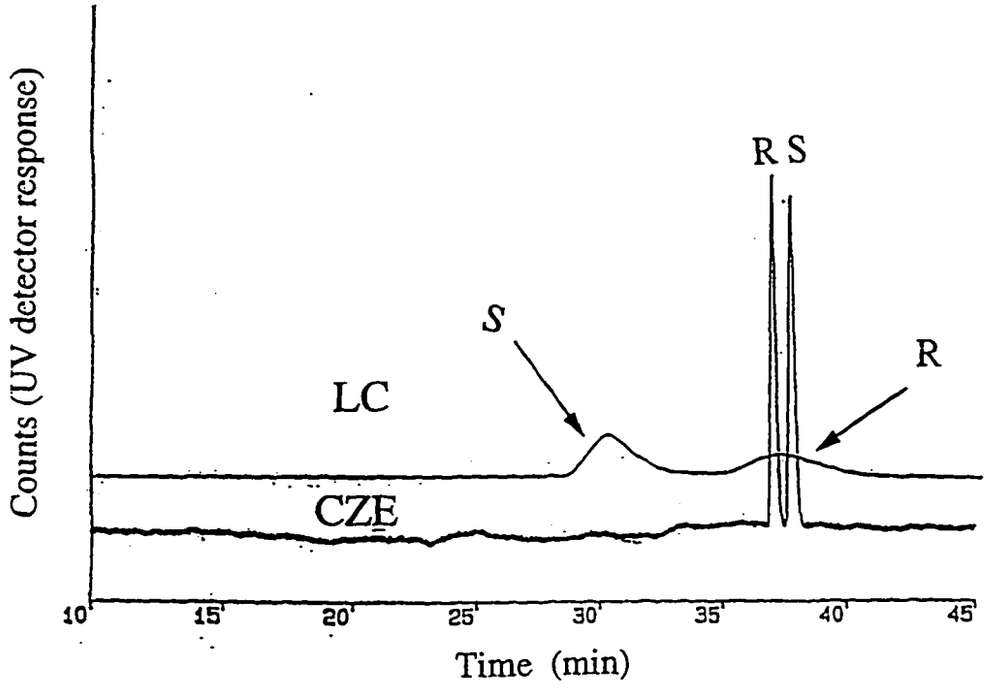


**Figure 3-2. Enantiomeric Separation for MK-0677 Using HPLC and CZE**

Experimental conditions for the HPLC: column: Ultra-ES OVM® with 150 x 4.6 mm; temperature: 27°C; mobile phase: 83:17 (v/v) of 15 mM ammonium phosphate aqueous solution:acetonitrile; flow rate: 1.0 ml/min; detector: UV at 210 nm.

Experimental conditions for the CZE: buffer solution: BF 1-1; fused-silica capillary, 52 cm effective length, 76 μm I.D. (72 cm total length); temperature: 25°C; voltage: 20 kV; detector: UV at 200 nm.

## 3-2 Experimental

### 3-2A Instrumentation

CZE experiments were performed using an ABI 270A (Applied Biosystems, Foster City, CA) and a $HP^{3D}CE$ systems. The ABI instrument was used with a 76 μm I.D., 52 cm effective length fused-silica capillary (72 cm total length) (Polymicro Technologies, Inc., Phoenix, AZ) and an UV detector at 200 nm. The capillary temperature was maintained at 25°C. Hydrodynamic sampling injection was applied for 2 seconds at 50 mbar pressure. The applied voltage was 20 kV. The $HP^{3D}$ CE instrument was used with a 75 μm I.D., 56 cm effective length (63 cm total length) fused-silica capillary (Hewlett-Packard, Piscataway, NJ) and a diode-array detector was employed and set at 200 nm. The injection mode, the injection time and the pressure were equivalent to those for the ABI instrument. The applied voltage was 20 kV. Data collection and integration were accomplished using the Nelson ACCESS CHROM data system (Perkin Elmer Corp, Cupertino, CA).

### 3-2B Reagents

MK-0677 and its *S*-isomer were prepared by the Process Research Department in Merck Research Laboratories (Rahway, NJ). *L*-tartaric acid (LTA) and mesityl

oxide were purchased from Aldrich (Milwaukee, WI) $NaH_2PO_4$, methanol (MeOH), ethanol (EtOH), isopropyl alcohol (IPA), and 50% NaOH solution were obtained from Fisher Scientific (Springfield, NJ). β-CD, citric acid, camphosulfonic acid, 3-(N-morpholinol)-propanesulfonic acid (MOPS), propanesulfonic acid (Na salt), butanesulfonic acid (Na salt) (BTSA), pentanesulfonic acid (Na salt), hexanesulfonic acid (Na salt), heptanesulfonic acid (Na salt), octanesulfonic acid (Na salt), and decanesulfonic acid (Na salt) were purchased from Sigma (St. Louis, MO). All commercial chemicals were used directly without any further purification. Water was purified with a Milli-Q system (Millipore Corp, Milford, MA).

### 3-2C. Electrolyte Solution and Sample Solution

Several electrolyte solutions were prepared as follows:

Buffer solution 3-1 (BF 3-1): BF 3-1 was prepared by dissolving 0.6 g LTA, 0.34 g $NaH_2PO_4$, and 3.4 g β-CD in a 25% EtOH (v/v) aqueous solution and adjusting the pH to 4.2 using 50% NaOH.

Other buffer solutions were prepared similarly to BF 3-1. The details are listed in Table 3-1. The pH of all buffer solutions is the apparent pH.

Sample solutions were prepared as follows:

Sample solutions (SP 3-1): SP 3-1 was prepared by dissolving 5 mg of each enantiomer of MK-0677 in 100 mL of BF 3-27. The concentration of each enantiomer of MK-0677 is 0.08 mM.

An neutral marker solution was prepared by dissolving 30 mg mesityl oxide in 100 mL of 99.99% methanol.

### 3-2D Procedure

All procedures for capillary and sample solution treatments are described in Section 1-3D, Chapter 1.

**Table 3-1 List of the Buffer Solutions and Sample Solutions**

| Solution I.D. | Purpose | Solution Composition |
|---|---|---|
| BF 3-1 | Validation | LTA: 40 mM; $NaH_2PO_4$: 24 mM; EtOH: 25% (v/v); β-CD: 30 mM; pH=4.2. |
| BF 3-2 | Effect of [β-CD] | LTA: 40 mM; $NaH_2PO_4$: 24 mM; EtOH: 25% (v/v); β-CD: 0 - 50 mM; pH=4.2. |
| BF 3-3 | Effect of [LTA] | $NaH_2PO_4$: 24 mM; EtOH: 25% (v/v); β-CD: 30 mM; LTA: 0 - 60 mM; pH=4.2. |
| BF 3-4 | Effect of [LTA] | $NaH_2PO_4$: 24 mM; EtOH: 25% (v/v); β-CD: 8 mM; LTA: 0-40 mM |
| BF 3-5 | Effect of [$NaH_2PO_4$] | EtOH: 25% (v/v); β-CD: 30 mM; LTA: 40 mM; $NaH_2PO_4$: 0 - 50 mM; pH=4.2. |
| BF 3-6 | Effect of [EtOH] | LTA: 40 mM; $NaH_2PO_4$: 24 mM; β-CD: 30 mM; EtOH: 10 - 30% (v/v); pH=4.2. |
| BF 3-7 | Effect of pH | LTA: 40 mM; $NaH_2PO_4$: 24 mM; EtOH: 25% (v/v); β-CD: 30 mM; pH: 2.2 - 8.0. |
| BF 3-8 | Temperature effect | $NaH_2PO_4$: 24 mM; EtOH: 25% (v/v); LTA: 40 mM; β-CD: 30 mM; pH=4.2. |
| BF 3-9 | Ion-pairing effect | $NaH_2PO_4$: 24 mM; EtOH: 25% (v/v); citric acid: 40 mM; β-CD: 30 mM; pH=4.2. |
| BF 3-10 | Ion-pairing effect | $NaH_2PO_4$: 24 mM; EtOH: 25% (v/v); MOPS: 40 mM; β-CD: 30 mM; pH=4.2. |
| BF 3-11 | Ion-pairing effect | $NaH_2PO_4$: 24 mM; EtOH: 25% (v/v); camphosulfonic acid: 40 mM; β-CD: 30 mM; pH=4.2. |
| BF 3-12 | Ion-pairing effect | $NaH_2PO_4$: 24 mM; EtOH: 25% (v/v); propanesulfonic acid (Na salt): 40 mM; β-CD: 30 mM; pH=4.2. |
| BF 3-13 | Ion-pairing effect | $NaH_2PO_4$: 24 mM; EtOH: 25% (v/v); butanesulfonic acid (Na salt): 40 mM; β-CD: 30 mM; pH=4.2. |
| BF 3-14 | Ion-pairing effect | $NaH_2PO_4$: 24 mM; EtOH: 25% (v/v); pentanesulfonic acid (Na salt): 40 mM; β-CD: 30 mM; pH=4.2. |
| BF 3-15 | Ion-pairing effect | $NaH_2PO_4$: 24 mM; EtOH: 25% (v/v); hexanesulfonic acid (Na salt): 40 mM; β-CD: 30 mM; pH=4.2 |
| BF 3-16 | Ion-pairing effect | $NaH_2PO_4$: 24 mM; EtOH: 25% (v/v); heptanesulfonic acid (Na salt): 40 mM; β-CD: 30 mM. |
| BF 3-17 | Ion-pairing effect | $NaH_2PO_4$: 24 mM; EtOH: 25% (v/v); octanesulfonic acid (Na salt): 40 mM; β-CD: 30 mM; pH=4.2 |
| BF 3-18 | Ion-pairing effect | $NaH_2PO_4$: 24 mM; EtOH: 25% (v/v); decanesulfonic acid (Na salt): 40 mM; β-CD: 30 mM; pH=4.2 |

**Table 3-1 List of the Buffer Solutions and Sample Solutions (continued)**

| Solution I.D. | Purpose | Solution Composition |
|---|---|---|
| BF 3-19 | Binding study | $NaH_2PO_4$: 30 mM; EtOH: 25% (v/v); β-CD: 0 - 50 mM; pH=4.2. |
| BF 3-20 | Binding study | $NaH_2PO_4$: 30 mM; EtOH: 25% (v/v); MOPS: 40 mM; β-CD: 0 - 50 mM; pH=4.2. |
| BF 3-21 | Binding study | $NaH_2PO_4$: 30 mM; EtOH: 25% (v/v); BTSA: 40 mM; β-CD: 0 - 50 mM; pH=4.2. |
| BF 3-22 | Binding study | $NaH_2PO_4$: 30 mM; EtOH: 25% (v/v); LTA: 40 mM; β-CD: 0 - 50 mM; pH=4.2. |
| BF 3-23 | Binding study | $NaH_2PO_4$: 30 mM; EtOH: 25% (v/v); β-CD: 0 - 18 mM; pH=4.2. |
| BF 3-24 | Binding study | $NaH_2PO_4$: 30 mM; MeOH: 25% (v/v); β-CD: 0 - 18 mM; pH=4.2. |
| BF 3-25 | Binding study | $NaH_2PO_4$: 30 mM; IPA: 25% (v/v); β-CD: 0 - 18 mM. |
| BF 3-26 | Binding study | $NaH_2PO_4$: 30 mM; EtOH: 25% (v/v); LTA: 40 mM; β-CD: 0 - 50 mM; pH=7.0. |
| BF 3-27 | Sample diluent | LTA: 40 mM; $NaH_2PO_4$: 24 mM; EtOH: 25% (v/v); pH=4.2. |

## 3-3 Results and Discussion

### 3-3A Effect of β-CD Concentration on Enantiomeric Separation

The effect of β-CD concentration on the separation of MK-0677 enantiomers was studied by determining the effective mobilities of the two enantiomers and the NM over the concentration range of β-CD from 0 to 50 mM. Their effective mobilities as a function of [β-CD] are shown in Figure 3-3a and 3-3b, respectively. The effective mobility of the *R*-isomer is identical to that of *S*-isomer with no β-CD, and both mobilities decrease as the [β-CD] increases. The mobility of the NM decreases slightly as the [β-CD] increases because the electrolyte viscosity increases. The resolution of the two enantiomers as a function of [β-CD] is also illustrated in Figure 3-3b.

Based on the same concepts for the *cis/trans* aminoindanol discussed in Chapter 2, if a dynamic equilibrium between the MK-0677 enantiomers and β-CD is assumed, the equilibrium should follow: [4-6]

$$S + \mathrm{CD} \rightleftharpoons \mathrm{S{:}CD} \qquad K_S = \frac{[\mathrm{S{:}CD}]}{[S][\mathrm{CD}]} \qquad [3\text{-}1]$$

$$R + \mathrm{CD} \rightleftharpoons \mathrm{R{:}CD} \qquad K_R = \frac{[\mathrm{R{:}CD}]}{[R][\mathrm{CD}]} \qquad [3\text{-}2]$$

where, *S* and *R* are the target *S*- or *R*- enantiomers, CD is the β-CD, S:CD and R:CD are the complexes formed by the *S*- and *R*- enantiomers with the β-CD, and

$K_S$ and $K_R$ are the formation constants for the [S:CD] and [R:CD] complexes. If the mobilities of the free and the complexed enantiomers are different, and if the exchange between the free and bound forms is very rapid, the chiral separation for the enantiomers is possible. The relationship between the effective mobility of each enantiomer and the concentration of free β-CD follows the Equation 2-5 as described in Chapter 2.

The binding constants (K) can be determined from the dependence of analyte mobility on the [CD]. The $\mu$ (after correction for viscosity) and $\mu_0$ were measured experimentally, and $\mu_\infty$, $K_R$ (14.2 $M^{-1}$), and $K_S$ (19.4 $M^{-1}$) were obtained by the non-linear least squares computer calculation based on Equation 2-5. The details of the calculation procedure have been described in Chapter II.

Equation 2-11 indicates that the maximum mobility difference, which is directly related to the resolution, is obtained at the optimized [β-CD]. Using $K_R$ and $K_S$ values determined experimentally from Equation 2-11, the optimum [β-CD] is calculated to be 60 mM based on Equation 2-12. The calculated results using the 1:1 [β-CD:analyte] complex equilibrium model are in good agreement with the experimental results. Figure 3-3b shows that the maximum resolution was achieved at the concentration range of 40 to 50 mM which is slightly lower than the calculated optimized concentration of β-CD. It is possibly related to the broader peaks with long migration times.

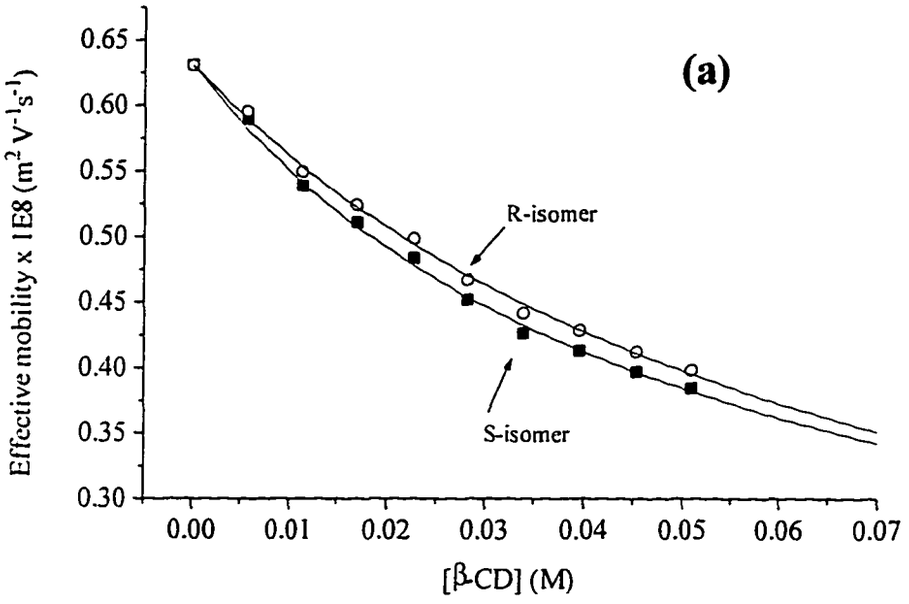


**Figure 3-3a. Effect of [β-CD] on Effective Mobility**

The solid square and the opened circle points are the experimental values and the lines are the calculated results based on the host:guest complex model calculation. Experimental conditions: buffer solution: BF 3-2; capillary: 76 μm I.D. and 52 cm effective length (72 cm total length); temperature: 25°C; voltage: 20 kV; detection: UV at 200 nm.

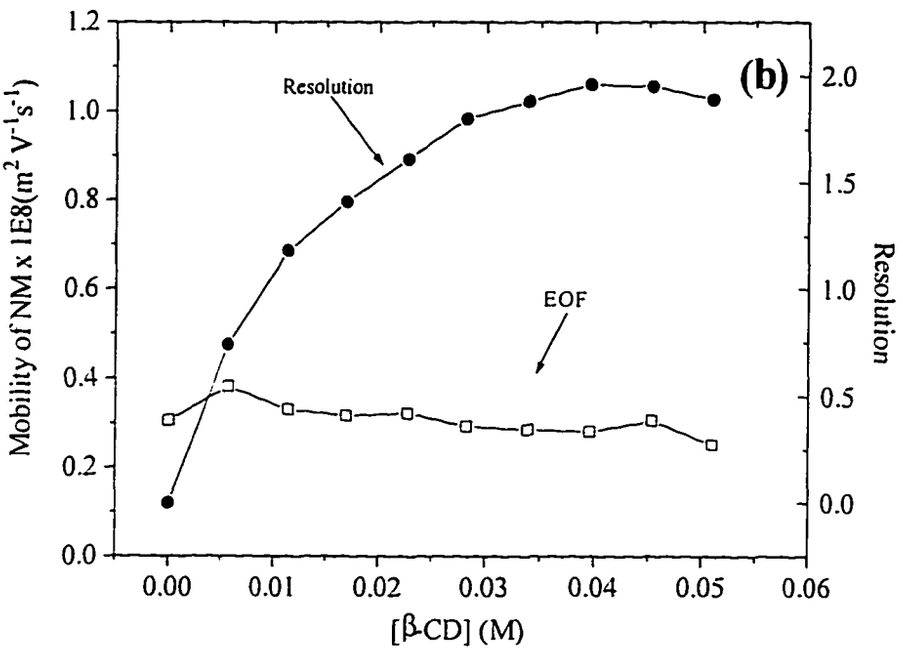


**Figure 3-3b. Effect of [β-CD] on Resolution and EOF**

Experimental conditions are the same as those in Figure 3-3a.

### 3-3B Effect of Organic Modifier on Enantiomeric Separation

Various amounts of EtOH were added to the buffer solution at levels from 10% to 30% (v/v) while keeping other components constant. The presence of EtOH in the buffer enhanced the solubility of β-CD. As shown in Figure 3-4a &b, the effective mobilities of the two enantiomers and the EOF decreased as the concentration of EtOH increased. The resolution is 1.18 at 10% and 2.17 at 30% EtOH level.

The complexation constants ($K_S$ and $K_R$) represent the extent of the hydrophobic interactions between the analyte and β-CD. It is expected that the addition of an organic modifier weakens these interactions and the binding constants of the two enantiomers to β-CD decreases due to the competitive binding from the modifier [4-6].

Based on Equation 2-12, if the $K_S$ and $K_R$ decrease, the optimum [β-CD] becomes higher. As a result, when the [β-CD] is equal or below the optimum value for the EtOH free buffer, the addition of EtOH should decrease the resolution because the optimum [β-CD] will shift to higher values. When [β-CD] is higher than the optimum value for the EtOH free buffer, the addition of EtOH should increase the resolution since the [β-CD] will be closer to the new optimum value, which

should be higher than that of EtOH free buffer. The results shown in Figure 3-4b demonstrate that the addition of EtOH increases the resolution.

The presence of EtOH causes the EOF to decrease; as a result, the migration times of the analyte ions increase. The reasons of the EOF change have been explained Section 1-4F in Chapter 1. They are mainly due to decrease of $\varepsilon/\eta$ ratio and $\xi$ potential.

In order to investigate the effect of the molecular size of organic modifiers, three different organic modifiers, MeOH, EtOH, and IPA were used. The concentration of β-CD in the electrolyte which contained 25% (v/v) of each organic modifier was varied. The results are given in Table 3-2.

As can be seen from Table 3-2, the order of the binding constants in the three organic modifiers is $K_{MeOH} > K_{EtOH} > K_{IPA}$. The larger the modifier size, the smaller the binding constants. This result implies the modifiers participate in the binding with β-CD, and compete with the analyte. Because larger modifier can fit into the cavity of β-CD better, stronger competitive binding results, and thus the binding constants are reduced.

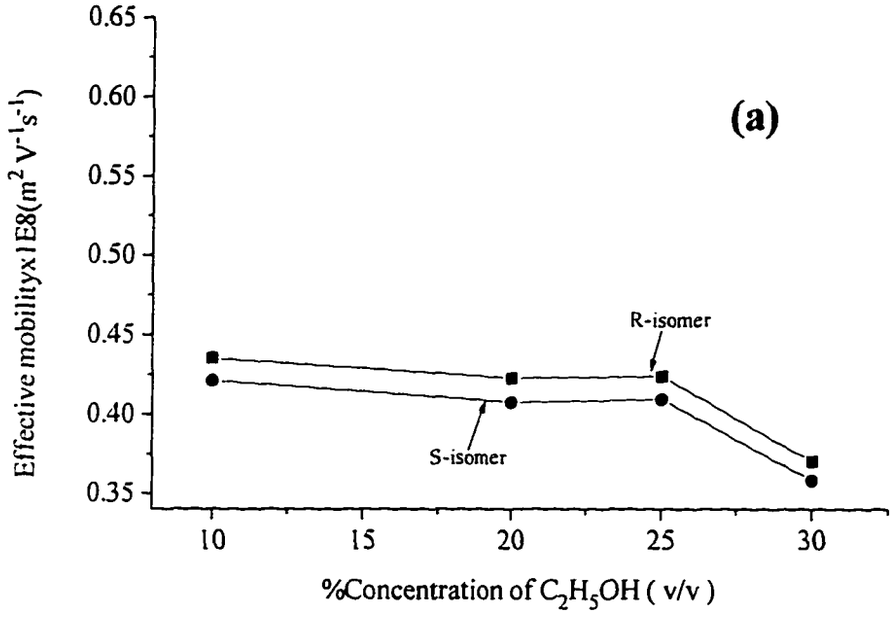


**Figure 3-4a. Effect of [EtOH] on Effective Mobility**

Experimental conditions: buffer: BF 3-6; Other conditions are the same as those in Figure 3-3a.

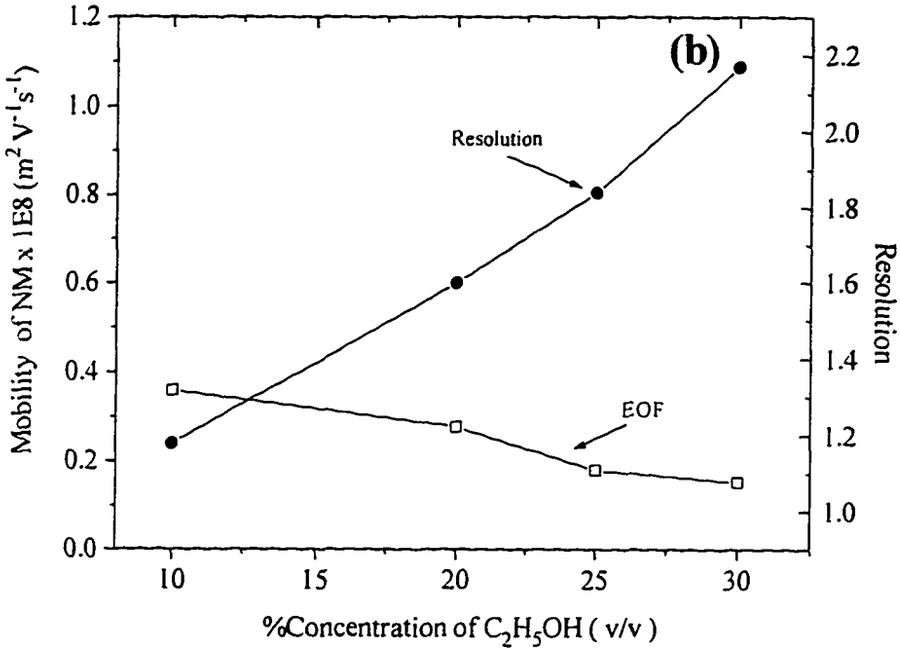


**Figure 3-4b. Effect of [EtOH] on Resolution and EOF**

Experimental conditions are the same as those in Figure 3-4a.

### 3-3C Effect of Temperature on Enantiomeric Separation

The resolution and migration time increase as the operating temperature decreases, as indicated in Figure 3-5(a). Since the temperature decreases, the viscosity of the buffer solution increases, and the mobilities of the analytes and the EOF decrease. Figure 3-5(b) shows the relationship between $\ln\alpha$ and 1/T, which is linear from 10°C to 45°C. The temperature and the current also show a linear relationship with a $R^2 = 0.997$, which indicated that Joule heating was sufficiently suppressed. The temperature studies indicate that the MK-0677 enantiomeric separation mechanism does not change within the studied temperature range [7-8].

**Table 3-2. Binding Constants Between MK-0677 and β-CD with Different Organic Modifiers**

| Organic Modifier | *R*-Isomer $K_R(M^{-1})$ | *S*-Isomer $K_S(M^{-1})$ |
|---|---|---|
| MeOH | 183.6 | 205.2 |
| EtOH | 97.9 | 101.6 |
| IPA | 19.3 | 29.1 |

Experimental conditions: buffer solution: BF 3-23 to 3-25; capillary: 75 μm I.D. and 56 cm effective length (63 cm total length); temperature: 25°C; voltage: 19 kV; detection: UV at 200 nm.

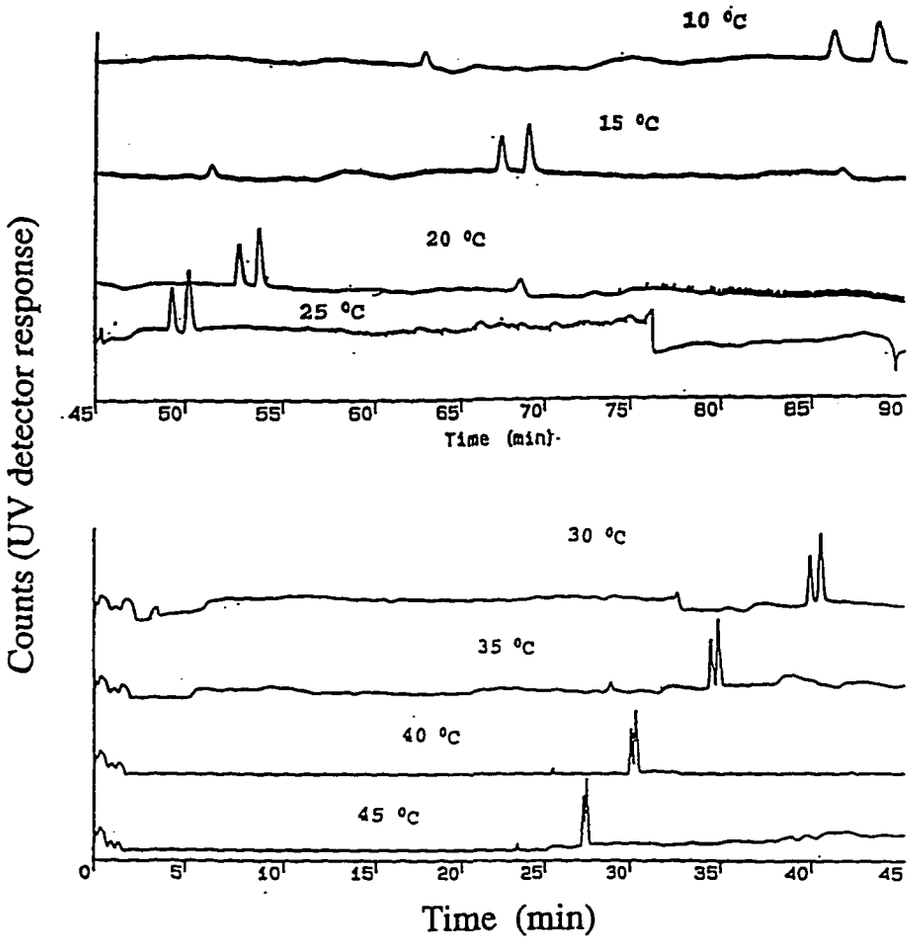


**Figure 3-5(a). Effect of Temperature on Resolution**

Experimental conditions: buffer solution: BF 3-8; capillary: 75 μm I.D. and 56 cm effective length (63 cm total length); voltage: 19 kV; detection: UV at 200 nm; temperature: 10-45°C.

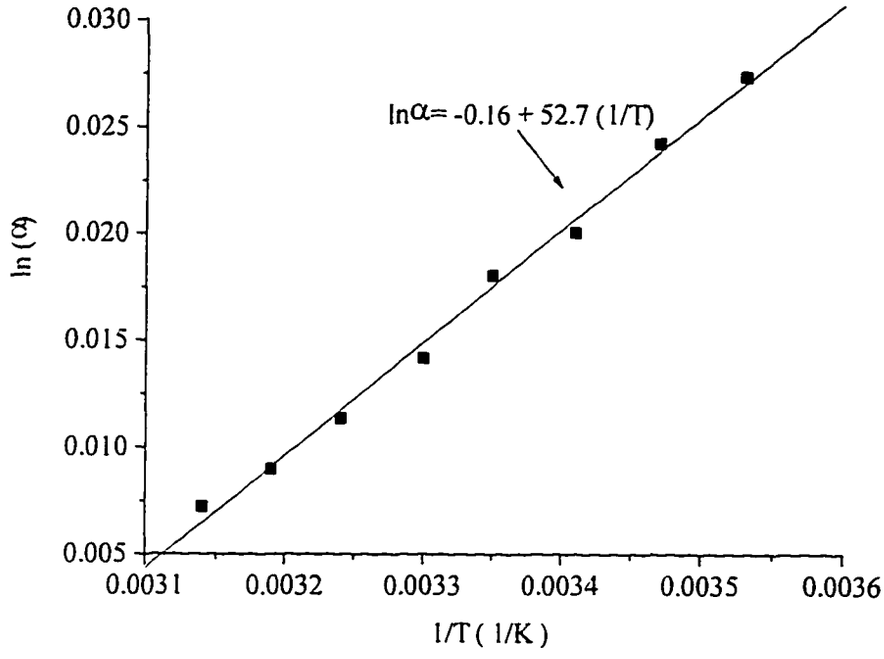


**Figure 3-5(b). van't Hoff Plot**

Experimental conditions are the same as those in Figure 3-5a.

### 3-3D Effect of buffer pH on Enantiomeric Separation

The pH studies were performed by keeping all the other conditions the same as described in Figure 2-2, except varying the pH from 2.5 to 8.0. The dependence of the effective mobility and enantiomeric separation on the pH is illustrated in Figure 3-6.

As discussed in Chapter 2, Vigh and Rawjee [9-13] developed a multiple-equilibria based model to account for the separation of chiral weak acids and bases as a function of both pH and β-CD concentration. Based on their model, for weakly basic enantiomers, three different types of CD-mediated CZE separation can be involved. In this application, since 25% EtOH was presented in the electrolyte, the pH measurements were not same as in the pure aqueous solution. However, the experimental data show clearly that the chiral separation is pH dependent. The effective mobilities gradually decrease in the pH range 2.5-6.0 due to the increasing ionic strength, which is caused by the increasing $Na^+$ concentration [10]. The most dramatic change is in the pH range 7-8, which is in agreement with the pKa =7.8 [1]. Similar behavior was observed for the change of the resolution. It is clear that both the EOF and the natural characteristics of the analytes play important roles in the resolution as discussed in Chapter 2. When the pH is below 4.0, the EOF is small and the resolution does not change significantly. As the pH is changed from 4 to 5, the EOF increases rapidly. The

resolution decreases rapidly although the MK-0677 is still fully charged. When the pH is changed from 5 to 8, the EOF still increases, but slowly and up to a maximum value. A dramatic loss of resolution is in the pH range 7-8 due to the EOF and the loss of positive charge on the analyte.

Binding constant were measured at pH 4.2 and 7.0. The results listed in Table 3-3 show K values decrease as the pH is increased. This contributes to the loss in resolution at a higher pH value.

**Table 3-3. Binding Constants Between MK-0677 and β-CD at Different Buffer pH**

| pH | *R*-Isomer $K_S(M^{-1})$ | *S*-Isomer $K_R(M^{-1})$ |
|---|---|---|
| 4.2 | 15.6 | 18.1 |
| 7.0 | 10.0 | 11.7 |

Experimental conditions: buffer solution: BF 3-22 and BF 3-26; capillary: 75 μm I.D. and 56 cm effective length (63 cm total length); temperature: 25°C; voltage: 19 kV; detection: UV at 200 nm.

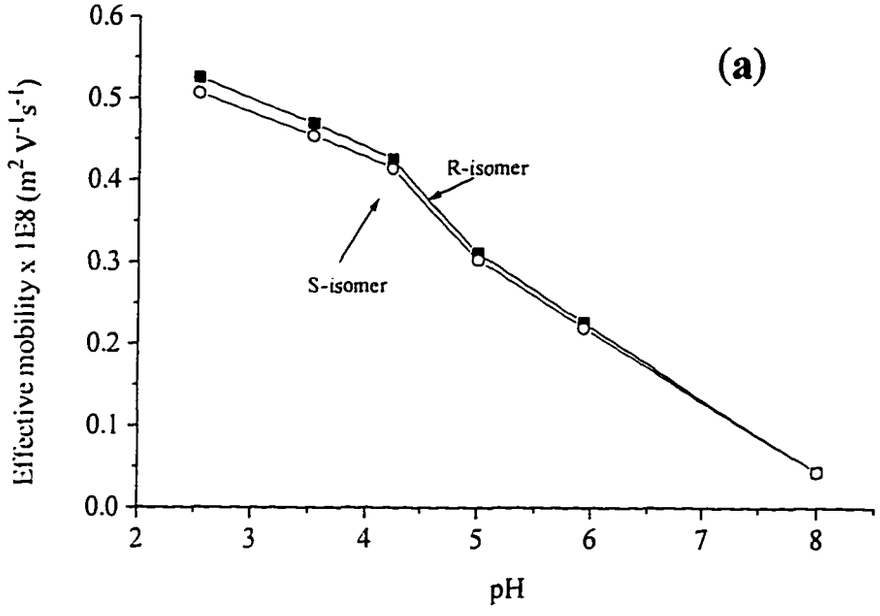


**Figure 3-6a. Effect of pH on Effective Mobility**

The experimental conditions are the same as those in Figure 3-3a, except the buffer is BF 3-7.

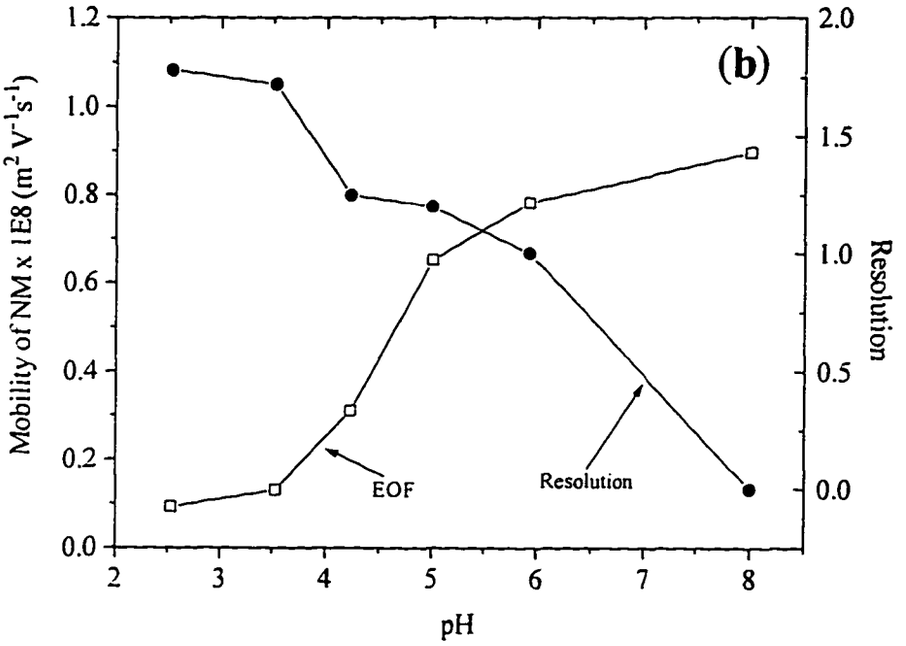


**Figure 3-6b. Effect of pH on Resolution and EOF**

Experimental conditions are the same as those in Figure 3-6a.

### 3-3F Effect of Ionic Composition on Enantiomeric Separation

The effect of ionic composition on the separation was investigated by varying the concentration of $NaH_2PO_4$ from 0-50 mM while keeping other concentrations constant and then varying the concentration of LTA from 0-60 mM while keeping all else constant.

As seen in Figures 3-7(a & b) and 3-8 (a & b), the effective mobilities of MK-0677 decrease and the resolution increases as the [LTA] and [$NaH_2PO_4$] are increased. One of the reasons is the increase in ionic strength which reduces electromigration dispersion and increases the separation efficiency. Rawjee and Vigh [13] demonstrated through a theoretical equilibrium model that peak shapes can be improved by mobility matching between the buffer counter ions and the analyte ions. The enantiomer peak shapes go from fronting through symmetric to tailing while the migration times change relatively slightly. However, in this experiment, a larger resolution enhancement and a greater migration time change were observed by addition of LTA. Consequently, the effective mobilities were decreased significantly since the EOF did not vary much over the entire concentration range. As indicated in Figure 7a, $\mu = 1.1 \times 10^{-8}$ ($m^2v^{-1}s^{-1}$) when [LTA]= 0 mM and [$NaH_2PO_4$] = 24 mM; $\mu = 0.5 \times 10^{-8}$ ($m^2v^{-1}s^{-1}$) when [LTA] = 20 mM and [$NaH_2PO_4$] = 24 mM. Further LTA concentration increases caused a slower mobility decrease. This large mobility change caused by LTA over the

concentration range 0-20 mM can not be explained by the ionic strength change alone. It may also be caused by ion pairing between the negatively charged LTA and the positively charged primary amine of the analytes, which could lead to a reduction in the overall electrophoretic mobility of the analyte.

The elution order of the two enantiomers was not affected when *D*-tartaric acid (DTA), instead of LTA, was used. This indicates that LTA did not function as a chiral recognition reagent in the enantiomeric separation of MK-0677.

Further investigation of the effects of ion-pairing reagents was conducted. As seen in Figure 3-9a, the separation is achieved in buffers containing various ion pair reagents. The migration time order of analytes is $t_{MOPS} > t_{camphorsulfonic\ acid} > t_{LTA} > t_{citric\ acid}$. The order of total negative charges for these ion-pairing reagents is MOPS < camphorsulfonic acid < LTA < citric acid. The MOPS and the camphorsulfonic acid are both mono acids, but the MOPS has a potential amine site, which could be protonated at pH=4.2, reducing the total negative charge on the MOPS. The LTA is a di-acid and the citric acid is a tri-acid.

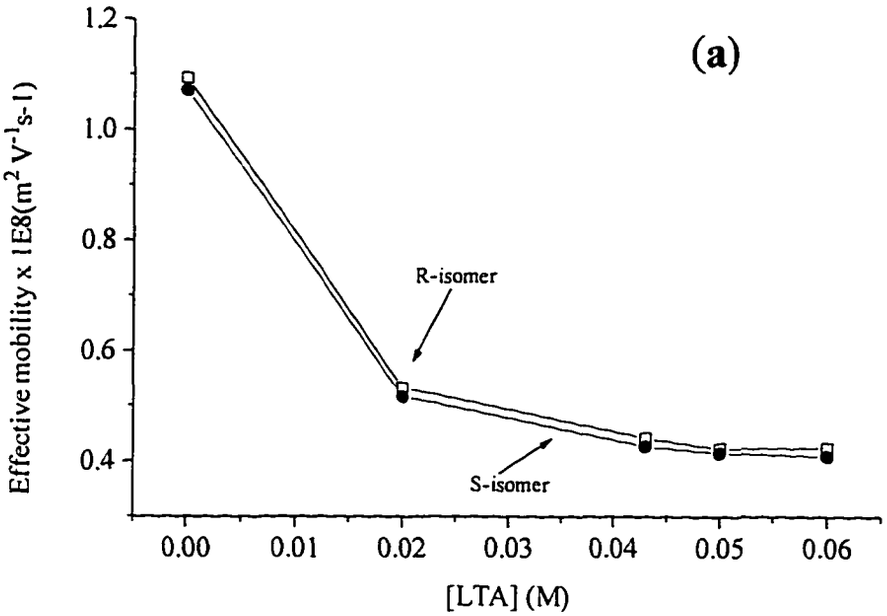


**Figure 3-7a. Effect of [LTA] on Effective Mobility**

Experimental conditions are the same as those in Figure 3-3a, except the buffer solution is BF 3-3.

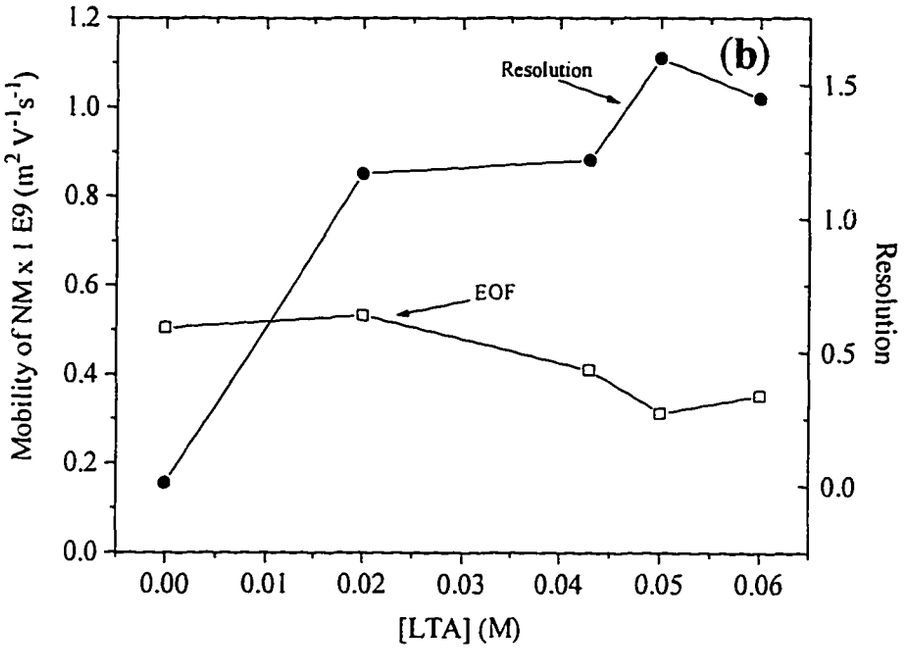


**Figure 3-7b. Effect of [LTA] on Resolution and EOF**

Experimental conditions are the same as those in Figure 3-7a.

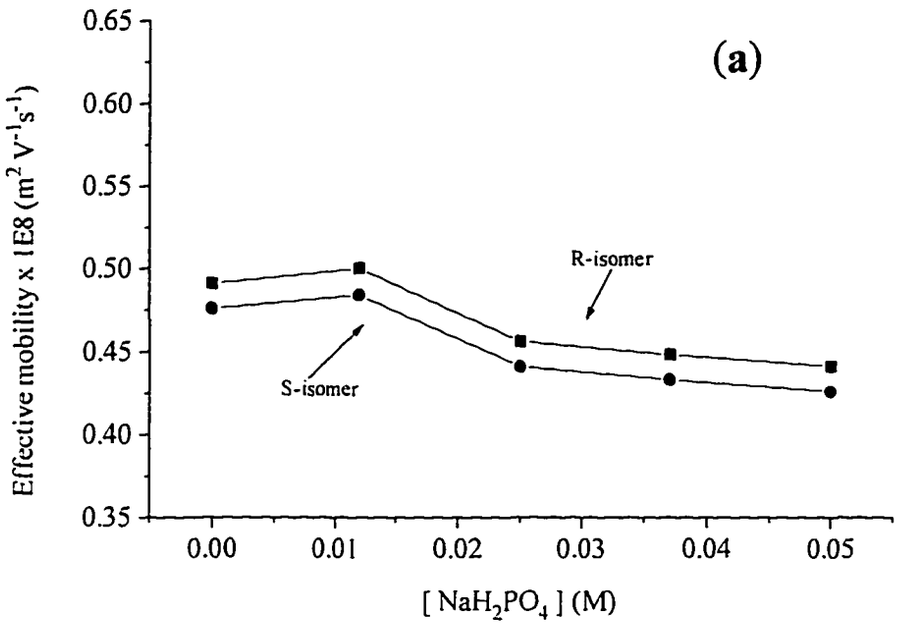


**Figure 3-8a. Effect of [$NaH_2PO_4$] on Effective Mobility**

The experimental conditions are the same as those in Figure 3-3a, except the buffer solution is BF 3-5.

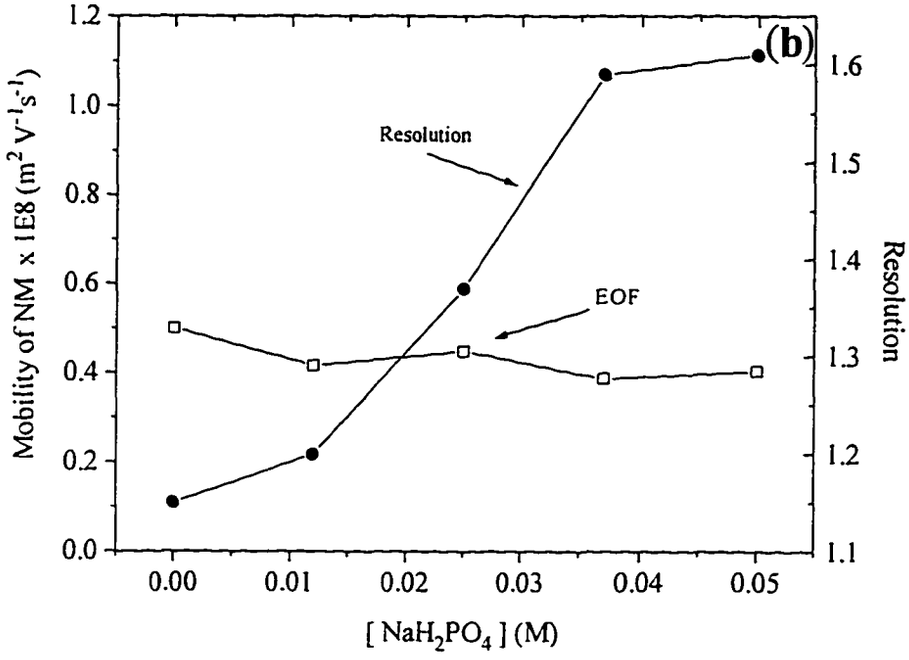


**Figure 3-8b. Effect of [$NaH_2PO_4$] on Resolution and EOF**

Experimental conditions are the same as those in Figure 3-8a.

The role of the ion-pairing reagent in the association between the analyte and the β-CD is also supported by the electropherograms shown in Figure 3-9b, which demonstrates that the resolution can be significantly affected by the length of the alkyl chain in the alkyl-sulfonic acids. The alkyl-sulfonic acids used in the experiment contain the same net charge, but vary in chain length. The migration time order of analytes in the presence of different alkyl-sulfonic acids is $t_{prop} > t_{but} > t_{pent} > t_{Hex} > t_{Hept} > t_{Oct} > t_{Decan}$. The resolution decreases when the carbon number of the alkyl chain is greater than 6, and completely disappears when the carbon number is 10. The changes in the migration time and the enantiomeric resolution can be attributed to the competition between the alkyl chain on the alkyl-sulfonic acids and the MK-0677 to interact with the hydrophobic cavity of the β-CD

As shown in Table 3-4, the binding constants for [MK-0677:β-CD] without ion-pairing reagents are much larger than those with ion-pair reagents. This confirms that the ion-pairing reagents participate in the binding with β-CD. Because of the competitive binding, the binding constant between the β-CD and MK-0677 is reduced and the optimum β-CD concentration is shifted higher.

**Table 3-4. Comparison of Binding Constants**

**Using Different Ion-pairing Reagents**

| Ion pair reagent | $K_R$ (25°C) | $K_S$ (25°C) | $C_{opt}$ (mM) |
|---|---|---|---|
| LTA | 15.6 | 18.1 | 59.4 |
| MOPS | 48.1 | 52.2 | 20.0 |
| BTSA | 47.0 | 50.4 | 20.5 |
| No Ion-pair Reagent (NIPR) | 97.9 | 101.6 | 10.0 |

Experimental conditions: buffer solutions: BF 3-19 to BF 3-22; other conditions are the same as those in Table 3-2.

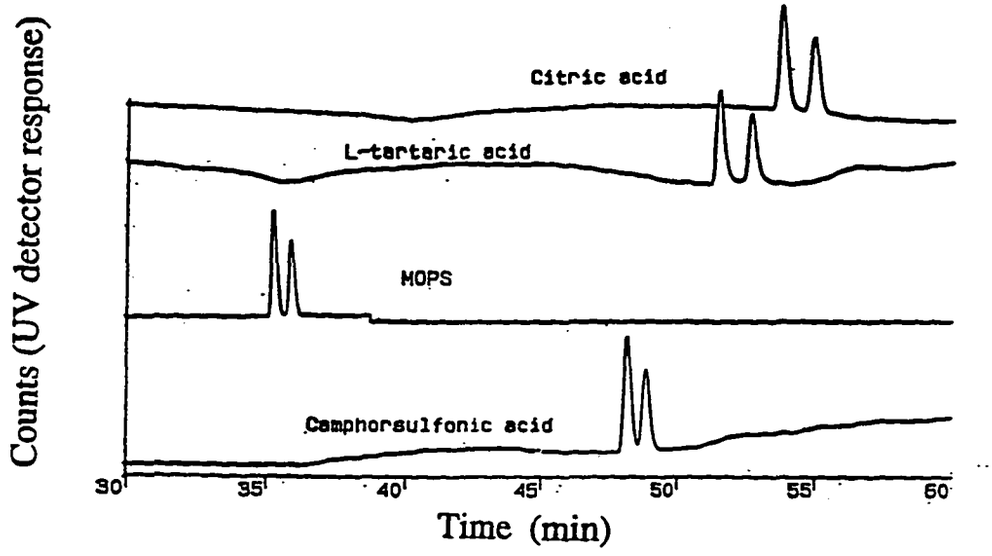


**Figure 3-9a. Separation of M-0677 in Presence Different Ion-pair Reagents**

The experimental conditions are the same as those in Table 3-2, except the buffer solutions used are BF 3-1, and BF 3-9 to BF 3-11

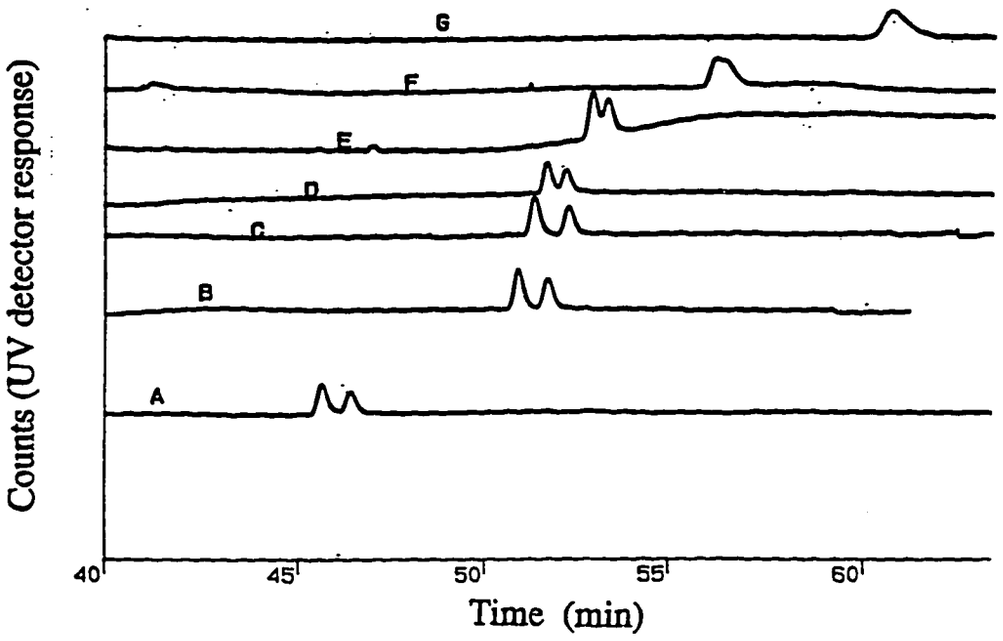


**Figure 3-9b. Separation of M-0677 in Presence Different Alkyl Sulfonic Acids**

A: propanesulfonic acid; B: butanesulfonic acid; C: pentanesulfonic acid; D: hexanesulfonic acid; E: heptanesulfonic acid; F: octanesulfonic acid; G: decanesulfonic acid. The experimental conditions are the same as those in Table 3-3, except the buffer solutions are BF 3-12 to BF 3-18.

According to Equation 2-12, the stronger the binding of the [β-CD:analyte] complex, the lower the optimum CD concentration, $C_{opt}$. The optimum β-CD concentrations for different ion-pairing reagents are listed in Table 3-4. The $C_{opt}$ without any ion-pairing reagent has the lowest value. As seen in Figure 3-10a, the range of the optimum [β-CD] matches the calculated values. Since the value of $C_{opt}$ becomes larger when an ion-pairing reagent is used, resolution should be inceased with ion-pairing reagents. Resolution is also related to the other factors, such as EOF, electromigration dispersion, ionic strength of the analyte, co-ions, etc. Figure 3-10b illustrates the resolution vs. concentration of β-CD with and without ion-pairing reagents. The LTA gives the best resolution for two reasons. The first is its higher ion strength. The second is the $C_{opt}$ has a higher value. As in the Figures 3-11 (a & b), at [β-CD] = 15 mM and [β-CD] = 50 mM, the peak shapes of the two enantiomers in the presence of LTA are much more symmetric than those without ion-pairing reagents. Symmetrical peaks lead to better resolution in the LTA buffer. If ionic strength were the only reason for the higher resolution, the difference in resolution between the two buffers should not change much over the entire concentration of β-CD. However, as shown in Figures 3-10b and 3-11(a & b), the resolution at [β-CD]=15 mM is almost the same for the two buffers but is much different at the [β-CD]=50 mM. The β-CD optimum concentration is about 10 mM for the buffer with no ion-pairing reagent (NIPR) and is 59 mM for the LTA buffer. At [β-CD]=50 mM, the $\Delta\mu$ is already over the maximum point for the NIPR buffer while it is still increasing for the LTA buffer.

Therefore, the differences of the resolution become large. For the buffers with MOPS or BTSA, although the $\Delta\mu_{max}$ appears in the same range as predicted, the resolution is not proportional to the binding constants. One possible explanation for this is that their hydrophobic tails not only interact with the cavity of the β-CD, but also with MK-0677 through hydrophobic interactions (surfactant effect). This reduces the enantioselectively binding and results in loss of the resolution.

As Wren and Rowe suggested if the [β-CD] is greater than the optimum value in the CD-free buffer solution, addition of organic modifier should increase the resolution. In contrast, if the [β-CD] is less than the optimum value in the CD-free buffer solution, addition of organic modify should decrease the resolution. This concept should also apply to the ion pairing reagents, as long as competitive interactions exist. The optimum value of the [β-CD] without LTA was determined to be 10 mM (Table 3-4). Figure 3-12 illustrates resolution as a function of [LTA] in the presence of β-CD at concentrations above and below that optimum value. Resolution increases as [LTA] is increased when the [β-CD]=30 mM and decreases as [LTA] is increased when the [β-CD] = 8 mM.

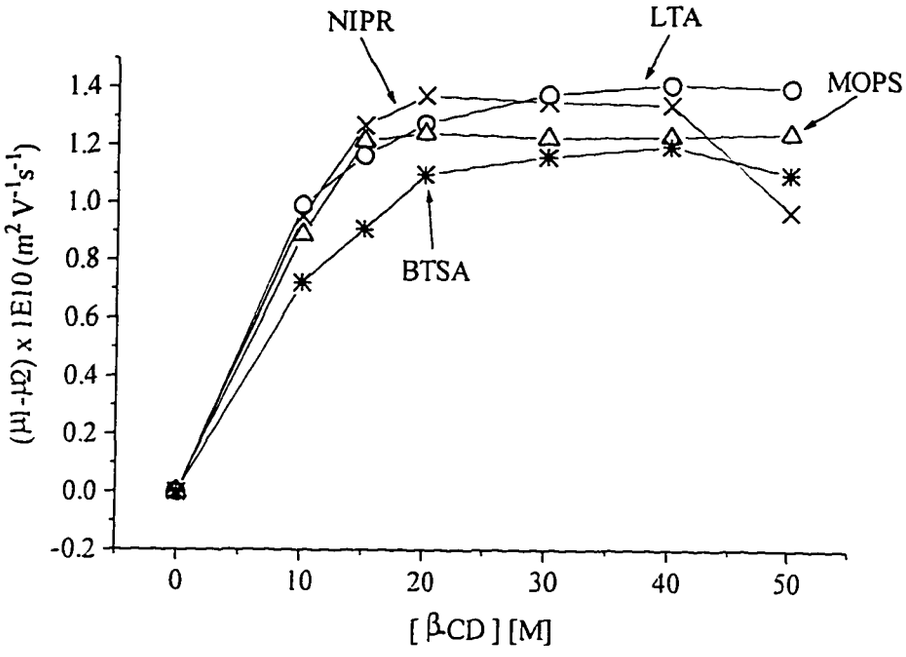


**Figure 3-10a. Mobility Difference of MK-0677 vs. [β-CD]**

The experimental conditions are the same as those in Table 3-2. × is NIPR; Δ is MOPS; o is LTA; * is BTSA.

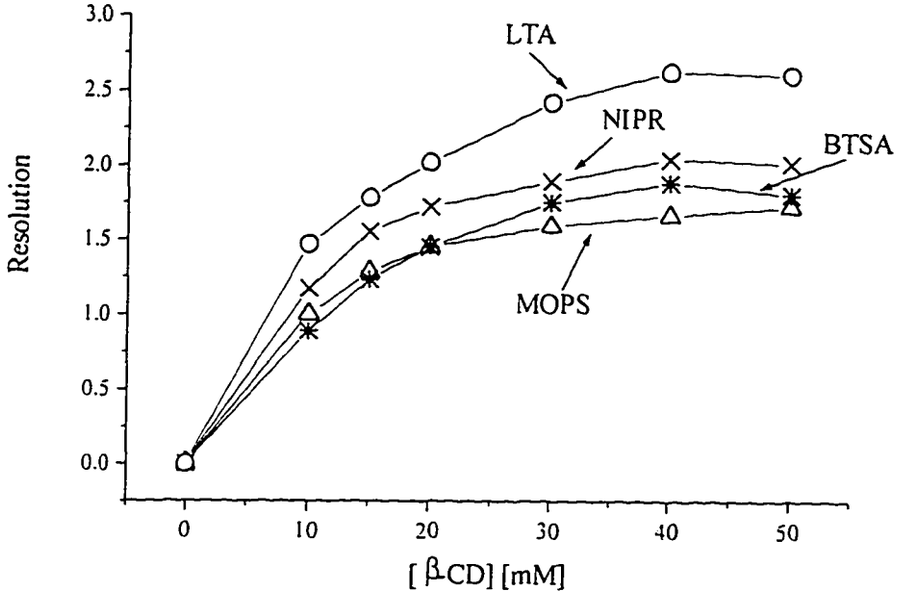


**Figure 3-10b. Resolution of MK-0677 in Different Ion-pairing Reagents**

The experimental conditions are the same as those in Table 3-3. × is NIPR; Δ is MOPS; o is LTA; * is BTSA.

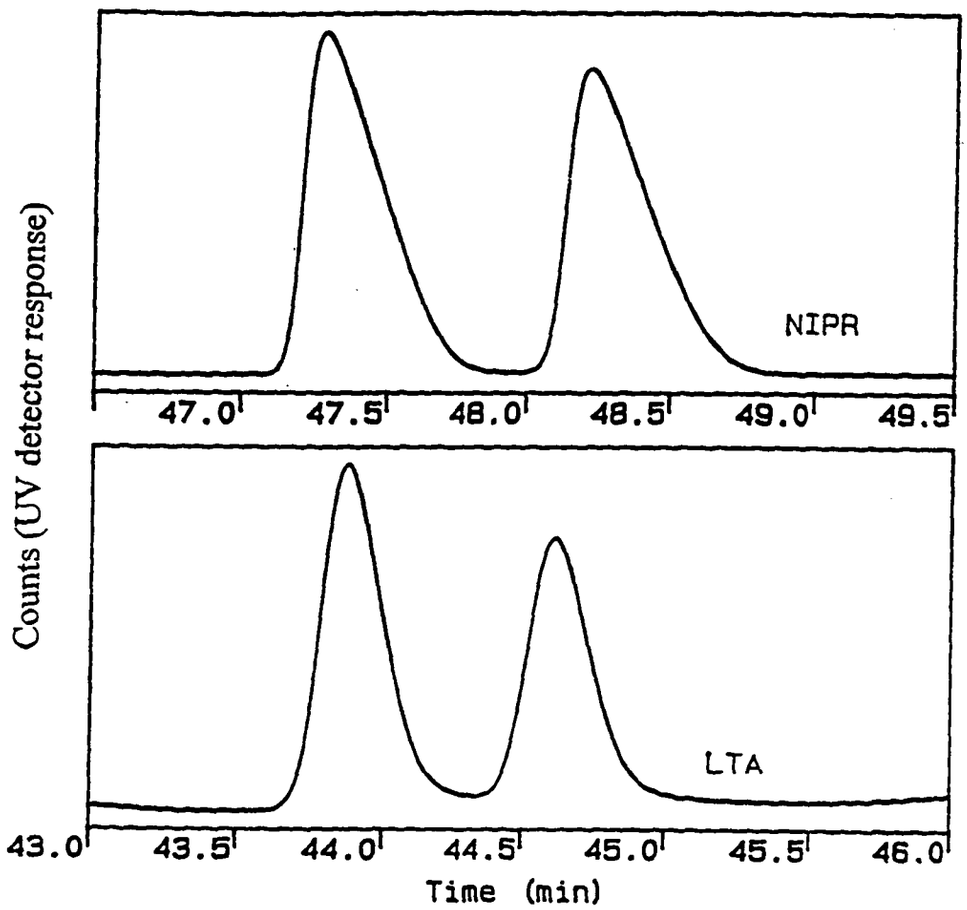


**Figure 3-11a. Comparison of Peak Shape at Different Buffer Solutions**

Experimental conditions: [β-CD)=15 mM; LTA: *L*-tartaric acid buffer solution (BF 3-22); NIPR: buffer solution without ion-pairing reagent (BF 3-19).

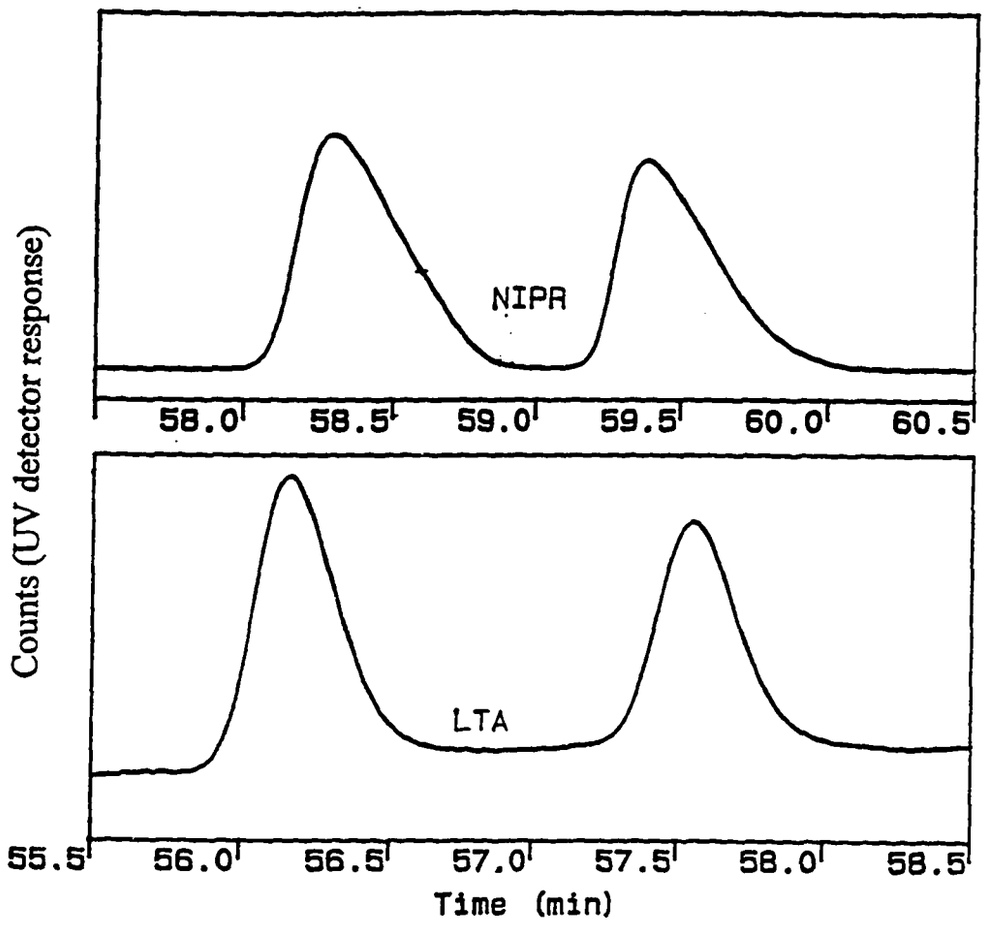


**Figure 3-11b. Comparison of Peak Shape at Different Buffer Solutions**

Experimental conditions: [β-CD)=50 mM; LTA: *L*-tartaric acid buffer solution (BF 3-22); NIPR: buffer solution without ion-pairing reagent (BF 3-19).

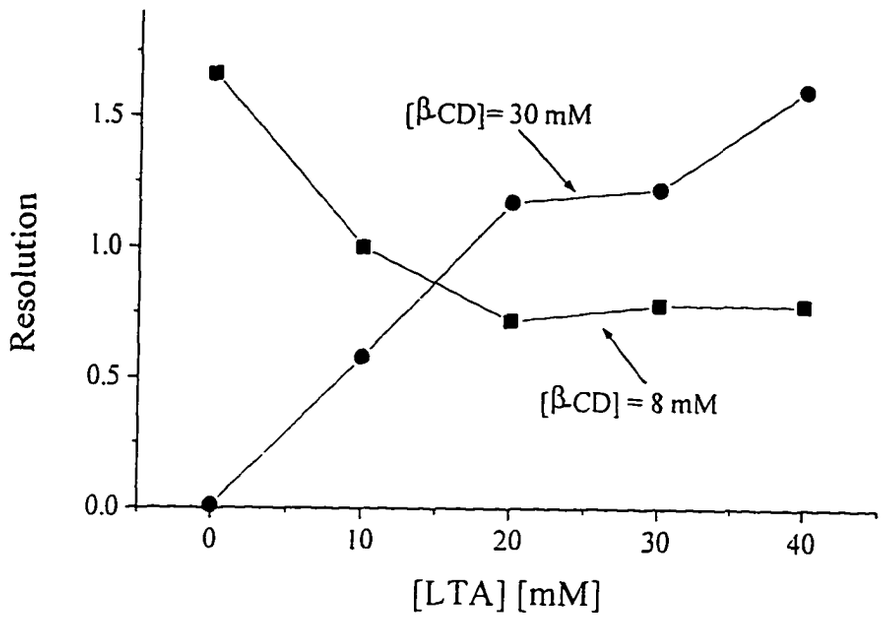


**Figure 3-12. Resolution vs. [LTA]**

The experimental conditions are the same as those in Table 3-2, except the buffer solutions are BF 3-3 and BF 3-4.

### 3-3G Effect of Voltage on Enantiomeric Separation

It was found that the analyte mobilities and the EOF increased as the increasing applied voltage. The resolution did not change significantly at the voltage range 16-20 kV, but decreased slightly at the range 20-30 kV. Based on the CZE theory, the higher the voltage, the shorter the migration time, and the higher the peak efficiency. However, too higher voltage will generate Joule heating which causes a band broadening and results a reduction in resolution.

## 3-4 Validation Study

The CZE method to enantiomerically separate MK-0677 has been validated based on the standard of cGMP [14]. The validation process includes evaluations of whether the method is suitable and practical in terms of accuracy, precision; limit of the detection (LOD), limit of quantitation (LOQ), linearity of the UV response, and ruggedness.

### Linearity of UV Response

The method linearity was evaluated by testing the UV responses to the concentrations of MK-0677 (*R*-isomer) at the range 0.32μg/mL - 0.54 mg/mL [0.08% (w/w) to 135% (w/w) of the target analyte concentration 0.4 mg/mL]. The

correlation coefficient, $R^2$, of the UV response to the concentration of MK-0677 was determined as 0.9997 based on duplicate injections of each solution.

**Limits of Detection (LOD) and Quantitation (LOQ)**

The LOD is the concentration of the analyte giving a signal-to-noise ratio of 3. The LOQ is defined as 3x(LOD). The lowest concentration tested in the linearity experiment, 0.32 μg/mL which corresponds to 0.1% of the target concentration, gave S/N=3. Therefore, the LOD and LOQ of the method are 0.1% and 0.3%, respectively.

**Accuracy**

The accuracy of the method was evaluated by assaying 5 times the *R*-isomer spiked with 0.35% (w/w) the *S*-isomer. The average recovery of the *S*-isomer was 103 %. Furthermore, the chiral HPLC method using the Ultron-ES OVM® protein column was also conducted in this test. The recovery results obtained from the CZE method and the HPLC method are in good agreement.

**Precision**

The injection precision was tested by making five consecutive injections of the MK-0677 solution (0.4 mg/mL) containing 0.35% of the *S*-isomer. The %RSD of all five assays is 0.03% for the *R*-isomer and 8.9% for the *S*-isomer.

**Ruggedness**

The solution stability was validated by repeatedly assaying a 0.4 mg/mL MK-0677 solution on different days over a one month period. The %RSD of the multiple assay results was 0.8% for the *R*-isomer, which indicates that the solution is stable for at least one month in the recommended diluent. The variations of capillary to capillary and electrolyte to electrolyte were verified by using two different capillaries and three different preparations of buffer solutions. 0.8% RSD of these assays was obtained, which indicates that the method is rugged with respect to day-to-day electrolyte variations and different capillaries. Overall, based on the day-to-day results, the resolution of the two enantiomers was less than 1.5, and the peak tailing factor for the *S*-isomer is less than 1.5.

## 3-4 Conclusions

1) The CZE method using β-CD as the chiral selector was developed for the enantiomeric separation of MK-0677. This method has also been validated based on standards of cGMP and demonstrated to be a linear, precise, accurate, and rugged method with 0.1% LOD and 0.3% LOQ.

2) The enantiomeric separation of MK-0677 was function of various experimental parameters, the concentration of β-CD, organic modifier, and ion pairing reagent. It was also affected by temperature, applied voltage, and buffer pH.

3) The binding study showed the organic modifiers participate in the complexing interaction between the analyte and the β-CD. The larger the organic modifier, the weaker the binding.

4) The binding constants of MK-0677 to the β-CD in the presence of the ion-pairing reagents are much less than those in the absence of the ion-pairing reagents.

# APPENDIX I

## SAS Computer Program to Calculate

## Inclusion Binding Constants from CZE Analysis

## (Non-Linear Regression Calculation in $c^+$ computer language)

```
OPTIONS LINESIZE=76;
DATA MAIN;
        INFILE 'TRIS_AMD_35.DAT';
        INPUT C U1 U2;
PROC PRINT;
        TITLE 'CALCULATION CZE INCLUSION CONSTANT';
PROC NLIN METHOD=NEWTON;
PARMS U8=.09 K1=1, 2, 5;
BOUNDS 0<U8<0.14, 0<K1<100000;
U0=0.1893483;
X1=U0-U8;
X2=1+K1*C;
MODEL U1=X1/X2+U8;
DER.U8=-1/X2+1;
DER.K1=-C*X1/X2/X2;
DER.U8.U8=0.0;
DER.K1.K1=2*C*C*X1/X2/X2/X2;
DER.K1.U8=C/X2/X2;
MODEL U1=X1/X2+U8;
DER.U8=-1/X2+1;
DER.K1=-C*X1/X2/X2;
DER.U8.U8=0.0;
DER.K1.K1=2*C*C*X1/X2/X2/X2;
DER.K1.U8=C/X2/X2;

PROC NLIN METHOD=NEWTON;
PARMS U8=0.0001 K2=1, 2, 5;
BOUNDS 0<U8<0.14, 0<K2<100000;
```

U0=0.1893483;

X1=U0-U8;

X3=1+K2*C;

MODEL U2=X1/X3+U8;

DER.U8=-1/X3+1;

DER.K2=-C*X1/X3/X3;

DER.U8.U8=0.0;

DER.K2.K2=2*C*C*X1/X3/X3/X3;

DER.K2.U8=C/X3/X3;

**Parameter Notification**

| Symbol in Program | Definition |
|---|---|
| U1 | $\mu_1$, the ionic mobility of enantiomer(I) at some concentration of CD [C], ($m^2V^{-1}s^{-1}$) |
| U2 | $\mu_2$, the ionic mobility of enantiomer(II) at some concentration of CD [C] ($m^2V^{-1}s^{-1}$) |
| U8 | $\mu_\infty$, the ionic mobility of the enantiomer at the [CD] $\rightarrow \infty$ ($m^2V^{-1}s^{-1}$) |
| U0 | $\mu_0$, the ionic mobility of the enantionmer in CD free buffer ($m^2V^{-1}s^{-1}$) |
| C | Concentration of free CD (M) |
| K1 | Binding constant of [enantiomer (I):CD] |
| K2 | Binding constant of [enantiomer (II):CD] |
| TRIS_AMD_35.DAT | Input data file which contains experimental data and for C, $\mu_1$, and $\mu_2$. |

## Reference

### Introduction


[1] F. A. Carey and R. J. Sunberg, *Advanced Organic Chemistry*, Part A, *Structure and Mechanisms*, Chapter 2, Plenum Press, New York, 1983

[2] P. Zurer, *Chem. Engr. News* 74 (1) (1996) 6.

[3] B. D. Dorsey, R. B. Levin, S. L. McDaniel, J. P. Vacca, J. P. Guare, P. L. Dark, J. A. Zugay, E. W. A. Schleif, J. C. Quintero, J. H. Lin, I.-W. Chen, M. Katharine Holloway, P. M. D. Fitzgerald, M. G. Axel, D. Ostovic, P. S. Anderson and Joel R. Huff, *J. Med. Chem*, 21 (1994), 3443.

[4] E. Gil-Av, B. Feibush and R. Charles-Siegler, *Tetrahedron Lett.*, (1966), 1009.

[5] S.-C. Chang, R. Charles and E. Gil-Av, *J.Chromatog.*,29 (1982) 238.

[6] D. W. Armstrong and W. DeMond, *J. Chromatogr. Sci.*, 22 (1984) 411.

[7] M. A. Tarr, G. Nelson. G. Patonary and I. M. Warner, *Anal. Lett.*, 21 (1988) 843.

[8] D. N. Heiger, *High Performance Capillary Electrophoresis*, Hewlett-Packard, France, 1992.

[9] S. Runge, R. Hirz, E. Kenndler and A. Rizzi, *J. Chromatogr.* A, 710 (1995) 339

[10] D. Gere, *Science* 222 (1983) 253

[11] P. Mourier, M.Caude, R. Rosset, *Anal. Chem.*, 57 (1985) 2819.

[12] R. Kuhn and S. H. Kuhn, *Chromatographia*, 34 (9/10) (1992) 505.

[13] F. E. P. Mikkers, F. M. Everaerts and T. P. E. M. Verheggen, *J. Chromatogr.*, 169 (1979) 11.

[14] J. W. Jorgenson and K. D. Lukacs, *Anal. Chem.*, 53 (1981) 1298.

[15] S. Hjerten, *J.Chromatogr.*, 270 (1983) 1.

[16] S. Terabe, K. Otsuka, K. Ichikawa, A. Tsuchiya and T. Ando, *Anal. Chem.*, 56 (1984) 111.

[17] S. Terabe, K. Otsuka and T. Ando, *Anal. Chem.*, 57 (1985) 834.

[18] J. W. Jorgenson, K. D. Lukacs, *J.Chromatogr.*, 218 (1981) 209.

[19] F. E. P. Mikkers, F. M. Everaerts, T. P. E. M. Verheggen, *J.Chromatogr.*, 169 (1979) 1.

[20] M.J. Gordon, X. Huang, S.L. Pentoney, Jr., R. N. Zare, *Science,* 242 (1988) 242.

[21] B. L. Karger, A. S. Cohen, A. Guttman, *J.Chromatogr.*, 492 (1989) 585.

[22] N. A. Guzman, L. Hernandez, B. G. Hoebel, *Biopharm Manufact.*, 2 (1989) 22.

[23] S. Terabe,Y. Milyashita, Y. Ishlhame and O. Shibata, *J.Chromatogr.* 636 (1993) 47.

[24] I. S. Lurie, *J. Chromatogr.*, 605 (1992) 269.

[25] A. D. Tran, T. Blance, E. J. Leoplod, *J. Chromatogr.*, 516 (1990) 241.

[26] H. Nishi, S. Terabe *J. Chromatogr. A*, 694 (1995) 245.

[27] H. J. Issaq, G. M. Janini; K.C. Chan, Z. El Rassi, *Adv.Chromatogr.* 35 (1995), 101.

[28] C. A. Monnig and R. T. Kennedy, *Anal. Chem.*66 (1994) 280R.

[29] H. Corstjens, H. A. Billiet, J. Frank and K. C. A. M. Luyben. *J. Chromatogr. A*, 715 (1995)1.

[30] S. Terabe, K. Otsuka and H. Nishi, *J. Chromatogr. A*, 666 (1994) 295.

[31] R. Vespalec and P. Bocek, *Electrophoresis* 15 (1994) 755.

[32] P. D. Grossman and J. C. Colburn, *Capillary Electrophoresis, Theory and Practice*, Academic Press, Inc., Califonia, 1992.

**Chapter One**

[1] T. A. Lyle, C. M. Wiscunt, J. P. Guare, W. J. Thompson, P. S. Anderson, P. L. Darke, J. A. Zugay, E. A. Emini, W. A. Schleif, J. C. Quintero, R. A. F. Dixon, I. S. Sigal and J. R. Huff, *J. Med. Chem.* 34 (1991) 1228.

[2] R. C. Williams, J. F. Edwards and C. R. Ainsworth, *Chromatographia,* 38 (1994) 441.

[3] G. N. Okafo, K. K. Rana and P. Camilleri, *Chromatographia*, 39 (1994) 627.

[4] S. Terabe, H. Ozaki, K. Otsuka and T. Ando, *J. Chromatogr.* 332 (1985) 211.

[5] T. Tadey and W. C. Purdy, *J. Chromatogr.* B 657 (1994) 365.

[6] D. N. Heiger, *High Performance Capillary Electrophoresis*, Hewlett-Packard, France, Chapter 2, 1992.

[7] J. L. Beckers, F. M. Everaerts and M. T. Ackermans, *J. Chromatogr.* 537 (1991) 407.

[8] R. R. Chadwick and J. C. Hsieh, *Anal.Chem.*, 63 (1991) 2377.

[9] Molecular Simulation Inc, *Cerius$^2$ Simulation Tools User's Reference*, Cambridge,U.K., 1994.

[10] G. S. Ponticello, M. B. Freedman, C. N. Habecker, P. A. Lyle, H. Schwam, S. L. Varga, M. E. Christy, W. C. Randall, J. J. Baldwin, *J. Med. Chem.*, 30 (1987) 591.

[11] A. Dovletoglou, S. M. Thomas, L. Berwick, D. K. Ellison and P. C. Tway, *J. Liq. Chromatogr.* 18 (1995) 2337.

[12] J. A. Dean, *Lange's Handbook of Chemistry*, thirteen edition, (1972) 5-22.

[13] R. S. Sahota and M. G. Khaledi, *Anal. Chem.* 66(1994), 1141.

[14] I. Bjørnsdottir and S. H. Hansén, *J. Pharm. Biomed. Anal.Chem.*, (1995), 1473.

[15] I. Bjørnsdottir and S. H. Hansén, *J. Chromatogr. A.* 711 (1995) 313.

[16] J. Cai, J. T. Smith and Z. E. Rassi, J. High Resol, *Chromatogr.*15 (1992) 30.

[17] J. A. Cleveland, Jr., M. H. Benko, S. J. Gluck and Y. M. Walbroehl, *J. Chromatogr. A.* 652 (1993) 301.

[18] F. A. Carey, *Organic Chemistry*, Plenum Press Inc., New York, 1987.

[19] F. A. Carey and R. J. Sundberg, *Advanced Organic Chemistry*, Part A: *Structure and Mechanisms*, Plenum Press Inc., New York, 1987.

[20] P. Sykes, *Mechanism in Organic Chemistry*, 6th edition, John Wiley & Sons, New York, 1986.

[21] P. D. Grossman and J.C.Colburn, *Capillary Electrophoresis, Theory and Practice*, 1992, Academic Press, Inc., Califonia.

[22] P. Camilleri, *Capillary Electrophoresis, Theory and Practice*, CRC Press, Inc., London,1994.

[23] L. G. Hargis, *Analytical Chemistry, Principles and Techniques*, Prentice-Hall Inc., New Jersey, 1988.

[24] C. Schweer and E. Kenndler, *Anal. Chem.*, 63 (1991) 1801.

[25] K. Salomon, D. S. Nurgiand, and J. C. Helmer, *J. Chromatogr.*, 559 (1991) 69.

**Chapter Two**

[1] S. Fanali, *J. Chromatogr.*, 474 (1989) 441.

[2] S. A. C. Wren and R. C. Rowe, *J. Chromatogr.*, 603 (1992) 235.

[3] Y. Y. Rawjee, R. L. Williams and G. Vigh, *J. Chromatogr.* A, 652 (1993) 233.

[4] D. W. Armstrong, Y. Tang, T. Ward and M. Nichols, *Anal. Chem.*, 65 (1993) 1114.

[5] S. Terabe, *TRAC*, 8 (1989) 129.

[6] G. E. Barker, P. Russo and R. A. Hartwick, *Anal. Chem.*, 64 (1992) 3024.

[7] S. Busch, J. C. Kraak and H. Poppe, *J. Chromatogr.*, 635 (1993) 119.

[8] R. Kuhn, F. Enri, T. Bereuter and J. Hanseler, *Anal. Chem.*, 64 (1992) 2815.

[9] E. Hohne, G. J. Krauss and G. Gubitz, *J. High Resolut. Chromatogr.*, 15 (1992) 698.

[10] A. D'Hulst and N. Verbeke, *J. Chromatogr.*, 608 (1992) 275.

[11] J. Szejtli, *Pharm. Technol. Int.*, 3 (1991) 15.

[12] R. J. Bergeron and M. P. Meeley, *Bioorg. Chem.*, 5 (1976) 197.

[13] S. A. C. Wren and R. C. Rowe, *J. Chromatogr.*, 609 (1992) 363.

[14] S. A. C. Wren and R. C. Rowe, *J. Chromatogr.*, 635 (1993) 113.

[15] S. A. C. Wren, *J. Chromatogr.*, 636 (1993) 57

[16] S. G. Penn, E. T. Bergstrom, D. M. Goodall and J. S. Loran , *Anal. Chem.*, 66 (1994) 2866.

[17] R. J. Bergeron and R. Rowan, *Bioorg. Chem.*, 5 (1976) 425.

[18] R. J. Bergeron and D. M. Pillor, G. Gibeily, W. P. Roberts, *Bioorg. Chem.*, 7 (1978) 263.

[19] *SAS/STAT User's Guide*, SAS Intitute, (1990) Chapt 29.

[20] D. N. Heiger, *High Performance Capillary Electrophoresis*, Hewlett-Packard, Gmblt, Waldbron, Germany, Chapt 2, 1992.

[21] W. L. Hinze, D. Y. Pharr, Z. S. Fu and W. G. Burkert, *Anal. Chem.* 61 (1989) 422.

[22] D. Y. Pharr, Z. S. Fu, T. K. Smith and W. L. Hinze, *Anal. Chem.* 61 (1989) 275.

[23] S. G. Penn, E. T. Bergström, I.Knights, G. Liu, A. Ruddick and D. M. Goodall, *J. Phys. Chem.* 99 (1995) 3875.

[24] *Cerius$^2$ Simulation Tools User's Reference,* Cambridge, U.K. Version 1.6 1994.

[25] *CSD.* Cambridge Crystallographic Data Center, Cambridge, U.K.

[26] Allen, F. H., Kennard. O. and Taylor. R., *Accts. Chem. Res.*, 16 (1983) 144.

[27] Y. Rawjee, R. L. Williams and G. Vigh, *Anal. Chem.*, 66 (1994) 619.

[28] Y. Rawjee, D. U. Staerk and G. Vigh, *J. Chromatogr.*, 635 (1993) 291.

[29] Y. Rawjee, R. L. Williams, L. A. Buckingham and G. Vigh, *J. Chromatogr.*, 688 (1994) 273.

[30] Y. Rawjee, R.L.Williams and G. Vigh, *Anal. Chem.*, 66 (1994) 3777.

[31] P. D. Grossman and J.C.Colburn, *Capillary Electrophoresis, Theory and Practice*, Academic Press, Inc., California, 1992.

[32] P. Camilleri, *Capillary Electrophoresis, Theory and Practice*, CRC Press, Inc., London,1994.

[33] H. Dodziuk, K. Nowinski, *J. Mol. Struct.*,304 1994 61.

[34] W. L. Hinze, *In Separation and Purification Methods:* vol. 10 C. J. van Oss, Ed.; Marcel Dekken, New York,1981, pp.159-237.

[35] *Chapter One*

[36] R. Stevenson, *Americ. Lab.*, GG (1993) 52.

[37] J. C. Reepmeyer, *Chirality*, 8 (1996) 11.

[38] R.M. Mohseni and R.J. Hurtubise, *J. Chromatogr.*, 499 (1990) 395.

[39] M. Yoshinaga and M. Tanaka, *J. Chromatogr.*,710 (1995) 331.

[40] J. Noroski, D. Mayo and J. J. Kirschbaum, *J. Pharm. & Biomed. Anal.*10 (1992) 447.

[41] R. Breslow and S. Halfon, *Proc. Natl, Acad. Sci. USA*, 89 (1992) 6916.

[42] G. Barone, G. Castronuovo, V. Eli and M. Muscetta, *J. Solu. Chem.*, 15 (1986) 2.

[43] S. G. Penn, G. Liu, E. T. Bergstrom and D. M. Goodall, *J. Chromatogr.*, 680 (1994) 147.

[44] S. Piperaki, S. G. Penn and D. M. Goodall, *J. Chromatogr.*, 700 (1995) 59.

[45] J. Debowski and D. Sybilska, *J. Chromatogr.*, 353 (1986) 409.

[46] T. J. Bahowick and R. E.Synovec, *Anal. Chem.* 64 (1992) 489.

[47] Z. D. Sybilska and J. Jurczak, *Anal. Chem.* 57 (1985) 2215.

[48] R. A. Kuharski and P. J. Rossky, *J. Am. Chem. Soc.*, 106 (1984) 5794.

**Chapter Three**

[1] R. G. Smith, K. Chang, W. R. Schoen, S. Pong, G. Hickey, T. Jacks, B. Butler, W. Chan, L.Chaung, F. Judith, J. Taylor, M. J. Wyvratt and M. H. Fisher, *Science,* 260 (1993) 1640.

[2] A. Patchett, R. P. Nargund, J. R. Tata, M. Chen, K. J. Barakat, D. B. R. Johnston, K. Cheng, W. Chan, B. Butler, G. Hickey, T. Jacks, K. Schleim, S. Pong, L.- Chaung, H.Y. Chen, E. Frazier, K. H. Leung, S. Chiu and R. G. Smith. *Proc. Natl. Acad. Sci. USA Medical Sciences,* 92 (1995) 700.

[3] US Pharmacopoeia,(621) Chromatography, 23 (1995) 1775.

[4] S. A. C Wren and R. C. Rowe, *J. Chromatogr.*, 603 (1992) 235.

[5] S. A. C. Wren and R. C. Rowe, *J. Chromatogr.*, 609 (1992) 363.

[6] S. G. Penn, E. T. Bergstrom, D. M. Goodall and J. S. Loran , *Anal. Chem.*, 66 (1994) 2866.

[7] R. Kuhn and F. Erni, *Anal. Chem.*, 64 (1992) 2815.

[8] W. Lindner, B. Bohs and V. Seidel, *J. Chromatogr.* A, 697 (1995) 549.

[9] Y. Rawjee, R. Williams and G. Vigh, *J. Chromatogr.*, 652 (1993) 233.

[10] Y. Rawjee, R. L. Williams and G. Vigh, *Anal. Chem.*, 66 (1994) 619.

[11] Y. Rawjee, D. U. Staerk and G. Vigh, *J. Chromatogr.*, 635 (1993) 291.

[12] Y. Rawjee, R. L. Williams, L.A.Buckingham and G. Vigh, *J. Chromatogr.*, 688 (1994) 273.

[13] Y. Rawjee, R. L. Williams and G. Vigh, *Anal. Chem.*, 66 (1994) 3777.

[14] US Pharmacopoeia,(1225) Validation of Compendial Methods, 23 (1995) 1982.